Infocommunications Journal

Technically Co-Sponsored by

IEEE ComSoc™
IEEE Communications Society

hte

IEEE
HUNGARY SECTION

HTE for 70 years

Infocommunications Journal: over 10 years – HTE: over Seven Decades – Guest Editorial

Pál Varga

INFOCOMMUNICATIONS – the domain that integrates information technology, telecommunications, audiovisual systems from user access to information storage and processing – has changed our quality of life in the last decades. The ever-increasing speed of data-exchange, the ultra-high resolution of affordable visual systems, or the "extraordinary" storage capacity that we instantly access every day became "ordinary" – we actually got used to the speed how things change around us. It is not simply that we realize such changes, but we build it into our everyday experience, and improve our "digitalized skills": we buy our train tickets, get around abroad, or communicate with our relatives much differently than one decade ago.

The last ten years changed our ways of life greatly. This is the eleventh year of Infocommunications Journal, which shows that the scientific society of our field has not just simply accepted its birth but keeps contributing to its growth. The scope of the journal is very broad, which can be seen as an advantage or as a drawback as well. Such a wide spectrum of interest – from radio communications to networking, from media delivery to security – makes it hard to build societies in the short run, but it always allows to choose from the most interesting topics and the most auspicious authors. Certainly, our journal has contributed well to the scientific society – hence, to our life in the long run – already significantly, and keeps doing so. Let us celebrate the first year of this new decade with impactful publications!

On the other hand, this year is remarkable for HTE, the Scientific Association for Infocommunications, our publisher. HTE has been formed in the January 29, 1949, in Hungary – hence celebrating its 70th anniversary this year. It was born when the Low Voltage and Radio-technical Section of Hungarian Electrotechnical Association (founded in 1900), merged with the Hungarian Kinotechnical Association. The name at the time reflected the technical interests and needs: Scientific Association for Communications Engineering, Precision Mechanics and Optics. This has changes twenty years ago to the current name – expressing the integration of information technology and communications –, although the abbreviation remained in Hungarian.

The current issue shows a true nature of our Journal: seven papers written by authors of 11 nationalities. Our international authors cover various domains of infocommunications: from radio propagation optimization problems through opto-electronic modulators to security and safety of cyber-phyiscal systems – including applications on robotic arms. Let us have a brief overview of the papers in this issue.

Addressing security, safety, and organizational standard compliance in Cyber-Physical Systems, A. Bicaku et. al. presents a monitoring and standard compliance verification framework for Industry 4.0 application scenarios, with the aim to provide an automated standard compliance.

In his contemporary survey, D. Kanellopoulos covers var- ious issues on multimedia synchronization. He presents the basic control schemes for Inter-Destination Multimedia Synchronization, and focuses on related solutions and standardization efforts for emerging distributed multimedia applications.

C. iftlikli and M. Al-Obaidi combined Alamouti space-time block code (STBC) with block diagonalization for downlink MU-MIMO system over Rician channel for 5G. Their results show that for best performance, this combined system should be extended with Alamouti STBC.

In their paper entitled "Cost function based soft feedback iterative channel estimation in OFDM underwater acoustic communication", G. Qiao et. al. propose an iterative receiver, which – according to simulation results and experiments at sea – outperforms current solutions.

Z. Luo et. al. proposes a minimum BER criterion based robust blind separation (BSS) for MIMO systems. Their results show that this method outperforms conventional ML-based BSS methods in speed of convergence and separation accuracy.

The opto-electronic oscillator with Mach-Zender modulator by A. Bortsov and M. Smolskiy offers a model for phasenoise analysis – and the model is applied successfully for the proposed system.

Finally, R. Szabo and A. Gontean demonstrate their results on applying the Six Sigma toolset for sun tracker robotic arm optical distance measurement evaluation at different positions.

Seventy years for our Association, and ten years for our Journal – this is a year for celebration: remembering some legendary achievements, and aiming for new challenges.

Pal Varga received the M.Sc. and Ph.D. degrees from the Budapest University of Technology and Economics, Hungary, in 1997 and 2011, respectively. He is currently an Associate Professor at the Budapest University of Technology and Economics. Besides, he is also the Director at AITIA International Inc. Earlier, he was working for Ericsson, Hungary, and Tecnomen, Ireland. His main research interests include communication systems, network performance measurements, root cause analysis, fault localisation, traffic classification, end-to-end QoS and SLA issues, as well as hardware acceleration. Recently he has been actively engaged with research related to Cyber-Physical Systems and Industrial Internet of Things. He has been involved in various industrial as well as European research and development projects in these topics. Besides being a member of HTE, he is a member of both the IEEE ComSoc (Communication Society) and IEEE IES (Industrial Electronics Society) communities, and the Editor-in-Chief of the Infocommunications Journal.

Security Safety and Organizational Standard Compliance in Cyber Physical Systems

Ani Bicaku, Christoph Schmittner, Patrick Rottmann, Markus Tauber and Jerker Delsing

Abstract—In Industry 4.0 independent entities should inter-operate to allow flexible and customized production. To assure the parties that individual components are secured to inter-operate, we investigate automated standard compliance. The standard compliance is defined based on given sets of security and safety requirements for which measurable indicator points are derived. Those reflect configurations of systems recommended by security, safety or process management relevant standards and guidelines, which help to demonstrate the state of compliance. We propose in this paper an approach to automate such an assessment when components are inter-operating with each other by using a monitoring and standard compliance verification framework. The framework will assure the parties that services or devices within their organizations operate in a secure and standard compliant way, without compromising the underlying infrastructure.

Index Terms—Security, safety, organizational, standard, compliance, monitoring, Cyber Physical Systems.

I. INTRODUCTION

THE increasing demand for flexible and customized production brings new challenges to the existing manufacturing systems. To address these challenges, lots of research has been conducted to pave the way for the fourth industrial revolution, known as Industry 4.0, which aims to optimize production by sharing physical and cyber resources [1]. This may also include inter-operation between individual companies or legal entities within large enterprises. Existing technologies, such as Internet of Things, System of Systems, Cyber Physical Systems, cloud computing and Service Oriented Architectures, allow for such inter-operation already [2]. Nevertheless, it is important for entities to assure that the components inter-operate in a safe and secure manner and prove it at any point of time.

In the industrial environments, the fulfilment of security, and safety requirements of devices autonomously communicating with each other plays a fundamental role. Consequences of security incidents in different areas or dimensions, can be for example interruption or modification of an operational process, or even sabotage with intention to cause harm. Manipulating or interrupting such systems could also affect safety, which can have consequences such as environmental damage, injury or loss of life [3]. To allow interoperability, flexibility and customized production from the industrial devices to the backend infrastructure and to prevent failures during business process execution, organizational aspects should be in place. According to Gaitanides et al., [4] the main goal of process management is customer satisfaction. To achieve this the quality products and services must be improved, cycle time must be reduced and cost must be kept as low as possible. A

correct configuration of systems is the key to support proper business process execution and audits or compliance checks of system configurations should provide a method to monitor and verify a valid state.

Security, safety and organizational incidents are tolerated more easily if one can show that they occurred despite system compliance with all applicable security regulations. This can be achieved via manual audits, which are often based on existing standards and guidelines.

The new technologies and requirements of Industry 4.0 create a new demand for standardization, which plays a key role in improving security and safety across different regions and communities. In the last years, different standard organizations have been established, mostly initiated from industry, and have published various standards in different fields and topics. Despite the extensive research [5], [6], [7], and a considerable number of widely accepted security, safety, legal and organizational standards, existing approaches are incapable of meeting the requirements imposed by challenges and issues in Industry 4.0.

In order to address the aforementioned concerns, in our previous work [8], we have proposed an initial approach to automatically verify standard compliance by using a monitoring and standard compliance verification framework, as shown in Figure 1. In this paper we extend the framework with MOIs to assure that the system is compliant with organizational standards.
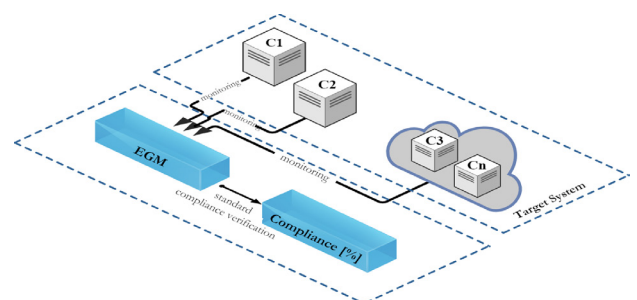
Fig. 1: High level view of standard compliance verification

The monitoring and standard compliance framework, built on our previous work [9], uses an Evidence Gathering Mechanism to collect evidence from a number of components in the target system based on a set of measurable indicator points. The Measurable Indicator Points, categorized in measurable security indicators, measurable safety indicators and measurable organizational indicators, are extracted from existing standards and guidelines to address target system

specific requirements (e.g. access control systems for the pro-duction line should be resistant against side-channel attacks). The information gained from the MIPs is then used by the compliance module to define if the target system is operating in a secure and standard compliant way.

The reminder of the paper is organized as follows. Section II reviews widely used security and safety standards/best practice guidelines and research on monitoring (security, safety and organizational) and compliance. Section III presents the overall architecture of the framework and the standard compliance verification approach. In Section IV an end-to-end communi-cation use case and a representative set of MIPs is provided and we conclude our work in Section V.

II. RELATED WORK

To enable the global usability of the products and systems, standardization in the industrial environment is of utmost im-portance. The new technologies and requirements of Industry 4.0 create a new demand for standardization, which plays a key role in improving security, safety and organizational aspects across different areas and in different communities. In the last years, several organizations have published various standards in different fields and topics. ENISA [1], ETSI [2], ISO [3] and IEC [4] are some of the most popular standardization bodies.

ISO 27000-series standards [10], also known as ISMS family of standards, deal with a different area of information security including requirements, implementation guidelines and risk management. The standards cover almost all the aspects of technology and business addressing cyber-security, privacy, confidentiality and other aspects of security issues by providing updates on the latest technologies and threats.

ISO/IEC 15408 [11], known as Common Criteria, provides a framework where the security functionality of IT products and the assurance requirements during a security evaluation can be specified. The CC evaluation is divided in three parts. The CC part 1, provides general concepts of IT security and defines the core concept of a TOE. The CC part 2 - Security functional components, includes a catalog of security functional components and categorizes them in a hierarchical order based on families, classes and components. The CC part 3 - Security assurance components, defines the assurance requirements of the TOE expressed in a PP or a ST. It also includes the EAL that defines the scale for measuring assurance for each component of the TOE. Nevertheless, CC has only focused on security evaluation without considering safety or legal aspects.

IoT Security Compliance Framework [12] is an assurance guideline for organizations used to provide structured evidence to demonstrate conformance with best practice guidelines. The compliance scheme in this document is based on risk profiles for different systems and environments including: (i) business processes, (ii) devices and aggregation points, (iii) networking and (iv) cloud and server elements. The compliance process is based on a set of requirements of organizations and products by defining five classes of compliance on a scale from 0

to 4. The compliance process determines also the levels of confidentiality, integrity and availability (C-I-A) for each compliance class. In order to apply the required level of security and to maintain the level of trust for IoT systems, each requirement includes an ID, the compliance class, and the applicability category.

A recent review of the literature on IoT security and trust is conducted in [13]. The authors evaluate relevant existing solutions related to IoT security, privacy and trust. The existing work is analyzed based on topics such as authentication, access control, privacy, policy enforcement, trust, confidentiality and secure middleware. In [13] the main research challenges in IoT security, the most relevant solutions and the questions that arise for future research related to security and trust in IoT are presented. The overview shows that available solutions involve different technologies and standards, but a unified vision for security requirements is still missing.

Julisch [14] introduces the compliance problem by focusing on security requirements. In this paper, security is the state of being safe from threats and the security compliance is the evidence (assurance) that a given set of requirements is met, which can be security requirements or other security mechanisms imposed by standards. He underlines that, in order to narrow the gap between academia and industry, it is necessary to focus more research on the question of security compliance to help organizations to comply with best practices guidelines and standards.

For safety the basic safety standard is IEC 61508 [15] "Functional Safety of Electrical / Electronic / Programmable Electronic Safety-Related System". This standard is developed as a domain independent standard which can be adapted for all domains without a domain-specific standard. The process industry, based on IEC 61508, IEC 61511 [16] developed the "Functional safety - Safety instrumented systems for the process industry sector". Such a domain specific instantiation is mainly developed to consider peculiarities from a specific domain. For the industrial sectors both standards are relevant. Compliance to both standards was mostly evaluated during the design time [17], [18]. It was assumed that safety-critical systems are stable and compliance can be completely checked during design time. Due to Industry 4.0 and the goal of increased production flexibility there is an increasing need to check compliance also during run-time. Existing approaches utilize mainly concepts from contract-based development [19]. This assumes that the basic blocks of a safety-critical system will stay the same and are assessed during design-time. Contracts are then used to check the compliance of different system compositions based on pre-checked blocks [20]. While such approaches make it possible to shift a part of the safety assessment towards run-time, there is still the challenge that with flexible and configurable systems components need to be checked if they are still compliant with their respective safety standard.

Standards such as ISO 9001:2015, ISO/IEC/IEEE 15288, ISO 18404, ISO/IEC 29169, ISO IEC TS 33052, etc., are some of the standards considering business process management.

ISO 9001 [21] is an international standard that specifies requirements for a QMS and is used by organizations to

demonstrate the ability to consistently provide products and services that meet customer and regulatory requirements. Additionally, a process approach is suggested including the PDCA-Cycle and risk based thinking. The PDCA-cycle helps organizations to define processes, execute them, measure the outcome and analyse the results to set actions for further improvement.

ISO 18404 [22] provides tools for organizations to improve the capability of their business processes. This increase in performance and decrease in process variation leads to defect reduction and improvement in profits, employee morale, and quality of products or services. It focuses on clarifying competencies required for personnel and organizations in SixSigma, Lean and "Lean&SixSigma". Moreover, this standard constitutes general requirements from personnel (e.g. Black Belt) or organizations due to the numerous existing combinations of Lean and Six Sigma. Therefore, competencies for individual skill levels are described in details, such as Black Belt, Green Belt, Lean practitioners and their organizations. However, a specification and design for Six Sigma is excluded.

ISO/IEC TS 33052 [23] is used to describe the structure of a process reference model to support information security management. The PRM includes processes, derived from ISO/IEC 27001, which can already exist in the context of a management system of a service provider. This standard is used to deploy and control the execution and performance of operational and organizational processes by supporting the efficient, timely and quality day-to-day operations.

Although the produced guidelines and scientific work help users to address industrial requirements, more standard compliance measurements are needed.

There are various frameworks and platforms supporting monitoring of CPS and IoT. Several approaches and prototypes are presente, both in literature [24], [25], [26] and in the scope of research projects such as Cumulus, NGcert, SECCRIT etc. However, there is no generally accepted method that allows mapping the security, safety and organizational compliance. In this context, the proposed monitoring and standard compliance verification framework advances the state of the art by considering security, safety and organizational related aspects without compromising the underlying infrastructure.

III. MONITORING AND STANDARD COMPLIANCE VERIFICATION FRAMEWORK

Standard compliance is the adherence to a given set of security and safety requirements, represented by measurable metrics, on the use and configuration of systems or any other security, safety or legal mechanism. These measurable metrics should be imposed by standardized bodies to make each system, device or application comply with the standards.

To assure that the system is operating in a secure and standard compliant manner a monitoring module is needed, which is responsible for gathering all the required measurements. Thus, in this paper we present a monitoring and standard compliance verification framework, which has been designed to support different use cases and viewpoints that should be considered and researched in Industry 4.0.

The monitoring and standard compliance verification framework, illustrated in Figure 2, makes it possible to gather security, safety and organizational evidence from the target system in a structured way (e.g. MSI, MSFI, MOI). The architecture of the framework has a pluggable and expendable architecture allowing easy adaptation to constantly analyze and monitor the status of the system or components of the system. It is possible to monitor a large number of measurable metrics (as shown in Section IV B-D) for different CPPS components by aggregating, scheduling, storing, retrieving and analyzing the monitoring data to provide standard compliance verification.
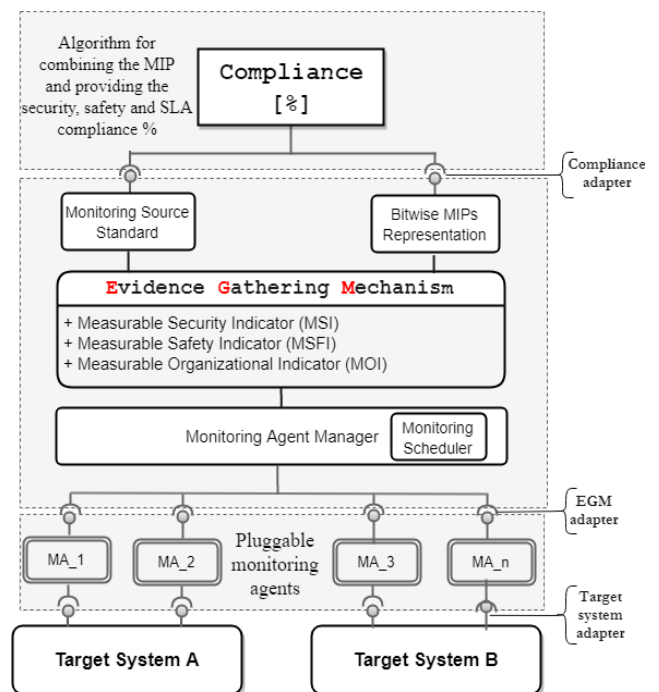
Fig. 2: Monitoring and standard compliance verification framework used to measure, aggregate, schedule, store, retrieve and analyze the monitoring data to provide standard compliance

The monitoring and standard compliance verification framework is composed of four main modules, including Monitoring Agents, Evidence Gathering Mechanism, Compliance and the Target System. The TS represents a system or component of a system that will be monitored by monitoring tool plugins or customized scripts.

A. Monitoring components

1) Monitoring Agents (MA): The MA module is used to gather data from the TS and should allow the integration of different pluggable monitoring agents (MA_i) from different monitoring tool plugins (e.g., Nagios plugin [27], Ceilometer plugin [28], Zabbix plugin [29], etc.) and customized scripts.

2) Evidence Gathering Mechanism (EGM): The EGM module is designed to acquire, store and analyze security, safety and legal related evidence [9]. It manages the incoming data from the monitoring agents and decides when/what data

to send to the Compliance module by using a writing buffer. It makes the mapping of the measurable metrics possible and their values with the standards to provide the necessary information for the compliance module. The EGM module consists of:

a) Monitoring Agent Manager: The Monitoring Agent Manager is the only contact point between the EGM module and the MA_i. It is responsible for organizing the MA_i based on the configurations and uses a Monitoring Scheduler to provide the run-time of each plugin in the corresponding component.

b) Monitoring Source Standard: The Monitoring Source Standard provides for each defined measurable metric the source from which standard/best practice guideline the metric is extracted. By mapping the MIPs to the specific standard, the compliance module can cross-check if the specific metric has been monitored in the target system.

c) Bitwise MIPs Representation: The Bitwise MIPs Representation module represents every MIP by a number, which can be converted to binary and operated on by a computer.

The EGM module gathers the monitoring data in a column structure based on the MIPs (MSI, MSFI, and MOI). For each MIP the following information is provided: (i) metric ID, (ii) value of the metric, which can be a binary value, true/false value, etc and (iii) the source based on the standard/best practice guideline from where the metric is extracted. A representative set of the information provided by the EGM module is shown in Figure 3. The information provided by

MIPs	Value TS_A	Value TS_B	S1	S2	S3
MSI-1,1	1	1	⊘		
MSI-2,1	0	1		⊘	
MSFI-1,1	1	1		⊘	
MSFI-2,1	0	1			⊘
MOI-1,1	0	1			⊘
MOI-2,1	1	1	⊘	⊘	

EGM
+ MSI
+ MSFI
+ MOI

MIP – Measurable Indicator Point
MSI – Measurable Security Indicator
MSFI – Measurable Safety Indicator
MOI – Measurable Organizational Indicator
TS_n – Target System n
Sn – Standard n

Fig. 3: A representative set of the information provided by the EGM module

the EGM module is used as input for the Compliance module for further analysis.

B. Standard Compliance Verification

In Industry 4.0 large monolithic organisations are moving towards multi-stakeholder cooperations, where cooperation is fostered by market requirements such as sustainable, flexible, efficient, competitive and customized production [1]. Despite the benefits, this brings new challenges in terms of security, safety and organizational related issues. Thus, it is of utmost importance to assure that independent entities inter-operate with each-other in a secure and standard compliant manner, without compromising the underlying infrastructure.

In this paper we present an initial approach for standard compliance verification. The Compliance module is responsible for assuring that the system is operating in a secure and standard compliant manner driven by the input provided by the EGM module. The compliance depends on a set of MIPs, which are extracted from a number of widely used standards

and best practice guidelines to address the target system specific requirements. Thus, in order to measure standard compliance one has to consider a set of MIPs and a set of standards, since a dynamic mix of new technologies, regulations and interactions of different organizations are involved. However, it is not easy to extract metrics for security, safety and organizational related issues [30], [31], since the indirect relationship and the dependability between them have to be considered as well. In the following section we present a representative set of MIPs for a specific target system and show how such a metric can be described.
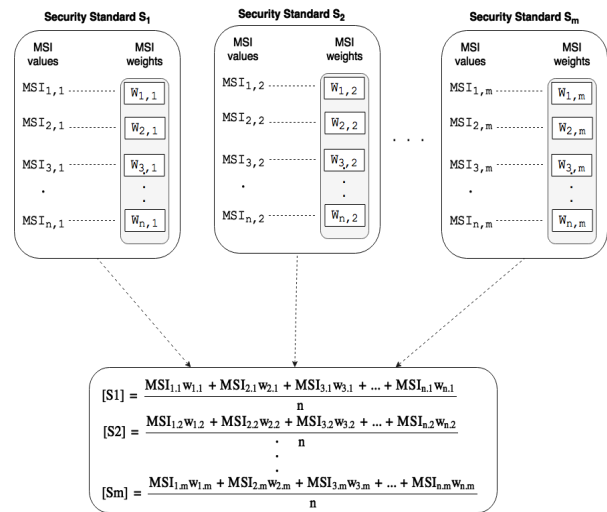
Fig. 4: Security standard compliance verification

To show the standard compliance verification approach, we have considered only MSIs. However, the same approach applies also for MSFIs and MOIs. Each MSI extracted from a standard is monitored using monitoring agents in the corresponding component of the target system. The monitoring data are than gathered by the EGM module, which is responsible for making them readable for the Compliance module. So, the EGM sends to the Compliance module for each MSI the source from which the metric is extracted and a binary value 1 or 0 that indicates if the metric is fulfilled or not. Depending on the specific target system requirements the Compliance module assigns to each MSI a weight value to indicate the importance in the range $[0, 1]$.

After gathering all the required evidence from the EGM module, the Compliance module first verifies the compliance $[\%]$ for a single standard as the ratio between the sum of each MSI measured value multiplied by its weight value and the total number of metrics per standard as shown in equation 1. It verifies the total compliance $[\%]$ as the ratio between the sum of each standard compliance and the total number of selected standards, as shown in equation 2.

$$MSI\_compliance_{(j)}[\%] = \frac{\sum_{i=1}^{n} MSI_{i,j}\omega_{i,j}}{n}100\% \quad (1)$$

$$MSI\_compliance[\%] = \frac{\sum_{j=1}^{m} compliance_{(j)}}{m}100\% \quad (2)$$

where:

n	total number of metrics per standard
m	total number of standards
$MSI_{i,j}$	measured value of "i" security metric from "j" standard
$\omega_{i,j}$	weight value of "i" security metric from the "j" standard

Introduction of Compliance Levels

In order to apply an appropriate level of security and safety standard compliance to a component or system depending on the requirements, four compliance levels [0-3] are arbitrarily defined:

Compliance Level	MIPs		
	MSI	MSFI	MOI
Level 0	basic	basic	basic
Level 1	basic	basic	high
	basic	high	basic
	high	basic	basic
Level 2	basic	high	high
	high	basic	high
	high	high	basic
Level 3	high	high	high

TABLE I: Arbitrary compliance levels based on MIPs

The compliance levels, shown in table I, depend on the standard compliance verification for MSIs, MSFIs and MOIs, whereas *basic* is defined as the compliance in the range $[0\%, 50\%]$ and *high* is defined as the compliance in the range $[50\%, 100\%]$.

- **Compliance Level 0** indicates that the compliance of all three MIP groups is basic
- **Compliance Level 1** indicates that at least the compliance of one MIP group is high
- **Compliance Level 2** indicates that at least the compliance of two MIP groups is high
- **Compliance Level 3** indicates that the compliance of all three MIP groups is high

IV. A REPRESENTATIVE SET OF MIPs FOR THE MONITORING AND STANDARD COMPLIANCE VERIFICATION FRAMEWORK

This section provides illustrative metrics that should be considered in an Industry 4.0 application scenario with the goal to address the requirements of access control systems for the production line. In that regard, the IEC 62443-3-3 (Industrial communication networks - Network and system security - System security requirements and security levels) [32] provides technical control system fundamentals requirements for industrial automation and control system capability, where

we have selected three MSIs to show how each MSI is documented and monitored. The IEC 61508-3 (Functional Safety of Electrical/Electronic/Programmable Electronic Safety-related Systems) [33], is the basic safety standard and intended as an umbrella standard by various industries to provide their own standards and guidelines, from which three MSFIs as representative examples are selected.

In contrast with security and safety standards, business management standards do not provide explicit technical measures. However, some standards provide a methodology on how to implement and execute assessments. ISO/IEC TS 33052 (Information Technology – Process reference model (PRM) for information security management) [23] provides process descriptions which relate to process purpose, process context, outcomes and traceable requirements. The traceable requirements give an indication which tasks and actives are relevant for certain processes and they are presented as actions that refer explicitly to ISO/IEC 27001 and relate to common tasks. It provides a process assessment model (PAM) from where we have selected three MOIs as representative examples.

A. Use Case

In order to extract MIPs, which can be used to evaluate the approach described in the previous section, we consider the use case depicted in Figure 5, from an ongoing research project addressing a secure end-to-end communication in CPPS [34].
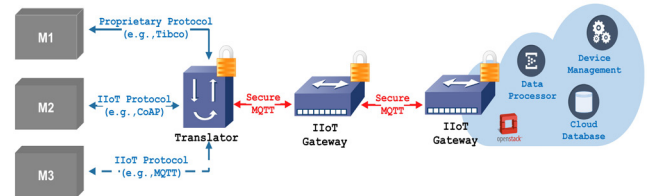
Fig. 5: CPPS end-to-end communication use case

To provide device management as a service, data is transmitted between devices (M1, M2, and M3), processed and sent to a private cloud for further processing and analysis. The communication protocol used between the edge devices, the IIoT components, and the cloud backend is the MQTT protocol, designed to be lightweight, flexible and simple to implement. In the production environment, the new industrial devices are already able to communicate using state of the art IIoT protocols, such as MQTT. However, this is not the case if a legacy device wants to establish a connection with the IIoT gateway. In this case, a translator system is needed to translate the device protocol into MQTT [35]. In such scenario, with different decentralized CPPS components, condition reports to the overall system are important. In order to observe the system behavior, several components can be monitored, including industrial devices, IIoT gateways and cloud services.

Once the requirements have been identified and the standards/best practice guidelines have been examined to see whether or not they address the specific requirement, the next step is to identify measurable indicator points. Based on this

use case and the access control requirements, we define a set of representative MSIs, MSFIs and MOIs extracted from security, safety and process management standards. For each MIP is provided: (i) an ID, (ii) the source and the definition based on the standards and best practice guidelines, (iii) possible monitoring solutions and (iv) a monitoring value are provided.

B. MSIs: Measurable Security Indicators

- **MSI-1.1**: Secure identification and authentication
  - *Source*: IEC 62443-3-3
  - *Definition*: The client and the server identify each other and assure their identities via secure log-on
  - *Monitoring Plugin*: Can be monitored with Nagios monitoring agent, which checks the configuration of the used protocol (or indeed any other client/server authentication method) to make sure that it uses a secure communication protocol.
  - *Monitoring Value*: True/False

- **MSI-2.1** : Strength of password-based authentication
  - *Source*: IEC 62443-3-3
  - *Definition*: The system shall be configurable by providing a degree of complexity such as minimum length, variety of characters and password rotation.
  - *Monitoring Plugin*: Can be implemented by performing checks on the PAM (Pluggable Authentication Module) to verify if a minimum length or complexity of passwords and password rotation is enabled.
  - *Monitoring Value*: True/False

- **MSI-3.1** : Concurrent session control
  - *Source*: IEC 62443-3-3
  - *Definition*: The system shall restrict the maximum number of concurrent sessions per system account or system type.
  - *Monitoring Plugin*: A script can be developed which checks *sshd_config* or *pam_limits* configuration.
  - *Monitoring Value*: True/False

C. MSFIs: Measurable Safety Indicators

- **MSFI-1.2** : Time-triggered architecture
  - *Source*: IEC 61508-3, Table A-2, Group 13
  - *Definition*: : Ensure that the system complies with the safety timing requirements
  - *Monitoring Plugin*: Can be checked via Nagios, send test packet to system and check if response time is inside allowed parameters. If Nagios is running on a separate system this achieves medium diagnostic coverage (based on IEC 61508-2). If the systems sends regular information about logical status high diagnostic coverage is achievable
  - *Monitoring Value*: Response time

- **MSFI-2.2** : Techniques and measures for error detection
  - *Source*: IEC 61508-3, Table A-18
  - *Definition*: Ensure that system modifications are protected against erroneous
  - *Monitoring Plugin*: Check that system modifications require a password

  - *Monitoring Value*: True/False
- **MSFI-3.2** : Control systematic operational failures
  - *Source*: IEC 61508-7
  - *Definition*: Ensure that all inputs via a safety-related system are echoed to the operator before being sent to the system. This should also consider abnormal human actions, e.g. speed of interaction
  - *Monitoring Plugin*: Can be monitored by a network module that checks the system behaviour
  - *Monitoring Value*: True/False

D. MOIs: Measurable Organizational Indicators

- **MOI-1.1**: Event Logging
  - *Source*: ISO/IEC TS 33052
  - *Definition*: The system shall forward event log information to a central security information and event management system
  - *Monitoring Plugin*: Can be monitored with a Nagios plugin checking syslog/event log configuration
  - *Monitoring Value*: True/False

- **MOI-2.1**: Restrictions on software installations
  - *Source*: ISO/IEC TS 33052
  - *Definition*: The system shall restrict software installation to approved products
  - *Monitoring Plugin*: Can be monitored with a custom Nagios plugin checking e.g. paket management (e.g. Linux) or other software management configuration
  - *Monitoring Value*: True/False

- **MOI-3.1** : Access to networks and network services
  - *Source*: ISO/IEC TS 33052
  - *Definition*: The system configuration must support access to mandatory networks and network services
  - *Monitoring Plugin*: : Can be monitored with a custom Nagios plugin checking network device and network service configuration (e.g., DNS, DHCP, Gateway, Netmask, NPS, 802.1x Cert etc.)
  - *Monitoring Value*: True/False

As illustrated in Figure 2, the monitoring agents defined for each MIP, will gather data from the target system (in this case the end-to-end communication use case) and will provide for the EGM the necessary information if the metric is fulfilled or not. The Compliance module maps the monitored metric with the corresponding standard and calculate the compliance [%] based on equation 2. The result will then be used to define the compliance level [0-3] of the system as shown in table I.

V. CONCLUSIONS

In this paper we have presented a monitoring and standard compliance verification framework for Industry 4.0 application scenarios with the aim to provide an automated standard compliance. The standard compliance is defined based on a set of MIPs extracted from existing standards and best practice guidelines. The MIPs are monitored in the target system using monitoring agents and the monitoring data are then used by the EGM to make them readable for the compliance module.

To give an example of how such an approach will work, we have extracted a representative set of MSIs, MSFIs and MOIs motivated by the requirements provided from an ongoing research project use case. We have provided the information on how the MSIs, MSFIs and MOIs can be measured by either existing monitoring tool plugins or customized scripts.

As part of our future work, we will implement and evaluate the monitoring and standard compliance verification framework and we will further analyze other security and safety standards that are relevant to the industrial environment.

Part of this analysis is also to determine other safety metrics that can be measured by the MSCV. Hardware based safety metrics like mean time between failures (MTBF) are difficult to monitor, and normally static. There are approaches to utilize contracts during run time to conduct safety assessment for systems which are composed during run time [36]. Other metrics which are oriented on hardware properties and need to be monitored, for example proof testing interval, can be monitored by setting a flag with time when the proof test is performed. We will also investigate how the information provided by the monitoring and standard compliance verification framework can be integrated in the Arrowhead Framework e.g., Arrowed Test Tool (ATT) [37], which enables the possibility to test producer and consumer interfaces for the Arrowhead services.

APPENDIX A
ACRONYMS

Acronym	Reference Abbreviation
ATT	Arrowhead Test Tool
CPPS	Cyber Physical Production System
CC	Common Criteria
CSCG	Cyber Security Coordination Group
CPS	Cyber Physical Systems
Cumulus	Certification Infrastructure for Multi-Layer Cloud Services
DNS	Domain Name System
DHCP	Dynamic Host Configuration Protocol
EGM	Evidence Gathering Mechanism
ENISA	European Network and Information Security
ETSI	European Telecommunications Standards Institute
EAL	Evaluation Assurance Levels
IoT	Internet of Things
ISO	International Organization for Standardization
IEC	International Electrotechnical Commision
ISMS	Information Security Management System
IIoT	Industrial Internet of Things
MIP	Measurable Indicator Point
MSI	Measurable Security Indicator
MSFI	Measurable Safety Indicator
MOI	Measurable Organizational Indicator
MA	Monitoring Agent
MA_i	Nr. of Monitoring Agents
MQTT	Message Queuing Telemetry Transport
NGcert	Next Generation Certification
PDCA	Plan-Do-Check-Act
PRMM	Process Reference Model
PRM	Process Reference Model
PAM	Pluggable Authentication Module
PP	Protection Profile
QMS	Quality Management System
SoS	System of Systems
SOA	Service Oriented Architecture
ST	Security Target
SECCRIT	Secure Cloud Computing for Critical Infrastructure IT
TOE	Target of Evaluation
TS	Target System

REFERENCES

[1] J. Delsing, "Iot automation: Arrowhead framework," 2017.
[2] A. W. Colombo, T. Bangemann, and S. Karnouskos, "Imc-aesop outcomes: Paving the way to collaborative manufacturing systems," in *12th IEEE International Conference on Industrial Informatics*, 2014.
[3] C. Schmittner, Z. Ma, and E. Schoitsch, "Combined safety and security development lifecylce," in *Industrial Informatics (INDIN), 2015 IEEE 13th International Conference on*. IEEE, 2015, pp. 1408–1415.
[4] M. Gaitanides, R. Scholz, and A. Vrohlings, "Prozeßmanagement-grundlagen und zielsetzungen," *Gaitanides, M., Scholz, R., Vrohlings, A., Raster, M.(Hrsg.)*, pp. 1–20, 1994.
[5] E. Jonsson, "Towards an integrated conceptual model of security and dependability," in *Availability, Reliability and Security, 2006. ARES 2006. The First International Conference on*. IEEE, 2006, pp. 8–pp.
[6] D. Basin, F. Klaedtke, and S. Müller, "Monitoring security policies with metric first-order temporal logic," in *Proceedings of the 15th ACM symposium on Access control models and technologies*. ACM, 2010.
[7] L. Hayden, *IT Security Metrics: A Practical Framework for Measuring Security & Protecting Data*. McGraw-Hill Education Group, 2010.
[8] A. Bicaku, C. Schmittner, M. Tauber, and J. Delsing, "Monitoring industry 4.0 applications for security and safety standard compliance," in *2018 IEEE Industrial Cyber-Physical Systems (ICPS)*. IEEE, 2018, pp. 749–754.
[9] A. Bicaku, S. Balaban, M. G. Tauber, A. Hudic, A. Mauthe, and D. Hutchison, "Harmonized monitoring for high assurance clouds," in *Cloud Engineering Workshop (IC2EW), 2016 IEEE International Conference on*. IEEE, 2016, pp. 118–123.
[10] G. Disterer, "Iso/iec 27000, 27001 and 27002 for information security management," *Journal of Information Security*, vol. 4, p. 92, 2013.
[11] C. C. Consortium *et al.*, "Common criteria (aka cc) for information technology security evaluation (iso/iec 15408), 2013."
[12] R. Atoui, J. Bennett, S. Cook, P. Galwas, P. Gupta, J. Haine, H. Trevor, C. Hills, R. Marshall, M. John, K. Munro, I. Philips, D. Purves, C. Robbins, D. Rogers, C. Shaw, R. Shepherd, and C. Shire, "Iot security compliance framework," *IoT Security Foundation*, 2016.
[13] S. Sicari, A. Rizzardi, L. A. Grieco, and A. Coen-Porisini, "Security, privacy and trust in internet of things: The road ahead," *Computer Networks*, vol. 76, pp. 146–164, 2015.
[14] K. Julisch, "Security compliance: the next frontier in security research," in *Proceedings of the 2008 workshop on New security paradigms*. ACM, 2009, pp. 71–74.
[15] D. J. Smith and K. G. Simpson, *Safety Critical Systems Handbook: A Straight forward Guide to Functional Safety, IEC 61508 (2010 EDITION) and Related Standards, Including Process IEC 61511 and Machinery IEC 62061 and ISO 13849*. Elsevier, 2010.
[16] K. Bond, "Iec 61511-functional safety: Safety instrumented systems for the process industry sector," in *Annual Symposium on Instrumentation for the Process Industries*, vol. 57, 2002, pp. 33–40.
[17] M. Lloyd and P. Reeve, "Iec 61508 and iec 61511 assessments-some lessons learned," 2009.
[18] R. K. Panesar-Walawege, M. Sabetzadeh, L. Briand, and T. Coq, "Characterizing the chain of evidence for software safety cases: A conceptual model based on the iec 61508 standard," in *Software Testing, Verification and Validation (ICST), 2010 Third International Conference on*. IEEE, 2010, pp. 335–344.
[19] A. Sangiovanni-Vincentelli, W. Damm, and R. Passerone, "Taming dr. frankenstein: Contract-based design for cyber-physical systems," *European journal of control*, vol. 18, no. 3, pp. 217–238, 2012.
[20] D. Schneider and M. Trapp, "Conditional safety certificates in open systems," in *Proceedings of the 1st workshop on critical automotive applications: robustness & safety*. ACM, 2010, pp. 57–60.
[21] E. ISO, "9001: 2015 quality managem5ent systems," *Requirements (ISO 9001: 2015), European Committee for Standardization, Brussels*, 2015.
[22] "Iso 18404:2015 - quantitative methods in process improvement – six sigma – competencies for key personnel and their organizations in relation to six sigma and lean implementation," https://www.iso.org/standard/62405.html.

[23] "Iso/iec ts 33052:2016 - information technology – process reference model (prm) for information security management," https://www.iso.org/standard/55142.html.

[24] M. T. Lazarescu, "Design of a wsn platform for long-term environmental monitoring for iot applications," *IEEE Journal on Emerging and Selected Topics in Circuits and Systems*, vol. 3, no. 1, pp. 45–54, 2013.

[25] Y. Liu, Y. Yang, X. Lv, and L. Wang, "A self-learning sensor fault detection framework for industry monitoring iot," *Mathematical problems in engineering*, vol. 2013, 2013.

[26] S. Tennina, M. Bouroche, P. Braga, R. Gomes, M. Alves, F. Mirza, V. Ciriello, G. Carrozza, P. Oliveira, and V. Cahill, "Emmon: A wsn system architecture for large scale and dense real-time embedded monitoring," in *Embedded and Ubiquitous Computing (EUC), 2011 IFIP 9th International Conference on.* IEEE, 2011, pp. 150–157.

[27] N. Enterprises, "Nagios," https://exchange.nagios.org/directory, 2017.

[28] OpenStack-Wiki, "Ceilometer," 2017.

[29] R. Olups, *Zabbix 1.8 network monitoring.* Packt Publishing Ltd, 2010.

[30] S. Pfleeger and R. Cunningham, "Why measuring security is hard," *IEEE Security & Privacy*, vol. 8, no. 4, pp. 46–54, 2010.

[31] W. Jansen, "Research directions in security metrics," *Journal of Information System Security*, vol. 7, no. 1, pp. 3–22, 2011.

[32] T. Phinney, "Iec 62443: Industrial network and system security," *Last accessed July*, vol. 29, 2013.

[33] I. IEC, "61508 functional safety of electrical/electronic/programmable electronic safety-related systems," *International electrotechnical commission*, 1998.

[34] S. Maksuti, A. Bicaku, M. Tauber, S. Palkovits-Rauter, S. Haas, and J. Delsing, "Towards flexible and secure end-to-endcommunication in industry 4.0," in *IEEE 15th International Conference of Industrial Informatics INDIN'2017*, 2017.

[35] A. Bicaku, S. Maksuti, S. Palkovits-Rauter, M. Tauber, R. Matischek, C. Schmittner, G. Mantas, M. Thron, and J. Delsing, "Towards trustworthy end-to-end communication in industry 4.0," in *IEEE 15TH International Conference of Industrial Informatics INDIN'2017*, 2017.

[36] D. Schneider and M. Trapp, "Conditional safety certification of open adaptive systems," *ACM Transactions on Autonomous and Adaptive Systems (TAAS)*, vol. 8, no. 2, p. 8, 2013.

[37] F. Blomstedt, "Arrowhead test tool," https://forge.soa4d.org/plugins/scmgit/cgi-bin/gitweb.cgi?p=arrowhead-f/arrowhead-f.git;a=blob;f=5_Compliance/1_Testtool/Arrowhead_SysD_Compliance+Test+Tool.pdf;h=f36e1b1cf63c5a05c79307a10d506739f15d9f4c;hb=HEAD.

Ani Bicaku is a PhD student at Luleå University of Technology and works as a researcher at the University of Applied Sciences Burgenland in the research field "Cloud and Cyber Physical Systems Security". Recently, he was working at the Austrian Institute of Technology in the AIT's ICT-Security Program and was responsible for evaluating data security, data privacy and high assurance in cloud computing. Also part of his duty was to build an OpenStack Cloud System testbed used for monitoring high assurance of critical infrastructure cloud services. He received the Dipl -Ing. degree in Communication Engineering from the Carinthia University of Applied Sciences, Klagenfurt - Austria and his B.Sc. degree in Telecommunication Engineering from the Polytechnic University of Tirana, Tirana - Albania.

Christoph Schmittner received his M.Sc. in System and Software Engineering at the University of Applied Sciences Regensburg in 2013. His main research area is safety and security co-engineering.
He works on safety, security analysis and coanalysis methods, connected and safety critical / fault & intrusion tolerant system architectures, functional safety and cybersecurity standards and interdepen-dence of safety and security in critical systems.
He is member of the Austrian mirror committees for ISO/TC 22 Road vehicles and IEC TC 56 Dependability and designated Austrian expert in corresponding international standardization groups (IEC 61508, IEC 62443 ISO 26262 and ISO/SAE 21434), member of TC65/WG20 "Industrial-process measurement, control and automation – Framework to bridge the requirements for safety and security", TC65/AHG2 "Reliability of Automation Devices and Systems" and TC65/AHG3 "Smart Manufacturing Framework and System Architecture" and coordinating the Austrian contribution to the development of ISO/SAE 21434 "road vehicles – cybersecurity engineering".

Patrick Rottmann recently finished his Master's thesis on "Monitoring and Standards Compliant Measurements in Industry 4.0" at the university of Applied Sciences Burgenland, in the Master program Cloud Computing Engineering. Prior to that he completed his BSc at the University of Applied Sciences Burgenland in the BSc Program IT Infrastructure Management. In parallel to his studies he was working as IT Engineer at the Umweltbundesamt GmbH where he still leads and coordinates IT Infrastructure projects.

Markus Tauber works as FH-Professor for the University of Applied Sciences Burgenland, where he holds the position: director of the MSc program "Cloud Computing Engineering" and leads the research center "Cloud and Cyber-Physical Systems Security". Between 2012 until 2015 he coordinated the research topic "High Assurance Cloud" at the Austrian Institute of Technology (AIT) part of AIT's ICT-Security Program. Amongst other activities he was the coordinator of the FP7 Project "Secure Cloud computing for CRitical infrastructure IT" - (www.seccrit.eu) and involved in the ARTEMIS Project Arrowhead. From 2004 to 2012 he was working at the University of St Andrews (UK) where he worked as researcher on various topics in the area networks and distributed systems and was awarded a PhD in Computer Science for which he was working on "Autonomic Management in Distributed Storage Systems".

Prof. Jerker Delsing received the M.Sc. in Engineering Physics at Lund Institute of Technology, Sweden 1982. In 1988 he received the PhD. degree in Electrical Measurement at the Lund University. During 1985 - 1988 he worked part time at Alfa-Laval - SattControl (now ABB) with development of sensors and measurement technology. In 1994 he was promoted to associate professor in Heat and Power Engineering at Lund University. Early 1995 he was appointed full professor in Industrial Electronics at Lulea University of Technology where he currently is the scientific head of EISLAB, http://www.ltu.se/eislab. His present research profile can be entitled IoT and SoS Automation, with applications to automation in large and complex industry and society systems.
Prof. Delsing and his EISLAB group has been a partner of several large EU projects in the field, e.g. Socrades, IMC-AESOP, Arrowhead, FAR-EDGE, Productive4.0 and Arrowhead Tools. Delsing is a board member of ARTEMIS, ProcessIT.EU and ProcessIT Innovations.

Inter-destination multimedia synchronization:
A contemporary survey

Dimitris Kanellopoulos

Abstract — **The advent of social networking applications, media streaming technologies, and synchronous communications has created an evolution towards dynamic shared media experiences. In this new model, geographically distributed groups of users can be immersed in a common virtual networked environment in which they can interact and collaborate in real-time within the context of simultaneous media content consumption. In this environment, intra-stream and inter-stream synchronization techniques are used inside the consumers' playout devices, while synchronization of media streams across multiple separated locations is required. This synchronization is known as multipoint, group or Inter-Destination Multimedia Synchronization (IDMS) and is needed in many applications such as social TV and synchronous e-learning. This survey paper discusses intra- and inter-stream synchronization issues, but it mainly focuses on the most well-known IDMS techniques that can be used in emerging distributed multimedia applications. In addition, it provides some research directions for future work.**

Index Terms — **Multimedia synchronization, IDMS, multipoint synchronization, RTP/RTCP**

Abbreviations

AMP	Adaptive media playout
DCS	Distributed control scheme
ETSI	European Telecommunications Standards Institute for Advanced Networking
IDMS	Inter-destination multimedia synchronization
IETF	Internet Engineering Task Force
M/S	Master/slave receiver scheme
MU	Media unit
QoE	Quality of experience
QoS	Quality of service
RTP	Real-Time Transport Protocol
RTCP	RTP Control Protocol
SMS	Synchronization maestro scheme
TISPAN	Telecoms & Internet Converged Services and Protocols
VTR	Virtual-time rendering synchronization algorithm

I. INTRODUCTION

NOWADAYS, novel media consumption paradigms such as social TV and synchronous e-learning are enabling users to consume multiple media streams at multiple devices together and having dynamic shared media experiences [1]. In order to provide an enjoyable dynamic shared media experience, various technical challenges must be faced. Examples are synchronization, Quality of Service (QoS), Quality of Experience (QoE), scalability, user mobility, intelligent media adaptation and delivery, social networking integration, privacy concerns, and user preferences management [2]. This survey focuses on the synchronization of media streams across multiple separated locations/consumers. This synchronization is known as *multipoint, group* or *Inter-Destination Multimedia Synchronization* (IDMS) and is required in many use cases such as social TV, synchronous e-learning, networked quiz shows, networked real-time multiplayer games, multimedia multi-point to multi-point communications, distributed tele-orchestra, multi-party multimedia conferencing, presence-based games, conferencing sound reinforcement systems, networked stereo loudspeakers, game-show participation, shared service control, networked video wall, and synchronous groupware [3]. These use cases require media synchronization as there are significant delay differences between the various delivery routes for multimedia services (e.g., media streaming). Meanwhile, broadcasters have started using proprietary solutions for over-the-top media synchronization such as media fingerprinting or media watermarking technologies. Given the commercial interest in media synchronization and the disadvantages of proprietary technologies, consumer-equipment manufacturers, broadcasters, and telecom and cable operators have started developing new standards for multimedia synchronization.

An important feature of multimedia applications is the integration of multiple media streams that have to be presented in a synchronized fashion [4]. *Multimedia synchronization* is the preservation of the temporal constraints within and among multimedia data streams at the time of playout. Temporal relations define the temporal dependencies between media objects [5]. An example of a temporal relation is the relation between a video and an audio object which are recorded during a concert. If these objects are presented, the temporal relation during the presentations of the two media objects must correspond to the temporal relation at the time of recording. *Discrete* media like text, graphics, and images are time-independent media objects, while the semantic of their content does not depend upon a presentation to the time domain. A discrete media object is frequently presented using one presentation unit. Conversely, a time-dependent media object

is presented as a *continuous* media stream in which the presentation durations of all *Media Units* (MUs) are equal [4]. For example, a video consists of a number of ordered frames, where each of these frames has a fixed presentation duration. Most of the components of a multimedia system support and address temporal synchronization. These components may include the operating system, communication subsystem, databases, documents, and even applications. In distributed multimedia systems, networks introduce random delays in the delivery of multimedia information. Actually, there are some sources of *asynchrony* that can disrupt synchronization [3],[6]:

- *Network Jitter*. This is an inherent characteristic of best-effort networks like the Internet.
- *Local Clock Drift* arises when clocks at users run at different rates. Without a synchronization mechanism, the asynchrony will gradually become more and more serious.
- *Different Initial Collection Times*. Let us consider two media sources, one providing voice and the other video. If these sources start to collect their MUs at different times, the playback of the MUs of voice and video at the receiver loses semantic meaning.
- *Different Initial Playback Times*. If the initial playback times are different for each user, then asynchrony will arise.
- *Network topology changes* and *unpredictable delays*. In mobile ad hoc networks (MANETs), the preservation of temporal dependencies among the exchanged real-time data is mainly affected: (1) by the asynchronous transmissions; (2) by constant topology changes; and (3) by unpredictable delays.
- *The encoding used*. If media streams are encoded differently, the decoding times at receiver may vary considerably.

Delay is a simple constraint when users are consuming non-time sensitive content from content-on-demand networks. However, delay and jitter (variation of end-to-end delay) become serious constraints when an interaction between the user and the media content (or interaction between different users) is needed. In those applications, delay and jitter could be harmful to the QoE and may prevent the inclusion of higher forms of interactivity in various group-shared services. Consequently, many multimedia synchronization techniques have been proposed to ensure synchronous sharing of content among users temporarily collocated, either being spatially distributed or even sharing a physical space.

This paper presents the basic control schemes for IDMS and discusses IDMS solutions and IDMS standardization efforts for emerging distributed multimedia applications. The structure of the paper is organized as follows. Section II discusses intra-stream and inter-stream synchronization issues. Section III reviews well-known schemes for IDMS, while Section IV presents standardization efforts on IDMS as well as effective IDMS solutions. Finally, Section V concludes the paper and gives directions for future work.

II. BACKGROUND

A. Intra-stream Synchronization

Intra-stream (also known as *intra-media* or *serial*) synchronization is the reconstruction of temporal relations between the MUs of the same stream. An example is the reconstruction of the temporal relations between the single frames of a video stream. The spacing between subsequent frames is dictated by the frame production rate. For instance, for a video with a rate of 40 frames per second, each of these frames must be displayed for 25 ms. Jitter may destroy the temporal relationships between periodically transmitted MUs that constitute a real-time stream, thus hindering the comprehension of the stream. *Playout adaptation algorithms* undertake the labor of the temporal reconstruction of the stream. This reconstruction is referred to as the '*restoration of its intra-stream synchronization quality*' [7]. *Adaptive Media Playout* (AMP) improves the media synchronization quality of streaming applications by regulating the playout time interval among MUs at a receiver. To mitigate the effect of the jitter, MUs have to be delayed at the receiver in order a continuous synchronized presentation to be achieved. Therefore, MUs have to be stored in a buffer and the size of this buffer may correspond to the amount of jitter in the network. As the synchronization requirements can vary according to the application on hand, we must control the individual sync requirements (i.e., delay sensitivity, error tolerance etc.) for each media separately. To this direction, Park and Choi [7] investigated an efficient and flexible multimedia synchronization method that can be applied at intra-media synchronization in a consistent manner. They proposed an adaptive synchronization scheme based on: (1) the delay offset; and (2) the playout rate adjustment that can match the application's varying sync requirements effectively. Park and Kim [8] introduced an AMP scheme based on a discontinuity model for intra-media synchronization of video applications over best-effort networks. They analyzed the temporal distortion (i.e., discontinuity) cases such as playout pause and skip, to define a unified discontinuity model. Finally, Laoutaris and Stavrakakis [9] surveyed the work in the area of playout adaptation. Actually, the problem of intra-stream synchronization has been solved efficiently as many intra-stream synchronization techniques in the literature achieved to avoid receiver buffer underflow and overflow problems.

B. Inter-stream Synchronization

Inter-stream (also known as *inter-media* or *parallel*) *synchronization* is the problem of synchronizing different but related streams. Precisely, it is the preservation of the temporal dependencies between playout processes of different, but correlated, media streams involved in a multimedia session. An example of inter-stream synchronization is the *Lip synchronization* that refers to the temporal relationship between an audio and a video stream for the particular case of human speaking [10]. Fig. 1 shows an example of the temporal relations in inter-stream synchronization.

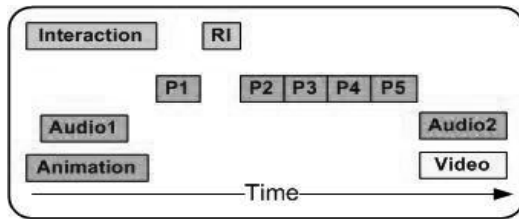Inter-destination multimedia synchronization:
A contemporary survey

Fig. 1. An inter-media synchronization example

It starts with an animation (Animation) which is partially commented using an audio sequence (Audio1). Starting the animation presentation, a multiple-choice question is presented to the user (Interaction). If the user has made a selection, a final picture (P1) is shown. Then, the replay of a recorded user interaction (RI) follows with a slide sequence (P2-P5), and a lip-synchronized audio/video sequence (Audio2 and Video). Blakowski and Steinmetz [5] illustrated the main specification methods that can describe synchronization scenarios. These methods are *interval-based specification, control flow-based specification, axes-based synchronization, event-based synchronization, scripts,* and *comments*. Among them, *Scripts* is one of the most powerful methods that describe the majority of synchronization scenarios. Scripts often become full programming languages extended by timing operations. Such language is SMIL (*Synchronized Multimedia Integration Language*) that became a standard (W3C SMIL 3.0, Dec. 2008). Scripts may rely on different specification methods. A typical script is a script that is based on a hierarchical method and supports three main operations: serial presentation, parallel presentation, and the repeated presentation of a media object. Below, we write a script for the application example depicted in Fig. 1.

```
activity Picture           Picture1("picture1.jpeg");
activity DigAudio          Audio1("animation.au");
activity RTAnima           Animation("animation.ani");
activity Xrecorder         Recorder("window.rec");
activity StartInteraction  Selection;
activity Picture           Picture2("picture2.jpeg");
activity Picture           Picture3("picture3.jpeg");
activity Picture           Picture4("picture4.jpeg");
activity Picture           Picture5("picture5.jpeg");

activity DigAudio          Audio2("audio2.au");
activity SMP               Video("video.smp");

script AniComment CC = Animation &
Audio1.Translate(GR);
script Picture_sequence
    4Pictures =            Picture2.Duration(3)>>
                           Picture3.Duration(3)>>
                           Picture4.Duration(3)>>
                           Picture5.Duration(3);
script Lipsynch  AV = Audio2 & Video;
script Multimedia
  Application_example {
                       ((Selection Picture1) & CC >>
                       Record.UI >>
                       4Pictures>>
                       AV
            }
```

Fig. 2. A script for the example depicted in Fig. 1

The symbols & and >> denote parallel and serial presentation correspondingly. Note that *activities* and *subscripts* compose the *script*. A *synchronization specification* of a multimedia object describes all temporal dependencies of the objects included in this object. It is comprised of:

- Intra-object synchronization specifications for the media objects of the presentation.
- QoS descriptions for intra-object synchronization.
- Inter-object synchronization specifications for media objects of the presentation.
- QoS descriptions for inter-object synchronization.

To achieve inter-stream synchronization, various algorithms have been applied. Also, there are several types of intra-stream synchronization control such as *Skipping* [11], *Buffering* [11], *Adaptive Buffer Control* (ABC) [12], *Queue Monitoring* (QM) [13], *Virtual-Time Rendering* (VTR) [14], and *Media Adaptive Buffering* [15]. Boronat et al. [16] have reviewed and compared the most powerful inter-stream synchronization algorithms. The building blocks of these algorithms are the synchronization techniques utilized both at the sender and the receiver sides. These algorithms can use multiple synchronization techniques to achieve synchronization aim even from different categories [17].

C. Classification of Inter-Media Techniques

Boronat et al. [16] categorized synchronization techniques according to the '*location*', '*content*', '*sync information used*' and '*purpose*'.

- **Location of synchronization technique:** The synchronization control can be performed either by source or receiver. If control is performed by the source, most of the time it will require some feedback information from the receiver. The receiver will tell the source about the degree of asynchrony at the current instance.
- **Live vs. Synthetic synchronization (Type of Media):** In *live* media, the temporal relations are exactly reproduced at a presentation as they existed during the capture process. Synthetic synchronization techniques are used for *stored* media.
- **Information used for synchronization technique:** The information included in the MU for the synchronization purpose can be different like *timestamp*, *sequence number*. Some techniques use either sequence number or timestamp, while others may use both. For example, the Real-Time Transport Protocol (RTP) provides timestamps to synchronize different media streams.
- **Purpose of synchronization technique:** The techniques can be divided into four subcategories with respect to their purpose:
  1. The *basic control* techniques are required in almost all synchronization algorithms. Examples are adding synchronization information in MUs at the source and buffering of MUs at the receiver.
  2. The *common control* techniques can be applied in both ways.
  3. The *preventive control* techniques are used to prevent the asynchrony in the streams. Preventive mechanisms minimize latencies and jitters and may involve disk-reading scheduling algorithms, network

transport protocols, operating systems, and synchronization schedules.

4. The *reactive control* (or *corrective*) techniques are designed to recover synchronization in the presence of synchronization errors. An example of corrective mechanisms is included in the Stream Synchronization Protocol (SSP).

Based on these criteria, Table I shows a classification of inter-media techniques.

TABLE I.
CLASSIFICATION OF INTER-MEDIA TECHNIQUES

Technique	Location	Description
Basic Control	Source control	• Add information useful for synchronization: timestamps, sequence numbers (identifiers), event information and/or source identifiers.
	Receiver control	• Buffering techniques
Common Control	Source control	• Skip or pause MUs in the transmission process. • Advance the transmission timing dynamically. • Adjust the input rate. • Media Scaling.
	Receiver control	• Adjust the playout rate. • Data Interpolation.
Preventive Control	Source control	• Initial playout instant calculation. • Deadline-based transmission scheduling. • Interleave MUs of different media streams in only one transport stream.
	Receiver control	• Preventive skips of MUs (e.g., discardings) and/or preventive pauses of MUs (repetitions, insertions or stops). • Change the buffering waiting time of MUs. • Enlarge or shorten the silence periods of the streams.
Reactive Control	Source control	• Adjust the transmission timing. • Decrease the media streams transmitted. • Drop low-priority MUs.
	Receiver control	• Reactive skips (eliminations or discardings) and/or reactive pauses (repetitions, insertions or stops). • Make playout duration extensions or reductions (playout rate adjustments). • Use of virtual time with contractions or expansions. • Master/slave scheme. • Late event discarding (Event-based). • Rollback techniques (Event-based)

III. INTER-DESTINATION MULTIMEDIA SYNCHRONIZATION

Inter-Destination (also known as *Inter-Receiver* or *group* or *multipoint*) *Multimedia Synchronization* (IDMS) has been gaining popularity due to the rise of social networking applications. IDMS involves the simultaneous synchronization of one or more playout receivers of one or several media streams at geographically distributed receivers to achieve fairness among them. Fairness implies that during a multimedia session, all the receivers must play the same MU at each media stream. For example, in a networked video wall scenario, wherein users are watching an on-line football match, all users should experience the goal event almost simultaneously (to have a fair shared experience).

Existing distribution technologies do not handle the IDMS problem in an optimal way. Thus, additional adaptive techniques must be provided to meet the IDMS synchronization requirements in practical content delivery networks. The levels of required synchrony among the receivers depend on the application on hand. However, the exact ranges of asynchrony levels (which could be tolerated by users for emerging distributed applications) have not sufficiently determined yet [3].

Akyildiz and Yen [6] introduced group synchronization protocols for real-time multimedia applications including teleconference, tele-orchestration, and multimedia on demand services. Their protocols achieve synchronization for all configurations (one-to-one, one-to-many, many-to-one, and many-to-many), and do so without prior knowledge of the end-to-end delay distribution, or the distribution of the clock drift. The only a-priori knowledge the protocols require is an upper bound on the end-to-end delay. Boronat et al. [16] reviewed the most-known multimedia group and inter-stream synchronization approaches. Group synchronization techniques can be classified at three schemes (discussed later). These schemes are based on the *Virtual-Time Rendering* (VTR) *media synchronization algorithm* to determine the output timing of each MU so that the timing can be the same at all the destinations. VTR algorithm is applicable to networks with unknown delay bounds. It makes use of globally synchronized clocks. VTR consists of the dynamic adjustment of the MUs rendering-time according to the network condition. For a better understanding of these schemes, let us consider that M sources and N destinations/receivers are connected through a network. MUs of M different streams have been stored with timestamps in M sources, and they are broadcasted to all the receivers. The timestamp contained in a MU indicates its generation time. The streams often fall into a *Master stream* and *Slave streams*. At each receiver, the slave streams are synchronized with the Master stream by using an inter-media synchronization mechanism.

A. Master/Slave (M/S) Receiver Scheme

In M/S scheme [18], the receivers are categorized into one *Master* receiver and *Slave* receivers. Multiple streams are received at each receiver and one of these streams acts as Master stream in order inter-media synchronization to be achieved at each receiver (Fig. 3).

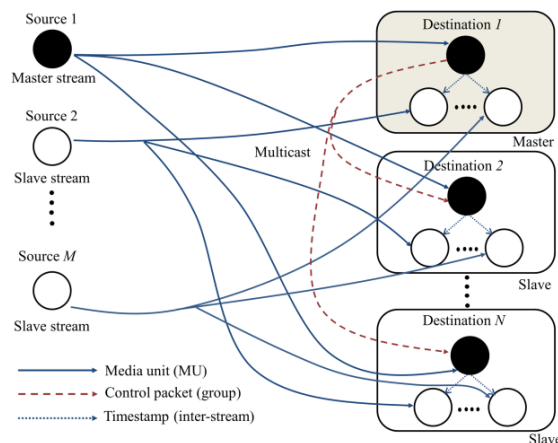Inter-destination multimedia synchronization:
A contemporary survey

Fig. 3. Master/Slave Receiver Scheme [19].

None of the slave receivers send any feedback information about the timing of the playout processes. It only adjusts the playout timing of MUs to that of the Master receiver. Only the Master receiver sends (multicasts) its playout timing to all the other (slave) receivers. The Master receiver controls and computes the presentation time of the MUs according to its own state of the received stream data. Group synchronization is achieved by adjusting the presentation time of the MUs of master stream at the slave receivers to that of the Master receiver. Therefore, the slave receivers should present MUs at the same timing as the Master receiver. The synchronization of the slave receivers is achieved as follows:

- The Master receiver multicasts a control packet to all slave receivers. This control packet includes the presentation time of its first MU of the master stream. This process is called "*initial presentation adjustment*".
- When the target presentation time of the Master receiver changes, the Master receiver notifies all the slaves about this modification by multicasting a control packet. This control packet contains the amount of time that is modified and the sequence number of the MU for which the target presentation time has been changed.
- The Master receiver periodically multicasts proper control packets to accommodate the newly joined slave receivers.

Boronat et al. [20] presented the M/S scheme by extending the RTP/RTCP (Real-time Transport Protocol/ RTP Control Protocol) messages for containing the synchronization information. Fig. 3 presents the different type of message exchanges in the basic M/S scheme. The advantage of the M/S technique is its simplicity and the decreased amount of information exchange (i.e., control packets) to support group synchronization. However, the selection of the Master receiver can influence the performance of the scheme because slave receivers must present MUs at the same timing as the Master receiver. If the fastest (more advanced) receiver is selected as the master, the playout point of this receiver is selected as the IDMS reference. This will result to poor presentation quality at slower (or more lagged) receivers. On the contrary, if the slowest receiver is selected as master, this will result in high packet drops at faster slave receiver(s). It is noteworthy that synchronization can also be based on the mean playout point (i.e., the IDMS reference is calculated by averaging the

playout timing reported from all the distributed receivers). A problem with the M/S technique is that the master can act as a bottleneck in the system. A second problem deals with the associated degree of unfairness with the slave receivers. Boronat et al. [21] discussed possible options with pros and cons for the master selection in this scheme.

B. Synchronization Maestro Scheme (SMS)

In SMS scheme [22], all the receivers are handled fairly as master and slaves do not exist. SMS involves a *Synchronization Manager* (SM) which can be performed by one of the source or receiver. For example, in Fig. 4, one receiver (destination) performs the role of SM.
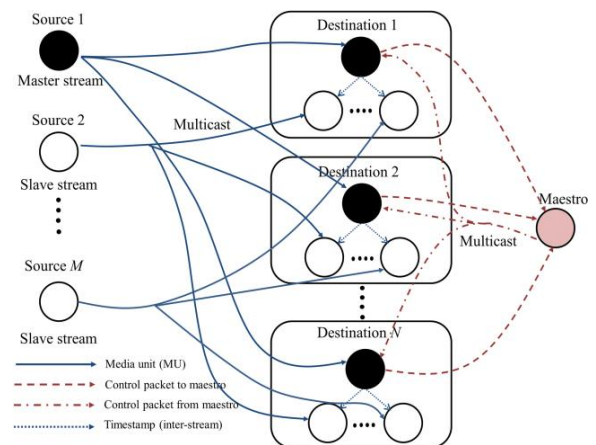
Fig. 4. Synchronization Maestro Scheme [19].

Each receiver estimates the network delay and uses the estimates to determine the local presentation time of the MU. Then, each receiver sends this estimated presentation time of MU to the SM. After that, the SM gathers the estimates from the receivers and adjusts the presentation timing among the receivers by multicasting control packets to receivers. The SMS scheme assumes that the clock speed at the sources and receivers is the same and that the current local times are also the same (i.e., globally synchronized clocks). Figure 4 depicts the basic principle of the SMS technique. Boronat et al. [16] presented the RTCP-based schemes which follow the same basic principle. The SMS scheme (like the M/S) is a centralized solution, and thus it can confront the bottleneck problem. The advantage of the SMS scheme over M/S is its fairness to the receivers because the feedback information of all the receivers is accounted for determining the presentation time of the MU. However, this fairness costs more communication overhead among the receiver and the Synchronization Manager (SM).

C. Distributed Control Scheme (DCS)

Figure 5 illustrates the DCS scheme [23]. Each receiver estimates the network delay, and then determines the presentation time of the MU. Then, it sends (multicasts) this presentation time to all the receivers. After that, every receiver will have the entire view of the estimated time of MU. Each receiver has the flexibility to decide the reference playout time among the timing of all the receivers. The DCS scheme provides higher flexibility to each receiver to decide the
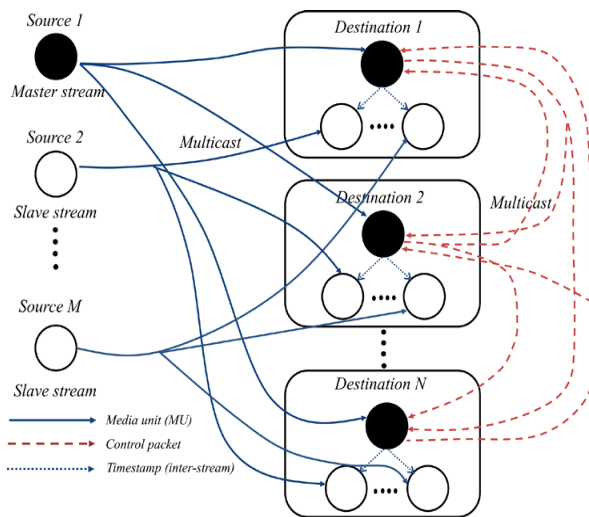
Fig. 5. The Distributed Control Scheme [19]

presentation time of MU. For example, it is possible that by selecting the presentation time of other receiver, it can achieve higher group synchronization quality, but it may cause the inter-media or intra-media synchronization degradation. In this case, the receiver has the flexibility to choose between the types of synchronization depending upon the nature of application on hand. If the application on hand requires the higher inter-media or intra-media synchronization and can sacrifice on the group synchronization to certain limit, then the receiver can select its own determined presentation time and vice versa. DCS is a distributed scheme by nature and does not suffer from the bottleneck problem. If one or more receivers leave the system, it will not disturb the overall scheme. This greater flexibility and the distributed nature of DCS make it complex in terms of processing. This happens because the receiver does more calculations and comparisons before deciding the presentation time of MU. Finally, DCS has a higher message complexity, because each receiver multicasts the estimated presentation time.

D. Comparison of Control Schemes - Lessons Learned

The following factors affect IDMS performance (i.e., the level of synchronicity among receivers). These factors can be used as evaluation criteria for the comparison of IDMS control schemes [3][16]:

Robustness: Disconnections and failures of some receivers/participants may affect the ability to perform the IDMS control. In a distributed control architecture (DCS), the failure of any of the participant has a slight effect on the other participants because each one of them is independent and has locally all the required information to compute the overall synchronization status at any time. In SMS, if the Maestro cannot communicate with the other terminals owing to some trouble, no destination can carry out the IDMS control. Generally, a centralized scheme (SMS or M/S) is *less robust* than distributed schemes. A distributed architecture (DCS) is more robust because it can simplify the deployment and maintenance of a distributed multimedia application.

Scalability: This is the ability to handle multiple concurrent participants/receivers in an IDMS session. SMS requires the maintenance of a dedicated server (Maestro) to which all the control information converges. Thus, SMS may present higher scalability constraints. For example, multiple receivers may send control packets almost simultaneously, thus originating a feedback-implosion problem because of the IDMS control. As the number of the receivers/participants increases, bursty traffic due to control packets can overwhelm the synchronization manager and may degrade the output quality of the media streams.

Traffic overhead: It is generated by two factors: (1) the distribution of the playout timing messages from the participants to the synchronization manager; and (2) the transmission of playout setting instructions. Generally, traffic overhead may be higher in DCS than in SMS.

Interactivity (*low delays*): Each slave destination can compute the detected playout asynchrony when it receives the control messages from the master destination. Consequently, the lowest delays may be achieved using the M/S scheme. In DCS, each participant must gather the overall status from all the other active participants. As a result, delays in DCS are bit larger. In SMS, the Maestro must gather the playout timing of all the receivers, and then send back to them new control messages including IDMS setting instructions. Therefore, the highest delay (smallest interactivity) occurs in SMS, but this delay depends on the network topology and on the routing tree structure.

Location of control nodes: The location of the multimedia source and the location of the synchronization manager affect the IDMS performance of the schemes. Centralized control schemes are more sensitive to these locations. Under heavily loaded network conditions, the IDMS performance with SMS can be slightly larger than the one with M/S and DCS schemes, if the media source is selected as the Maestro. This is due to the fact that IDMS control packets sent by the Maestro are sent through the same path as the MUs (e.g., video frames, encapsulated in data packets). In SMS scheme, IDMS control messages scarcely increase the network load. But, if the bandwidth availability is limited, some (data or control) packets may be dropped. If a control packet is dropped (lost), the destination cannot get the reference output timing until receiving the next control packet. On the other hand, in M/S scheme, if the most heavily loaded destination is selected as the master, the data packets are less likely dropped on the intermediate links because it does not need to receive control packets and their own sent control packets may be transmitted in the opposite direction to the media data packets.

Consistency: In media-sharing applications, consistency is required to guarantee concurrently synchronized playout states in all the distributed participants. In centralized schemes, inconsistency between receivers' states occurs less likely, since all of them always receive the same control information about IDMS timing from the Maestro (in SMS) or the Master receiver (in M/S scheme). On the contrary, in a DCS scheme, there is no guarantee that the same reference IDMS timing, from among all the collected IDMS control reports, will be selected in all the distributed receivers since each one takes its own decisions locally. This leads to a more probable potential inter-receivers inconsistency.

Security: Centralized architectures provide higher security than distributed architectures. In DCS architectures, we have

lack of control because each participant has the responsibility of what is doing, and some participants may be malicious. Synchronization entities (Maestro in SMS, or each destination in DCS and in M/S) must consider inconsistent playout information (exceeding configuration limits) as a malfunctioning service and reject that information in the calculation of the necessary playout adjustments (synchronization actions).

Coherence: This is the ability to synchronously and simultaneously coordinate the media playout timing according to a reference timing for IDMS. For this reason, the maximum playout asynchrony (between the most lagged and the most advanced receiver) must be estimated. And this is easy in DCS and SMS schemes. But, in M/S scheme, each receiver can only know the asynchrony between its local playout process and that of the Master. Using M/S scheme, the reactive synchronization actions will not be performed simultaneously because slave receivers adjust their playout timing when they detect an asynchrony value (regarding the playout state of the master) exceeding an allowable threshold and this situation may not be detected at the same time in all the slave receivers. Consequently, SMS outperforms the M/S and DCS in terms of coherence.

Fairness: M/S scheme is appropriate for applications in which a single receiver has a certain priority level over the others. For example, in multi-point video conferencing (e.g., synchronous e-learning), the teacher's terminal can be selected as the Master receiver, which directs to the students' devices the required playout adjustments to get in sync. However, M/S scheme cannot treat all the receivers fairly. This problem is minimized when SMS or DCS are employed because the reference output timing is selected after a comparison among the output timing of all the receivers.

Flexibility: Using M/S scheme, there is no option for selecting the reference output timing since it is taken from the one reported by the master destination. Conversely, the Maestro, in SMS, and the distributed receivers, in DCS, can employ several dynamic policies for selecting an IDMS reference from the collected output timings.

Conclusively, M/S scheme can provide the best performance in terms of scalability, traffic overhead, and interactivity. Moreover, M/S scheme can be proper in those scenarios in which the bandwidth availability is limited, and also in those use cases in which a single participant (e.g., a teacher in a synchronous e-learning scenario) has a certain priority level over the others. However, the M/S scheme presents serious drawbacks, if some features such as robustness, coherence, flexibility, and fairness are required. Finally, M/S and SMS control schemes are the most appropriate in terms of consistency. Centralized schemes (M/S and SMS) have larger network delays (low interactivity), lower robustness with poorer flexibility and scalability.

E. Classification of Group Synchronization Solutions

In Table II, we summarize the most well-known synchronization solutions by presenting the above schemes and other features of interest such as the following ones:
- *Group synchronization schemes*: The control schemes (M/S receiver scheme, SMS, and/or DCS) included in the solutions are indicated.

- *Synchronization information*: The information used for synchronization (included in the transmitted MUs) is indicated.
- *Location of the synchronization techniques*: The synchronization control is made by the source(s) or by the receiver(s) or both.
- *Synchronization techniques*: The most representative techniques included in each solution have been indicated in Table II.

In the first column (Table II), the *Name* of the group synchronization solution and the corresponding cited work are included. Several solutions use RTP/RTCP protocols [32]. Particularly, they use feedback and time information (timestamps) included in the RTP/RTCP. These solutions exploit the use of control RTCP report packets for including feedback information for multimedia synchronization purposes. The VTR media synchronization algorithm [18] has been used in media synchronization between voice and movement of avatars in networked virtual environments. The synchronization maestro scheme (SMS) for group synchronization, employed together with the VTR media synchronization algorithm, has been enhanced so that the SMS scheme can be used efficiently in a networked real-time game with collaborative work [31], and in a P2P-based system [28].

TABLE II:
CLASSIFICATION OF SOME GROUP SYNCHRONIZATION SOLUTIONS

Name	Sche-me	Sync information	Loca-tion	Synchronization techniques
VTR [18]	Master/Slave receiver scheme	Timestamps Seq. number	Source and Recei-ver	Change of the buffering time according to the delay estimation. Decreasing the number of media streams. Preventive pauses. Reactive skips and pauses. Skips at the source side. Playout duration extensions or reductions. Virtual local time expansions or contractions.
[6]	DCS	Timestamp in 1st packet	--	Initial transmission and playout instant. Playout rate adjustments (receiver's clock). Master/slave receiver switching (chairman).
BS [24]	DCS	Timestamps Seq. number	Recei-ver	Skips (discarding) and pauses (duplicates). Late events are dropped.
LL-TW [23]	DCS	Timestamps	Recei-ver	Event-based synchronization control. Playout duration extension. Rollback-based techniques.
DCS [25]	DCS	Timestamps	Recei-ver	VTR techniques
TSS [26]	DCS	Timestamps	Recei-ver	Event-based synchronization control. Playout duration extension. Rollback-based techniques.
ILA [27]	DCS	Timestamps	Recei-ver	Event-based synchronization control. Preventive MDU/event discarding. Reactive events discarding.
ESMS	SMS	Timestamps	Source	Skipping and VTR

[28]		Seq. number	and Recei- ver	techniques for intra- stream synchronization.
RTP-FGP [29]	SMS	Timestamps Source id.	Source and Recei- ver	Initial playout instant. Reactive skips and pauses at the receiver side. Playout rate adjustment. Virtual time expansion. Master/slave receiver switching (group synchronization).
SMS [11], [18], [30], [31], [22]	SMS	Timestamps Seq. number	Recei- ver	Initial transmission instant (only in [22])

BS: bucket synchronization; DSC: distributed control scheme;
ILA: interactivity-loss avoidance;
LL-TW: local-lag and time warp algorithms;
RTP-FGP: RTP-based feedback-global protocol;
SMS: synchronization maestro scheme; TSS: trailing state synchronization;
VTR: virtual time rendering algorithm

Moreover, many different reactive techniques have been proposed. For example, receivers can discard late events in [24]. In addition, receivers in [25] can use rollback techniques, such as maintaining late events and using them to compensate for inconsistency at the receiving end. In the *Timewarp* algorithm [23], this can cause an extra overhead in terms of memory space and computation for inconsistency compensation. To re-establish the consistency of the game state, rollback-based techniques were developed in [23]. Copies of the states are maintained after command executions and events received after their playout time are stored locally instead of being dropped and used to compensate for the inconsistency among receivers' views. Then, visual rendering of significant events can be delayed (to avoid inconsistencies if corrections occur). In this case, the difficulty is that the use of these realignment techniques may further impact on the responsiveness of the system. The *Trailing State Synchronization* (TSS) algorithm [26] uses dynamically changing states as the source of rollbacks as opposed to static snapshots, which is the fundamental difference between it and *Timewarp* [23]. TSS preserves more than a few instances of the applications running with different synchronization delays. In TSS, inconsistencies are noticed by detecting when the leading state and the correct state diverge, and at that point are corrected. From another perspective, a proactive event discarding mechanism is used in [27]. This mechanism is based on the discrimination of obsolete events. In particular, obsolete events are discarded with a probability depending on the level of interactivity.

In the next section, we present IDMS standardization efforts and some state-of-the-art IDMS solutions.

IV. RECOMMENDATIONS AND SOLUTIONS

A. Standardization efforts

ETSI (European Telecommunications Standards Institute) TISPAN (Telecoms & Internet converged Services & Protocols for Advanced Networking) has been carried out standardization efforts of IDMS. This standardization is also a highlight for the IETF AVTCORE WG (Internet Engineering

Task Force - Audio/Video Transport Core Maintenance Working Group). The specification [33] does pose IDMS and the synchronization of media streams from different sources as a requirement for providing synchronization-sensitive interactive services. These use cases are mostly in the categories of 'low' or 'medium' synchronization, and not very high requirements are posed to delay differences between various user equipments. However, Montagud et al. [3] presented up to 19 use cases for IDMS, each one having its own (very high) synchronization requirements. The most of these use cases are not supported by the protocol specification, which gives a delay difference of between 150 and 400 ms as a guideline for achieving transparent interactivity, based on ITU guidelines for interactivity in person-to-person communication.

ETSI TISPAN has done the first work on standardizing RTCP usage for IDMS. The ETSI proposal is a dedicated solution for use in large scale IPTV deployments with 'low' to 'medium' level synchronization requirements. The ETSI solution [34] is an evolved version of an RTCP-based IDMS approach including an AMP scheme that adjusts the playout timing of each one of the geographically distributed consumers in a specific cluster if an allowable asynchrony threshold between their playout states is exceeded. Still, there are use cases [3] that require higher levels of synchronization and are not supported efficiently by the ETSI solution.

Within the Internet Engineering Task Force (IETF), the AVTCORE working group [35] carries out standardization of the RTCP-based IDMS protocol. This is the core group that is responsible for the RTP and accompanying RTCP protocol. Actually, most RTCP extensions are developed within the IETF. van Deventer et al. [36] provided an overview of recently published standards for media synchronization from the most relevant bodies: IETF, ETSI, MPEG, DVB, HbbTV, and W3C.

B. Solutions

Boronat et al. [16] described most IDMS solutions that define new proprietary protocols with specific control messages which increase the network load. Montagud et al. [37] reviewed the existing sync reference models by examining the involved features, components, and layers in each one of them. Their study reflects the need for a new modular and extensible theoretical framework to efficiently comprehend the overall media sync research area. From another perspective, Huang et al. [38] presented a historical view of temporal synchronization studies focusing on continuous multimedia. They demonstrated how the development of multimedia systems has created new challenges for synchronization technologies. They concluded with a new application dependent, multi-location, multi-requirement synchronization framework to address these new challenges.

The realization of synchronous shared experiences requires that users feel that they are coherently communicating with each other. Vaishnavi et al. [1] analyzed challenges that need to be tackled to achieve coherence: QoS, mobility, and distributed media synchronization. They presented their solution to distributed media synchronization. Their design uses the local lag mechanism over a distributed control or master–slave signaling architecture. Montagud et al. [39]

presented an IDMS solution based on extending the capabilities of RTP/RTCP protocols. To enable an adaptive, highly accurate, and standard compliant IDMS solution, they specified RTCP extensions in combination with several control algorithms and adjustment techniques.

Focused on the TV area, Costa and Santos [40] surveyed the existing media sync solutions, classifying them in terms of types of involved devices, types of media content, types of sync techniques, targeted applications or scenarios, and evaluation methodologies. The following sync specific aspects were considered to classify the existing solutions: protocols, algorithms, delivery channels, specification methods, architectural schemes, allowable asynchrony levels, and evaluation metrics. Marfil et al. [41] presented an adaptive, accurate and standard-compliant IDMS solution for hybrid broadcast and broadband delivery. Their solution can accomplish synchronization when different formats/versions of the same (or even related) contents are being played out in a shared session. It can also independently manage the playout processes of different groups of users. Their IDMS solution has been integrated within an end-to-end platform, which is compatible with the *Hybrid broadcast broadband TV* (HbbTV) standard. It has been applied to digital video broadcasting-terrestrial technology and tested for a social TV scenario, by also including an ad-hoc chat tool as an interaction channel.

Ishibashi et al. [42] carried out QoE assessment of fairness between players in a networked game with olfaction. They investigated the influence of the time it takes for a smell to reach a player on fairness. They illustrated that fairness is hardly damaged when the constant delays are smaller than about 500 ms. The used media synchronization algorithm considers the human perception of intra-stream and inter-stream synchronization errors. Ghinea and Ademoye [43] conducted a perceptual measurement of the impact of a synchronization error between smell sensory data and audiovisual content, assuming the audiovisual lip skew is zero. Their results showed a synchronization threshold of 30 s, when olfaction is ahead of audiovisual data, and of 20 s when olfaction is behind. In joint musical performance, multiple users play their respective same or different types of musical instruments together. However, the media synchronization quality and interactivity may seriously be deteriorated owing to the network delay. Sithu and Ishibashi [19] proposed a new media synchronization control called the '*dynamic local lag control*'. By QoE assessment, they demonstrated that this new control can achieve a high quality of media synchronization and keep the interactivity high in joint musical performance.

Bello et al. [44] presented a distributed multimedia synchronization protocol oriented to satisfy logical and temporal dependencies in the exchange of real-time data in mobile distributed systems by using logical mapping, avoiding the use of global references. Two main aspects of their protocol include: (1) the computation of the deadline for messages by using only relative time points, and (2) by dividing the processing stage to achieve synchronization with an asymmetric principle of design. Simulations results showed that their protocol is effective in diminishing the synchronization error. Furthermore, their protocol is efficient as regards processing and storage costs at the mobile hosts,

and in the overhead attached per message with a reduced usage of bandwidth across the wired and wireless channels in comparison with the RTP.

Internet-based video services can also benefit from IDMS. We can achieve a smooth multiple-stream distributed multimedia presentation over the Internet if we apply presentation adaptation and flow control. Huang et al. [45] proposed the *Pause-And-Run* approach for *k*-stream (PARK) multimedia presentations over the Internet to achieve reliable transmission of continuous media. They evaluated the application of the PARK approach over the Internet. The evaluation results revealed a suitable buffering control policy for the audio and video media respectively. The characteristics of the PARK approach are:

- PARK adopts TCP to achieve reliable transmission for continuous media.
- A novel flow adaptation scheme reduces the overhead of the network and end-hosts because the slow-start scheme is embedded in TCP. The server adapts its transmission rates to the buffer situation of the client and prevents the client's buffers from overflow and underflow as much as possible.
- With the provision of multiple-stream synchronization and the multi-level adaptation control, the client achieves smooth multimedia presentations and graceful presentation degradation.

From another perspective, *Wersync* [46] is a novel web-based platform that enables distributed media synchronization and social interaction across remote users. By using Wersync, users can create or join on-going sessions for concurrently consuming the same media content with other remote users in a synchronized manner.

Rainer et al. [47] presented *Merge and Forward*, an IDMS scheme for adaptive HTTP streaming as a distributed control scheme and adopting the MPEG-DASH standard [48] as a representation format. They introduced so-called IDMS sessions and described how an unstructured peer-to-peer overlay can be created using the session information and using the MPEG-DASH. They assessed the performance of *Merge and Forward* with respect to convergence time (time needed until all clients hold the same reference time stamp) and scalability. After the negotiation on a reference time stamp, the clients have to synchronize their multimedia playback to the agreed reference time stamp. In order to achieve this, the authors proposed a new AMP approach minimizing the impact of playback synchronization on the QoE. The proposed AMP was assessed subjectively using crowdsourcing.

Kwon et al. [49] proposed a media sharing scheme (named *PlaySharing*) for scalable media streaming and precise group synchronization services. PlaySharing combines event-based synchronization, local adjustment of playback position errors, and rare and periodic synchronization. It achieves sustained precise synchronization by minimizing synchronization control packets during network congestion. Event-based synchronization manages the synchronization between a media source device and client devices using event messages from the source device. To reduce the number of synchronization control packets, the local adjustment of

playback position errors corrects those on the media client devices according to the expected playback position for the time elapsed since the last synchronization. Rare and periodic synchronization is applied in preparation for control packet loss, correcting the local adjustment errors when no event occurs. To evaluate the performance of PlaySharing, the average synchronization errors (between the source device and the client devices) were measured in an IEEE 802.11 infrastructure network configuration and a hierarchical wireless media streaming network (HSN) configuration. For these measurements, two protocols were used: the user datagram protocol unicast and broadcast for control packet transmission. The experimental results showed that PlaySharing, with user datagram protocol unicast transmission of control messages in the HSN, has the lowest synchronization errors in the experiments.

Last but not least, an additional challenge in IDMS is securing group communication that involves *Multicast Group Key Management*. Such management is the management of the keys in a group communication. Developing group key management faces additional challenges in wireless mobile networks (e.g., MANETs) due to their inherent complexities. The constraints of wireless devices in terms of resources scarcity and the mobility of group members increase the complexity of designing a group key management scheme. Daghighi et al. [50] surveyed existing group key management schemes that consider the host mobility issue in secure group communications in wireless mobile environments.

V. Conclusion and Future Work

This paper has illustrated various issues on multimedia synchronization. It has presented the basic control schemes for IDMS and has focused on IDMS solutions and standardization efforts for emerging distributed multimedia applications.

Lessons Learned

IDMS is essential in various emerging distributed multimedia applications such as social TV, hybrid broadcast/broadband services, networked quiz shows, networked video wall, multi-party multimedia conferencing, and interactive 3D tele-immersive applications. 3D tele-immersive applications provide geographically distributed users with a realistic and immersive multimedia experience [51]. The protocol software developer must take into account: (1) the context and space in which the IDMS solution is going to be deployed; and (2) the multimedia application requirements that must be satisfied. The key-point in IDMS is to minimize the delay differences among different receivers by introducing proper buffering mechanisms. The primary latency in IDMS scenario is the playout delay that consists of the sending buffer delay, packet transfer delay, and receiving buffer delay. The transfer delay (which includes packet transmission and path propagation delay) of the same (media) video packet to different destinations often differs significantly because of the variations in available bandwidth and path propagation delays. These packet transfer delay differences are the main barrier for IDMS because they affect the receivers' synchronous playout possibility substantially.

Existing control schemes (i.e., M/S, SMS, DCS) for IDMS have their own strengths and weaknesses. However, the choice between these schemes is largely application-dependent. For their evaluation, certain metrics must be used such as robustness, fairness, scalability, traffic overhead, interactivity (low delay), location of control nodes, consistency, coherence, security, and flexibility.

Precise group synchronization schemes can be deployed by using *event-based synchronization*. This kind of synchronization implies that the synchronization controller can transfer a synchronization control message to the media client devices when an event (e.g., Play, Pause, Resume, Stop, and Seek) in a media source device occurs. The control message may include an event time, an event type, a playback position, etc. Then, media client devices could synchronize their playback states with the media source device after correcting errors, based on the received control message.

The current industry pushes for new IDMS services, both at the IP media stream level (IETF RTCP, ETSI TISPAN) and the MPEG-2 transport stream level (DVB CSS, MPEG TEMI). It also includes more fundamental standards [(W3C SMIL and ITU - NCL (Nested Context Language)] that can serve as models for future and more general synchronization primitives. The standardization of IDMS will facilitate the uptake of implementations and of the interoperability between different implementations. Such standardization will ensure a more extensive use of IDMS.

Future Work

- The basic control schemes for IDMS must be compared and evaluated under various types of wireless networks (e.g., MANETs, VANETs). The evaluation metrics must cover many aspects such as robustness, interactivity, etc.

- Future IDMS techniques could benefit from cross-layer optimization. Such optimization allows communication between OSI-RM layers by permitting one layer to access the data of another layer to exchange information and enable interaction [52]. It contributes to an improvement of QoS under various operational conditions. The cross-layer control mechanism can provide feedback on concurrent quality information for the adaptive setting of control parameters of a multimedia system. As a result, it could help to the utilization of synchronization techniques such as preventive control. A comprehensive multimedia synchronization subsystem will integrate preventive and reactive methods and will use a cross-layer optimization method and other components (e.g., the IP Multimedia Subsystem).

- In RTP-based multimedia streaming services, client-driven media synchronization mechanisms must be developed to provide accurate media synchronization such as to reduce: (1) the initial synchronization delay; (2) the processing complexity at the client device; (3) the number of required user datagram protocol ports; and (4) the amount of control traffic injected into the network. Such a synchronization mechanism was recently proposed in [53]. In this mechanism, the server does not need to send any RTCP sender report packets for synchronization.

Instead, the client device derives the precise normal play time for each video and audio stream from the received RTP packets containing an RTP timestamp.

- Intelligent distributed control schemes are required to develop IDMS for pull-based streaming. Such schemes must negotiate a reference playback timestamp among the peers participating in an IDMS session. The MPEG-DASH standard can be used to incorporate these IDMS sessions in the Media Presentation Description (MPD). In this way, the proposed solutions will remain compliant to the MPEG-DASH because non-IDMS peers will ignore the additional session description when parsing the MPD.

- Finally, we must introduce and evaluate transmission schemes that will minimize the transmission loss rate, while still ensuring the synchronous arrival of video packets. The main principle of their design will be to leverage the packet transfer delay differences among different destinations for spreading the departures of video/audio packets. The integration of such transmission schemes with dynamic AMP solutions will be a challenge.

REFERENCES

[1] Vaishnavi, I., Cesar, P., Bulterman, D., Friedrich, O., Gunkel, S., and Geerts, D. "From IPTV to synchronous shared experiences challenges in design: Distributed media synchronization," *Signal Processing: Image Communication,* vol. 26, no. 7, pp.370-377, 2011.

[2] Kernchen, R., Meissner, S., Moessner, K., Cesar, P., Vaishnavi, I., Boussard, M., and Hesselman, C. "Intelligent multimedia presentation in ubiquitous multidevice scenarios," *IEEE Multimedia*, vol. 17, no. 2, pp. 56-63, 2010.

[3] Montagud, M., Boronat, F., Stokking, H., and van Brandenburg, R. "Inter-destination multimedia synchronization: Schemes, use cases and standardization," *Multimedia Systems,* vol. 18, no. 6, pp. 59-482, 2012.

[4] Li, M., Sun, Y., and Sheng, H. "Temporal relations in multimedia systems," *Computers & Graphics*, vol. 21, no. 3, pp. 315-320, 1997.

[5] Blakowski, G., and Steinmetz, R. "A media synchronization survey: Reference model, specification, and case studies," *IEEE J. Sel. Areas Commun.*, vol. 14, no. 1, pp. 5-35, 1996.

[6] Akyildiz, I.F., and Yen, W. "Multimedia group synchronization protocols for integrated services networks," *IEEE J. Sel. Areas Commun.*, vol. 14, no. 1, pp. 162-173, 1996.

[7] Park, S., and Choi, Y. "Real-time multimedia synchronization based on delay offset and playout rate adjustment," *Real-Time Imaging*, vol. 2, no. 3, pp.163-170, 1996.

[8] Park, S., and Kim, J. "An adaptive media playout for intra-media synchronization of networked-video applications," *Journal of Visual Commun. and Image Representation*, vol. 19, no. 2, pp.106-120, 2008.

[9] Laoutaris, N., and Stavrakakis, I. "Intrastream synchronization for continuous media streams: A survey of playout schedulers," *IEEE Network*, vol. 16, no. 3, pp. 30-40, 2002.

[10] Aggarwal, S. and Jindal, A. "Comprehensive overview of various lip synchronization techniques," *Int. Symposium on Biometrics and Security Technologies*, ISBAST 2008, pp.1-6, 23-24 April 2008.

[11] Ishibashi, Y., Tasaka, S., and Miyamoto, H. "Joint synchronization between stored media with interactive control and live media in multicast communications," *IEICE Trans. on Communications*, vol. E85-B, no. 4, pp.812–822, 2002.

[12] Wongwirat, O., and Ohara, S. "Haptic media synchronization for remote surgery through simulation," *IEEE MultiMedia*, vol. 13, no. 3, pp.62–69, 2006.

[13] Hikichi, K., Morino, H., Arimoto, I., Sezaki, K., and Yasuda, Y. "The evaluation of delay jitter for haptic collaboration over the Internet," In *Proc. of IEEE Global Commun. Conference (GLOBECOM)* (pp. 1492-1496), 2002.

[14] Ishibashi, Y., Tasaka, S., and Hasegawa, T. "The Virtual-Time Rendering algorithm for haptic media synchronization in networked virtual environments," In *Proc. of the 16th Int. Workshop on Communications Quality and Reliability* (pp. 213-217), 2002.

[15] Isomura, E., Tasaka, S., and Nunome, T. "QoE enhancement in audiovisual and haptic interactive IP communications by media adaptive intra-stream synchronization," In *Proc. of IEEE TENCON* (pp. 1085-1089), 2011.

[16] Boronat, F., Lloret, J., and García, M. "Multimedia group and inter-stream synchronization techniques: A comparative study," *Information Systems*, vol. 34, no. 1, pp. 108-131, 2009.

[17] Din, S., and Bulterman, D. "Synchronization techniques in distributed multimedia presentation," *MMEDIA 2012: The Fourth Int. Conferences on Advances in Multimedia* (pp.1-9), 2012.

[18] Ishibashi, Y., Tsuji, A., and Tasaka, S. "A group synchronization mechanism for stored media in multicast communications," In *Proc. of the Sixth Annual Joint Conference of the IEEE Computer and Communications Societies* (INFOCOM), (vol. 2, pp. 692–700). Kobe, Japan: IEEE Press, 1997.

[19] Sithu, M., and Ishibashi, Y. "Media synchronization control in multimedia communication," In D. Kanellopoulos (Ed.), *Emerging Research on Networked Multimedia Communication Systems* (pp.25-61). Hershey, PA: Information Science Publishing, 2015.

[20] Boronat, F., Guerri, J.C., and Lloret, J. "An RTP/RTCP based approach for multimedia group and inter-stream synchronization," *Multimedia Tools Appl J*, vol. 40 no. 2, pp. 285-319, 2008.

[21] Boronat, F., Montagud, M., and Vidal, V. "Master selection policies for inter-destination multimedia synchronization in distributed applications," In *Proc. of the IEEE 19th Int. Symposium on MASCOTS*, (pp. 269-277), 2011.

[22] Ishibashi, Y., and Tasaka, S. "A group synchronization mechanism for live media in multicast communications," In *Proc. of the IEEE GLOBECOM' 97*, November 1997, (pp.746–752), 1997.

[23] Mauve, M., Vogel, J., Hilt, V., and Effelsberg, W. "Local-lag and timewarp: Providing consistency for replicated continuous app," *IEEE Trans. Multimedia*, vol. 6, no. 1, pp. 47-57, 2004.

[24] Diot, C., and Gautier, L. "A distributed architecture for multiplayer interactive applications on the Internet", *IEEE Network*, vol. 13, no. 4, pp. 6-15, 1999.

[25] Ishibashi, Y., and Tasaka, S. "A distributed control scheme for causality and media synchronization in networked multimedia games", in *Proc. of the 11th Int. Conference on Computer Communications and Networks*, Miami, USA, October 2002, pp. 144–149.

[26] Cronin, E. Filstrup, B. Jamin, S. and Kurc, A.R. "An efficient synchronization mechanism for mirrored game architectures", *Multimedia Tools Appl.*, vol. 23 no. l, pp. 7-30, 2004.

[27] Palazzi, C.E., Ferretti, S., Cacciaguerra, S., and Roccetti, M. "On maintaining interactivity in event delivery synchronization for mirrored game architectures", in *IEEE Global Telecommunications Conference Workshops*, Dallas, TX, USA, November/December 2004, pp. 157–165.

[28] Hashimoto, T. and Ishibashi, Y. "Group synchronization control over haptic media in a networked real-time game with collaborative work", in *Proc. of the Fifth ACM SIGCOMM workshop on Network and System Support for Games,* Singapore, October 2006.

[29] Boronat, F., Guerri, J.C., Esteve, M., & Murillo, J.M. "RTP-based feedback global protocol integration in Mbone tools", EUROMEDIA 2002, Modena, Italy (Best Paper Award) April 2002.

[30] Kaneoka, H., and Ishibashi, Y. "Effects of group synchronization control over haptic media in collaborative work", in: *Proc. of the 14th Int. Conference on Artificial Reality and Telexistence* (ICAT'04), Coex, Korea, November/December 2004, pp. 138–145.

[31] Kurokawa, Y., Ishibashi, Y., and Asano, T. "Group synchronization control in a remote haptic drawing system", in: *Proc. of the IEEE International Conference on Multimedia and Expo*, Beijing, China, July 2007, pp. 572–575.

[32] Schulzrinne, H., Casner, S., Frederick, R., and Jacobson, V. "RTP: a transport protocol for real-time applications", RFC–3550, July 2003.

[33] ETSI TS 181 016 V3.3.1 (2009-07). *Telecommunications and Internet converged Services and Protocols for Advanced Networking (TISPAN); Service Layer Requirements to integrate NGN Services and IPTV.*

[34] Montagud, M., and Boronat, F. "Enhanced adaptive RTCP-based inter-destination multimedia synchronization approach for distributed applications," *Computer Networks*, vol. 56, no. 12, pp. 2912-2933, 2012.

[35] van Brandenburg, R.H.O.F.M.K., Stokking, H., van Deventer, O., Boronat, F., Montagud, M., and Gross, K. "Inter-Destination Media Synchronization (IDMS) using the RTP Control Protocol (RTCP)", RFC–7272, 2014.

[36] van Deventer, M. O., Stokking, H., Hammond, M., Le Feuvre, J., and Cesar, P. "Standards for multi-stream and multi-device media synchronization," *IEEE Communications Magazine*, vol. 54, no. 3, pp.16-21, 2016.

[37] Montagud, M., Jansen, J., Cesar, P., and Boronat, F. "Review of media sync reference models: Advances and open issues," *MediaSync2015 Workshop*, ISBN: 978-90-5968-463-4, 2015.

[38] Huang, Z., Nahrstedt, K., and Steinmetz, R. "Evolution of temporal multimedia synchronization principles: A historical viewpoint," *ACM Trans. on Multimedia Computing, Commun., and Applications*, vol. 9, no.1. Article 34, 23 pages, 2013.

[39] Montagud, M., Boronat, F., Stokking, H., and Cesal, P. "Design, development and assessment of control schemes for IDMS in a standardized RTCP-based solution," *Computer Networks*, vol. 70, no. 9, pp.240-259, 2014.

[40] Costa, R., and Santos, C.A.S. "Systematic review of multiple contents synchronization in interactive television scenario," *ISRN Commun. and Networking*, Volume 2014, Article ID 127142, pp. 1-17, 2014.

[41] Marfil, D., Boronat, F., Montagud, M., and Sapena, A. "IDMS solution for hybrid broadcast broadband delivery within the context of HbbTV standard". *IEEE Transactions on Broadcasting*, 2018.

[42] Ishibashi, Y., Hoshino, S., Zeng, Q., Fukushima, N., and Sugawara, S. "QoE assessment of fairness in networked game with olfaction: Influence of time it takes for smell to reach player," *Multimedia Systems*, vol. 20, no. 5, pp. 621-631, 2014.

[43] Ghinea, G., and Ademoye, O. A. "Perceived synchronization of olfactory multimedia," *IEEE Trans. on Systems, Man and Cybernetics*, vol. 40, no. 4, pp. 657-663, 2010.

[44] Bello, M. A. O., Dominguez, E. L., Hernandez, S. E. P., and Cruz, J. R. "Synchronization protocol for real time multimedia in mobile distributed systems," *IEEE Access*, vol. 6, pp.15926-15940, 2018.

[45] Huang, C.-M., Kung, H.-Y., and Yang, J.-L. "Synchronization and flow adaptation schemes for reliable multiple-stream transmission in multimedia presentations," *Journal of Systems and Software*, vol. 56, no. 2, pp. 133-151, 2001.

[46] Belda, J., Montagud, M., Boronat, F., Martinez, M., and Pastor, J. "Wersync: A web-based platform for distributed media synchronization and social interaction," In *Proc. ACM Int. Conf. on Interactive Experiences for Television and online Video (TVX 2015)*, 2015.

[47] Rainer, B., Petscharnig, S., and Timmerer, C. "Merge and Forward: A self-organized inter-destination media synchronization scheme for adaptive media streaming over HTTP," In *MediaSync* (pp. 593-627). Springer, Cham., 2018.

[48] Sodagar. I. "The MPEG-DASH standard for multimedia streaming over the Internet," *IEEE MultiMedia*, vol. 18 no.4, pp.62-67, 2011.

[49] Kwon, D., Kim, H., and Ju, H. (2018). "PlaySharing: A group synchronization scheme for media streaming services in hierarchical WLANs," *Int. J. of Netw. Management*, vol. 28 no. 6, e2024, 2018.

[50] Daghighi, B., Kiah, M.L.M., Shamshirband, S., Iqbal, S., and Asghari, P. "Key management paradigm for mobile secure group communications: Issues, solutions, and challenges," *Computer Communications*, vol. 72, pp. 1-16, 2015.

[51] Huang, Z., Wu, W., Nahrstedt, K., Rivas, R., and Arefin, A. "SyncCast: synchronized dissemination in multi-site interactive 3D tele-immersion". In *Proc. of the second annual ACM conference on Multimedia systems* (pp. 69-80). ACM. 2011.

[52] Bin-Salem, A., and Wan, T. "Survey of cross-layer designs for video transmission over wireless networks," *IETE Technical Review*, vol. 29, no. 3, pp. 229-247, 2012.

[53] Jung, T., and Seo, K. "A client-driven media synchronization mechanism for RTP packet-based video streaming," *Journal of Real-Time Image Processing*, vol. 12 no. 2, pp. 455-464, 2016.

Dimitris N. Kanellopoulos is a member of the Educational Software Development Laboratory in the Department of Mathematics at the University of Patras, Greece. He received a Diploma in Electrical Engineering and a Ph.D. in Electrical and Computer Engineering from the University of Patras. Since 1990, he was a research assistant in the Department of Electrical and Computer Engineering at the University of Patras and involved in several EU R&D projects. He is a member of the IEEE Technical Committee on Multimedia Communications. He serves as a reviewer for highly-respected journals such as: *J. Netw. Comput. Appl.* (Elsevier), *Int. J. of Commun. Systems* (Wiley), *J. of Systems and Software (Elsevier), Information Sciences* (Elsevier), *IETE Technical Review, Electronics* (MDPI), etc. He has served as a technical program committee member to many international conferences. His current research interests are multimedia networking and wireless ad hoc networks. He has many publications to his credit in international journals and conferences at these areas. He has edited two books on Multimedia Networking, while he serves as an editorial board member in some refereed journals.

Combining Alamouti STBC with Block Diagonalization for Downlink MU-MIMO System over Rician Channel for 5G

Cebrail ÇiFTLiKLi and Musaab AL-OBAIDI

Abstract— **Wireless communication faces a number of adversities and obstacles as a result of fading and co-channel interference (CCI). Diversity with beamformer techniques may be used to mitigate degradation in the system performance. Alamouti space-time-block-code (STBC) is a strong scheme focused on accomplishing spatial diversity at the transmitter, which needs a straightforward linear processing in the receiver. Also, high bit-error-rate (BER) performance can be achieved by using the multiple-input multiple-output (MIMO) system with beamforming technology. This approach is particularly useful for CCI suppression. Exploiting the channel state information (CSI) at the transmitter can improve the STBC through the use of a beamforming precoding. In this paper, we propose the combination between Alamouti STBC and block diagonalization (BD) for downlink multi-user MIMO system. Also, this paper evaluates the system performance improvement of the extended Alamouti scheme, with the implementation of BD precoding over a Rayleigh and Rician channel. Simulation results show that the combined system has performance better than the performance of beamforming system. Also, it shows that the combined system performance of extended Alamouti outperforms the combined system performance without extended Alamouti. Furthermore, numerical results confirm that the Rician channel can significantly improve the combined system performance.**

Index Terms— **Fading, CCI, STBC, Alamouti, MIMO, Beamforming, BD, CSI.**

I. INTRODUCTION

Today's wireless network's customers need to more quality of service (QoS). Therefore, fifth generation (5G) of wireless networks promises to deliver that and much more. It is highly expected that future 5G networks should achieve a 10-fold increase in connection density, i.e., 10^6 connections per square kilometers [1] and increase in the volume of mobile traffic, e.g., beyond a 500-1000-fold increase in mobile traffic [2]. Unfortunately, the current radio access technology, within the limited available time/frequency spectrum, is facing challenges to meet the requirements of technological advances presented by the 5G network. Therefore, new solutions must be identified and developed that can make significant gains in capacity and QoS for network customers to ensure continued sustainability of radio access technologies. To date, 5G is still being studied; and research groups and companies are working together to determine the exact nature of 5G. On the other hand, it is not yet clear which technologies will do the most for 5G in the long run, but a few early favorites have emerged. The front-runners include beamforming technology. At once, it is possible to achieve signal-to-noise-plus-interference-ratio (SINR) improvements through the adoption of beamforming precoding at the transmit side [3]. There is the potential to utilise a block diagonalization (BD) initiative to design transmitting beamforming vectors without any degree of complexity. One such approach is to secure a precoding matrix for all mobile stations. This type of matrix will lie in the null spaces of other mobile stations' channel matrix, and thus, the beamforming approach may be seen to depend on each mobile station's spatial data [4]. Unfortunately, the desired power of the received signal will be decreased. The BD algorithm that supports multiple-stream transmissions for multi-user MIMO (MU-MIMO) systems, in which every user has several antennas trying to connect with the base station, can eliminate the co-channel interference (CCI) completely [5]. When no information concerning the channel state information (CSI) is held by a MIMO system sender, spatial multiplexing and multi-user diversity are not possible [6]. Additional profits can accrue when the CSI at the transmitter is available and using a MIMO system with a liner precoding technique [7]. If all mobile stations' channel state information is available in the transmitter, the precoder would then have the ability to completely remove CCI. By removing CCI, each user can communicate with the transmitter over an interference-free way, as single-user channel [3]. Therefore, through an imperfect feedback channel, reconnaissance of limited CSI and employment of CSI are critical points for a MIMO system [8]. CSI is very important, because when it is fully available at the base station, the MIMO system performs best in numerous ways via using the precoding method. For example, to mitigate symbol interference, precoding can be used with spatial diversity and spatial multiplexing provided by the MIMO system. Besides high gain coding, if space-time-block-code (STBC) can be combined with precoding, maximum gain diversity is available [9]. Owing to the use of wireless fading channels, it is common for error performance to demonstrate further degradation in terms of the wireless network's mobile communication system.
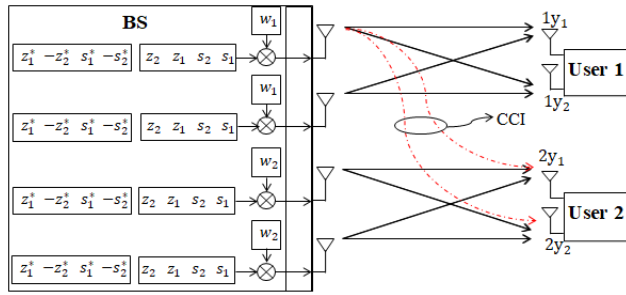
Fig. 1. Block diagram of the proposed MU-MIMO system, s is the data of 1st
user and z is the data of 2nd user.

It is important to note that, diversity has become recognised as a key communication approach when seeking to enhance the performance of wireless systems without incurring significant expense [10] [11]. Diversity, in essence, may be achieved at the transmitter and/or the receiver side [10]. However, should diversity be received in an instance of downlink, there will be a notably high consumption of power, owing to the fact that the majority of computational burden is assigned to the mobile side. Accordingly, a non-complex decoding processing can be achieved at the mobile side through the base station-located application of STBC [10] [12] [13] [14].

The primary and most well-recognised diversity is identified as the STBC, which has come to be accepted as a powerful and extremely valuable diversity approach in overcoming the effects of wireless channel fading. In this regard, the Alamouti scheme is seen to be a complicated orthogonal STBC; this affords simplistic decoding and encoding processing at the receiver and transmitter side, respectively. This was originally devised and presented by Alamouti [15]. In an effort to decrease error performance degradation levels in mobile units and accordingly attain greater improvements in wireless links, the Alamouti scheme can be combined with beamforming precoding [16] [17] [18] [19]. Beamforming scheme based on BD technology combined with STBC enables the multi-user MIMO (MU-MIMO) system to provide good QoS, thereby absorbing more users, and makes it promising to address the 5G requirement of massive connectivity, specifically in the Internet of things (IoT) and massive machine-type communications (mMTC) scenarios, which are considered as types of 5G application scenarios [20]. In these scenarios, users may be low-cost sensors deployed in a small area, where both the line-of-sight (LoS) and the non-line-of-sight (NLoS) exist, which can be better modeled by the Rician fading channel. In [21] and [22], 5G cellular systems on MU-MIMO transmitters use linear precoding. In this report, the system performance within regards to the Alamouti scheme undergoes both analysis and evaluation, with BD precoding applied when there is the presence of CSI. Furthermore, the performance of an MU-MIMO beamforming system, alongside the utilisation of BD with the extended Alamouti scheme, is discussed, with the signal in the NLoS setting transmitted (Rayleigh fading channel) as well as in the LoS environment (correlated realistic Rician fading channel).

The superscripts$(\cdot)^{T}$, $(\cdot)^{*}$ and $(\cdot)^{H}$ denote transpose, complex conjugate, and Hermitian operations, respectively.

II. ALAMOUTI CODING

The Alamouti code is recognised as being the first and most widely known STBC, and is described as being a complicated orthogonal spice-time-code most applicable in the case of two transmits antennas [15].

Primarily, the Alamouti space-time-coding approach is taken into account, with generalisation in relation to the three transmits antennas then considered [23].

a. Alamouti Space-Time Code

Alamouti designed and presented a complicated orthogonal space-time block code for two transmit antennas [15]. In the case of the Alamouti encoder, there is the encoding of s_1 and s_2 , notably two consecutive symbols complete with the space-time codeword matrix outlined below:

$$S_{A\ 2.antenna} = \begin{bmatrix} s_1 & -s_2^* \\ s_2 & s_1^* \end{bmatrix} \tag{1}$$

As can be seen when reviewing the equation (1), there is the transmission of the Alamouti encoded signal from the two transmit antennas over the two different symbol periods. Throughout the preliminary symbol period, s_1 and s_2 are transmitted at the same time from the two transmit antennas. Throughout the secondary period, there is the repeated transmission of the symbols, with the first transmit antenna transmitting $-s_2^*$ whilst the second transmit antenna transmits s_1^*.

b. Extended Alamouti

As has been discussed in other works [24], the Alamouti scheme has the underpinning foundation of extension, which is seen to derive through extension for 4x1-diversity order. In this case, it is further extended in mind of the 3x3-diversity order [10]. Accordingly, it is necessary to take into account the block diagram representation depicted in the Fig. 2 below, which shows the extended Alamouti code for 3 transmit antennas and 3 receive antennas over the eight different symbol periods for four symbols s_1, s_2, s_3 and s_4.

$$S_{A\ 3.antenna} =$$

$$\begin{bmatrix} s_1 & -s_2 & -s_3 & -s_4 & -s_1^* & s_2^* & s_3^* & s_4^* \\ s_2 & s_1 & s_4 & -s_3 & s_2^* & s_1^* & s_4^* & s_3^* \\ s_3 & -s_4 & s_1 & s_2 & -s_3^* & -s_4^* & s_1^* & s_2^* \end{bmatrix} \tag{2}$$
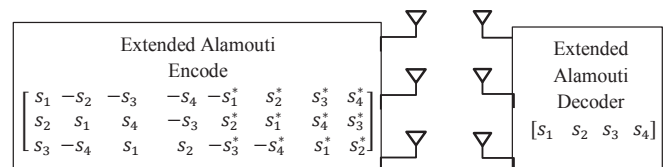

Fig. 2 Extended Alamouti Scheme for 3x3.

III.   MU-MIMO BEAMFORMING SYSTEM MODEL

In MU-MIMO system we have considered an environment of U geographically sparse mobile stations as multi-user (MU) communicates with the MIMO base station (BS) which has M antennas. In such a system environment, each mobile station is independent and employing N_u antennas of user u. These users will receive their own signal, as shown in Fig.1 (block diagram of 2 users). The total number of users' antennas is defined as;

$$N_T = \sum_u^U N_u \qquad (3)$$

Also, this system has an operation condition which is $N_T = M$ with the independent channels of flat fading. The meant message signal for the uth user is the scalar S_u. Thereby, the transmitted symbol vector to U users is:

$$S_T = [s_1, \ldots, s_u, \ldots, s_U]^T \qquad (4)$$

It should be mentioned that $S_u = S_{A\ 2.antenna}$ for two transmit antennas and $S_u = S_{A\ 3.antenna}$ for three transmit antennas. In the second step, we denote to precoding matrix step as:

$$W = [w_1, \ldots, w_u, \ldots, w_U] \qquad (5)$$

where $w_u \in C^{N_u \times M}$ is the joint beamforming coefficients for uth user. Then the transmitted symbol vector is multiplied by the precoding matrix as third step to produce the precoding data as:

$$X = \sum_{u=1}^U w_u s_u = WS \qquad (6)$$

The symbol s_u and the coefficients of beamforming precoding w_u will be normalized as follows:

$$E|s_u|^2 = 1, \|w_u\|^2 = 1$$
$$for\ u=\{1, \ldots, U\}.$$

In the broadcast step, we assumed that signals $WS \in C^{N_u \times M}$ are broadcasted over the channels denoted as:

$$H = [H_1^T, \ldots, H_u^T, \ldots, H_U^T]^T \qquad (7)$$

where $H_u \in C^{N_u \times M}$ describes the channel coefficients between N_u receiver antenna at uth user and BS antennas as:

$$H_u = \begin{bmatrix} h_u^{(1,1)} & \cdots & h_u^{(1,M)} \\ \vdots & \ddots & \vdots \\ h_u^{(N_U,1)} & \cdots & h_u^{(N_U,M)} \end{bmatrix} \qquad (8)$$

where $h_u^{(n,m)}$ denotes the channel matrix ingredient, which is located between the mth transmitter array antenna of base station and the nth receiver array antenna of uth user. Thus, at users' antennas the received signals are:

$$y = [y_1^T, \ldots, y_u^T, \ldots, y_U^T]^T = H\ WS + n \qquad (9)$$

where $y_u \in C^{N_u \times M}$ is representing the signal which is received at uth recipient, whilst for the additive noise is denoted by n. When we have given careful consideration to each user separately, we will find the received signal at an ith recipient as:

$$y_i = H_i \sum_{u=1}^U w_u s_u + n_i$$

$$y_i = H_i w_i s_i + H_i \sum_{u=1,u\neq i}^U w_u s_u + n_i$$

$$y_i = H_i x_i + H_i \sum_{u=1,u\neq i}^U x_u + n_i \qquad (10)$$

where x_i is precoding data of ith user and x_u is precoding data of other users as interference for uth user. The H_i vector has complex Gaussian variable components with unit-variance and zero-mean. Moreover, the components of the additive noise n_i have distribution as $N(0,\sigma_i^2)$ and are temporarily white.

IV.   DOWNLINK CHANNEL MODEL

Due to LoS propagation the strongest propagation component of MIMO channel corresponds to deterministic component (also referred to as specular components). On the other hand, all the other components are random components (due to NLoS also referred to as scattering components) [10]. The broadcast channel distribution has been following the Rayleigh channel distribution, which is Gaussian distribution with a variance of σ^2 and zero mean. That means there is no component of LoS ($K= 0$): $\sigma = \sqrt{\frac{1}{K+1}}$. On the other hand, when there is any component of LoS (For $K > 0$) the broadcast channel distribution has been following the Gaussian distribution with a variance of σ^2 and mean of q or Rician distribution when K increases as: $q = \sqrt{\frac{K}{K+1}}$, $\sigma = \sqrt{\frac{1}{K+1}}$.

Therefore, in this work, channel matrix of the MIMO system described as [25]:

$$H = \sqrt{\frac{K}{K+1}}\ H_d + \sqrt{\frac{1}{K+1}}\ H_r \qquad (11)$$

where H_d representing the component of the normalized deterministic channel matrix, while H_r representing the component of random channel matrix, with $\|H_d\|^2 = N_T\ M$, $E\{|[H_r]_{i,j}|^2\} = 1$, $i = 1: N_T$, $j = 1: M$ [25]. While K is known

as factor of the Rician channel which is the relation between the component of the specular power c^2 and the component of scattering power $2\sigma^2$, displayed as [10]:

$$K = \frac{\|H_d\|^2}{E\left\{|[H_r]_{i,j}|^2\right\}} = \frac{c^2}{2\sigma^2} \qquad (12)$$

V. BLOCK DIAGONALIZATION PRECODING

Block Diagonalization precoding (BD) method is compatible with the multiple users, every user has multiple antennas. By the precoding process of this method, the interference signal which is coming from other user signals will be canceled. Therefore, MU-MIMO channel model will be converted into multiple independent single user MIMO channels model by BD method [10].

Briefly, definition of BD precoding matrix starts from the channel of all users except ith user as:

$$\tilde{H}_i = [H_1 \ldots H_{i-1} \ H_{i+1} \ldots H_U]^T \qquad (13)$$

where $\tilde{H}_i$ is H with out H_i , then we should compute the null space $\tilde{V}_i^{ns}$ of all users except ith user by singular value decomposition (SVD) to $\tilde{H}_i$:

$$SVD \ of \ \tilde{H}_i = \tilde{U}_i \ \tilde{\Lambda} \ [\ \tilde{V}_i^b \ \ \tilde{V}_i^{ns} \ ]^H \qquad (14)$$

where $(.)^H$ denotes Hermitian transposition. To prevent other users interference multiplies H_i by $\tilde{V}_i^{ns}$, and then uses SVD again:

$$SVD \ of \ H_i \tilde{V}_i^{ns} = U_i \ \Lambda \ [\ V_i^b \ V_i^{ns} \ ]^H \qquad (15)$$

where V_i^{ns} is the null space of ith user, while V_i^b is the beam of ith user. Therefore, we can get the precoding matrix w_i for ith user from $\tilde{V}_i^{ns}$ and V_i^b under the condition $N_T \leq M$ as:

$$w_i = [\tilde{V}_i^{ns} \ V_i^b \ ] \qquad (16)$$

Now under the condition $\tilde{H}_i \tilde{V}_i^{ns} = 0$, we substitute (16) into (10), we can obtain:

$$y_i = H_i x_i + 0 + n_i \qquad (17)$$

where y_i represents the received signal which is consisted of the required signal of ith user and noise without multiuser interference. Note that x_i is Alamouti space-time coding. Therefore, y_i is represented by $1y_{1a}$, $1y_{2a}$, $2y_{1a}$ and $2y_{2a}$:

$$\begin{bmatrix} 1y_{1a} & 2y_{1a} \\ 1y_{2a} & 2y_{2a} \end{bmatrix} = H_i \ w_i \begin{bmatrix} s_1 & -s_2^* \\ s_2 & s_1^* \end{bmatrix} + n_i \qquad (18)$$

where $1y_{1a}$ and $1y_{2a}$ represents the received signals at the first time in first and second antenna respectively, while $2y_{1a}$

and $2y_{2a}$ represents the received signals at the second time in first and second antenna respectively:

1st time

$$1y_{1a} = \left[h_i^{(1,1)} \ldots \ h_i^{(1,M)}\right] w_i \begin{bmatrix} s_1 \\ s_2 \end{bmatrix} + n_i \qquad (19)$$

$$1y_{2a} = \left[h_i^{(2,1)} \ldots \ h_i^{(2,M)}\right] w_i \begin{bmatrix} s_1 \\ s_2 \end{bmatrix} + n_i \qquad (20)$$

2nd time

$$2y_{1a} = \left[h_i^{(1,1)} \ldots \ h_i^{(1,M)}\right] w_i \begin{bmatrix} -s_2^* \\ s_1^* \end{bmatrix} + n_i \qquad (21)$$

$$2y_{2a} = \left[h_i^{(2,1)} \ldots \ h_i^{(2,M)}\right] w_i \begin{bmatrix} -s_2^* \\ s_1^* \end{bmatrix} + n_i \qquad (22)$$

then:

$$1y_{1a} = C \, s_1 + D \, s_2 + n_i, \quad 2y_{1a} = D \, s_1^* - C \, s_2^* + n_i \quad (23)$$

$$1y_{2a} = Q \, s_1 + P \, s_2 + n_i, \quad 2y_{2a} = P \, s_1^* - Q \, s_2^* + n_i \quad (24)$$

where C, D, Q and P represents the multiplication of channel by precoding of each antenna.

To find s_1 and s_2, we assume that CSI at the mobile stations is available. Then multiplying the received signals by the Hermitian transpose of the CSI matrix and using Maximum Likelihood (ML) concepts:

$$\hat{s}_1 = \frac{C^* \, 1y_{1a} \ + \ Q^* 1y_{2a} \ + \ D \, 2y_{1a}^* \ + \ P \, 2y_{2a}^*}{C^*C \ + \ Q^*Q \ + \ D^*D \ + \ P^*P} \qquad (25)$$

$$\hat{s}_2 = \frac{D^* \, 1y_{1a} \ + \ P^* \, 1y_{2a} \ - \ C \, 2y_{1a}^* \ - \ Q \, 2y_{2a}^*}{C^*C \ + \ Q^*Q \ + \ D^*D \ + \ P^*P} \qquad (26)$$

where $\hat{s}_u$ denote noisy version of s_u.

VI. SIMULATION RESULTS AND EVALUATION

In the present work, the signal-to-noise ratio (SNR) in comparison to the BER undergoes assessment as a precoding efficiency scale. A common MU-MIMO scheme was completed in mind of predicting the performance of the MU-MIMO beamforming precoding suggestion, alongside with the Alamouti STBC scheme over a Rician fading channel in contrast to the same scheme in the case of a Rayleigh fading channel. The parameter samples have been devised up to 10,000, encompassing elements created as zero-mean in the case of the Rayleigh fading channel, whereas for the Rician fading channel, there was the m-mean and unit-variance independently and identically distributed (i.i.d) complex Gaussian random variables. Notably, the M antennas of BS transmitted the signal across all users over the noise and flat fading channel, while each user employed Nu antennas to receive the signal. There was the application of a QPSK signal

constellation as a form of broadcast modulation across all
instances of simulation, with the findings then undergoing
averaging through the implementation of different channel
investigations. For all receivers, the noise variance per
receiver antenna should be equal, $\sigma_1^2 = \ldots = \sigma_K^2 = \sigma^2$. The
typical values and simulation parameters are presented in
Table 1.

Table 1.
Typical values and simulation parameters

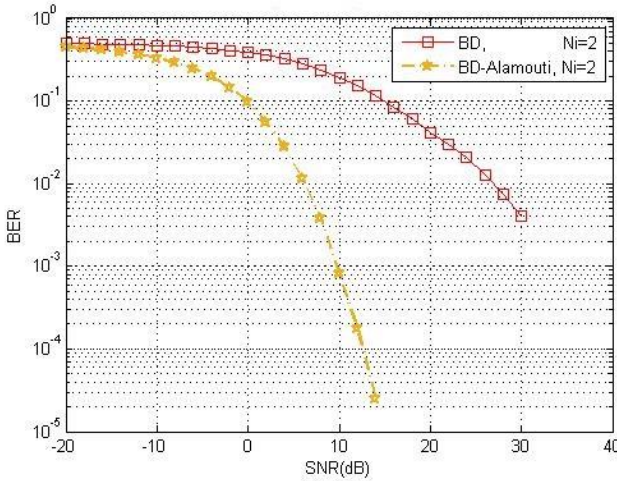| Parameters	Definition
Channel type	Rayleigh and Rician
Number of users (U)	2, 3
Number of antenna for BS (M)	4, 6, 9
Number of antenna for each user (Ni)	2, 3
Rician channel factor (K)	5, 10, 15

Fig. 3. A MU-MIMO system over Rayleigh channel, $U = 2$ and
Ni=2.

As can be seen in Fig. 3, in the scenario of classical BD
beamforming precoding scheme, system performance
demonstrates improvement, albeit in a gradual but continuous
pattern, with SNR values showing increases. While in the case
of combined BD beamforming with Alamouti STBC,
significant improvement could be seen at any value of SNR.
In other words, the combined scheme enjoys better
performance than the classical BD beamforming precoding
scheme. This is because we use both BD beamforming and
Alamouti STBC: for multiuser interference, we use the
advantage of BD beamforming; for fading channel, we use the
advantage of STBC.

scheme. This is because we use both BD beamforming and
Alamouti STBC: for multiuser interference, we use the
advantage of BD beamforming; for fading channel, we use the
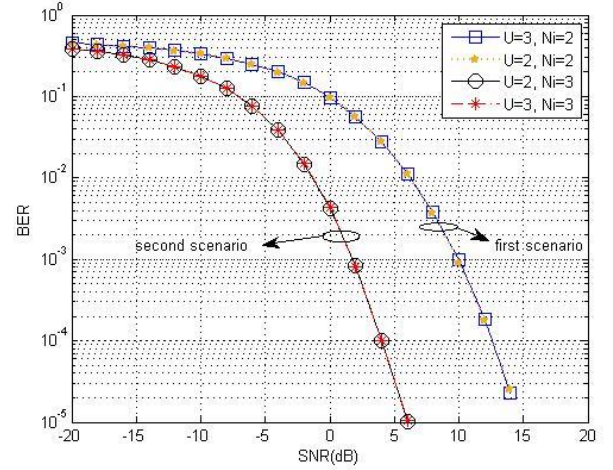advantage of STBC.

Fig. 4. A combined scheme over Rayleigh channel for different
scenarios

Fig. 4 demonstrates the performance of the combined BD
beamforming with Alamouti STBC scheme with different
value of N_i and U. In the first scenario, each user has two
receives antennas ($N_i = 2$), two cases are investigated: two
users system with 4 transmit antennas at the BS; and 3 users
system with 6 transmit antennas at BS. The second scenario
has the extended Alamouti STBC scheme when each user has
three receives antennas ($N_i = 3$), two cases are investigated:
two users system with 6 transmit antennas at the BS; and 3
users system with 9 transmit antennas at BS. In Fig. 4, it is
shown that the two user system achieves almost the same
performance with a 3-user system in first scenario, which is
consistent with our analysis in BD beamforming and Alamouti
STBC. The downlink precoder completely eliminates
multiuser interference at each mobile, and full spatial diversity
is achieved by Alamouti codes. Similarly, in the second
scenario, the two user system achieves the same performance
with a 3-user system. In the second scenario higher diversity
gain greatly improves the BER performance, as compared to
the performance of the first scenario. Figs. 5 and 6 further
show that in the LoS environment (over a correlated realistic
Rician fading channel) the performance of combined system is
greater when contrasted alongside the performance of the
NLoS (over a Rayleigh fading channel) setting. The high
value of Rician's factor has the ability to decrease error rate.
To better understand the behavior of the combined scheme,
the BER is plotted with different values of K to show and
compare the two cases of first scenario in Fig. 5 and the two
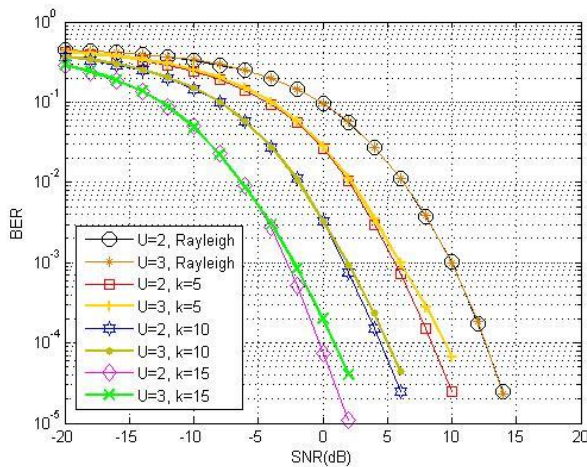cases of second scenario in Fig. 6.

Fig.5 A MU-MIMO system employed BD precoding with Alamouti STBC in
the LoS and NLoS environment with Ni=2.

The traditional combined beamforming with STBC have sensitive BER performance depending on the coefficient of the channel (K). This sensitivity of the system is also increased by increasing the value of SNR.
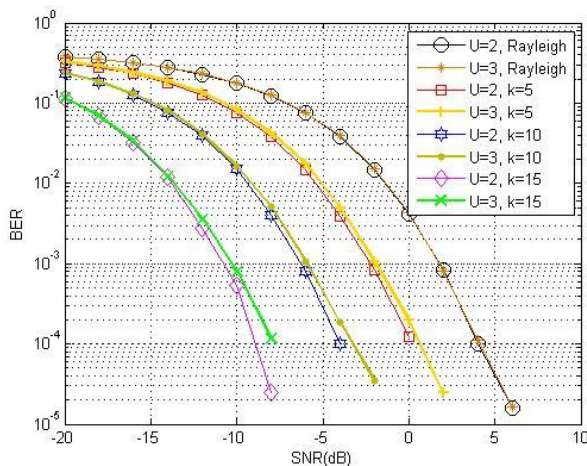

Fig. 6 A MU-MIMO system employed BD precoding with extended
Alamouti STBC in the LoS and NLoS environment with Ni=3.

In other words, unfortunately, the desired power of the signal reception will be reduced because the BD algorithm spends some of power as leakage power, which is represented as the interference power and it does completely cancel after the transmission. Therefore, the system over wireless channel will suffer from low desired power of the received signal, impact of fading channel and noise factors. For the system over Rayleigh fading channel (K< 0), the number of users does not affect the performance of the system along of SNR's values because the effect of fading channel was bigger than the effect of the leakage power and noise. Therefore, the

system of two users and the system of three users have same performance.

On the other hand, for the system over Ricain fading channel (K > 0), the low number of users does affect the performance of the system at high value of SNR because the major factor limiting the performance of the system was the leakage power and noise. Thus, over Ricain fading channel, the combined system with low number of users enjoys better performance when compared to high number of users at high SNR.

VII.   CONCLUSION

This report has suggested MU-MIMO download fading channel frameworks with the implementation of pragmatic beamforming through the approach of downlink precoding, encompassing STBC system's spatial diversity. Moreover, it further provides an analysis and evaluation centred on the application of a simple BD precoding method, which is seen to entirely eradicate CCI between any and all users at the same cell location. The broadcast through the downlink MU-MIMO channel by any transmitter uses the BD beamforming algorithm to look like as the broadcast through a downlink multiple independent single-users MIMO (SU-MIMO) channel system.

Consequently, a suitable environment for the use of Alamouti STBC scheme, which works in SU-MIMO system, was provided. It can be seen, when reviewing the simulation results, that the BD precoding with Alamouti STBC scheme's BER performance is better than only BD precoding performance, because BD beamforming precoding achieves more diversity when it combines with Alamouti STBC scheme. Furthermore, an extended Alamouti STBC scheme is able to provide significant improvements in performance of a combined system. The findings further demonstrate the effect of Rician fading channel on the proposed system, which it is represented the environment of some typical of 5G application scenarios.

REFERENCES

[1] F. Boccardi, R. W. Heath, A. Lozano, T. L. Marzetta, P. Popovski, "Five disruptive technology directions for 5G," IEEE Commun. Mag., vol. 52, no. 2, pp. 74–80, Feb. 2014.

[2] Y. Saito, A. Benjebbour, Y. Kishiyama, T. Nakamura, "System-level performance evaluation of downlink non-orthogonal multiple access (NOMA)," 24th Annual International Symposium on Personal, Indoor, and Mobile Radio Communications (PIMRC), London, 2013, pp. 611-6152013 IEEE.

[3] R. Chen, J. G. Andews, R. W. Health, "Multiuser Space-Time Block Coded MIMO System with Downlink Precoding" Communications, IEEE International Conference on (Volume:5) 2004.

[4] H. Liu, X. Cheng, Z. Zhou, G. Wu, "Block Diagonalization Eigenvalue Based Beamforming precoding design for Downlink Capacity Improvement in Multiuser MIMO channel," International Conference on Wireless Communications and Signal Processing (WCSP) 2010.

[5] Q. H. Spencer, A. L. Swindlehurst, and M. Haardt, "Zero-Forcing Methods for Downlink Spatial Multiplexing in Multiuser MIMO Channels," IEEE Trans. Signal, Process. vol. 52, no. 2, pp.461-471, February 2004.

[6] S. A. Jafar and A. Goldsmith, "On the capacity region of the vector fading broadcast channel with no CSIT," in Proc. IEEE ICC, Paris, Jun. 2004.

[7] D. Love, R. Heath, V. Lau, D. Gesbert, B. Rao, M. Andrews, "An overview of limited feedback in wireless communication systems," IEEE Journal on Selected Areas in Communications, vol. 26, no. 8, pp. 1341 1365, October 2008.

[8] F. Han, Y.-Z. Liu, G.-X. Zhu, J. Sun," A Multi-user Multi-beam Selection Scheme based on Orthonormal Random Beamforming for MIMO Downlink System, " Communications, Circuits and Systems. ICCCAS 2007. International Conference.

[9] X. Shi, C. Siriteanu, S. Yoshizawa, and Y. Miyanaga, "MIMO precoding performance for correlated and estimated Rician fading," in Proc. 11th Int. Symp. on Communications and Information Technologies, (ISCIT '11), Hangzhou, China, October 2011.

[10] Y. S. Cho, J. Kim, W. Y. Yang, C. G. Kang, "MIMO-OFDM Wireless Communications with Matlab," Wiley-IEEE Press, New York, p.544, 25 Aug 2010.

[11] V. Tarokh, H. Jafarkhani, and A .R. Calderbank, "Space-time block codes from orthogonal design," IEEE Trans. Info., vol. 45, no. 5, pp. 1456-1467, Jul. 1999.

[12] V. Tarokh, N. Seshadri, A.R. Calderbank, "Space-time codes for high data rate wireless communication: performance criterion and code construction," IEEE Trans. Inform. Theory, vol. 44, no. 2, pp. 744–765, 1998.

[13] B.L. Hughes, "Differential space-time modulation," IEEE Trans. Info. Theory, vol. 46, no. 7, pp. 2567–2578, 2000.

[14] B.M. Hochwald, and W. Sweldens, "Differential unitary space-time modulation," IEEE Trans. Commun., vol. 48, no. 2, pp. 2041–2052, 2000.

[15] S.M. Alamouti, "A simple transmit diversity scheme for wireless communications," IEEE J. Select. Areas Commun. vol. 16, no. 8, pp. 1451–1458, 1998.

[16] G. Jongrem, M. Skoglund, and B. Ottersten, "Combining beamforming and orthogonal space-time block coding," IEEE Trans. Info. Th., vol. 48, pp. 611-627, Mar. 2002.

[17] A. Scaglione, P. Stoica, S. Barbarossa, and G. B. Giannakis, "Optimal designs for space-time linear precoders and decoders," IEEE Trans. Sig. Proc., vol. 50, no. 5, pp. 1051-1064, May 2002.

[18] Y. Xin, Z. Wang, and G. B. Giannakis, "Space-time diversity systems based on linear constellation precoding," IEEE Trans. Wireless Commun., vol. 2, no. 2, pp. 294-309, Mar. 2003.

[19] D. J. Love, R. W. Heath, "Limited feedback unitary precoding for orthogonal space-time block codes," IEEE Trans. Signal Process, vol. 53, pp. 64-73, no. 1, Jan. 2005.

[20] R. Jiao, L. Dai, J. Zhang, R. MacKenzie, and M. Hao, "On the performance of NOMA-based cooperative relaying systems over Rician fading channels," IEEE Trans. Veh. Technol., vol. 66, no. 12, pp. 11409-11413, Dec. 2017.

[21] E. L. Bengtsson, F. Rusek, S. Malkowsky, F. Tufvesson, P. C. Karlsson, O. Edfors, "A simulation framework for multiple-antenna terminals in 5G massive MIMO systems," IEEE Access, vol. 5, no. 99, pp. 26819–26831, 2017.

[22] A. Gupta, R. K. Jha, "A survey of 5G network: Architecture and emerging technologies," IEEE Access, vol. 3, pp. 1206–1232, 2015.

[23] V. Tarokh, H. Jafarkhani, A.R. Calderbank, "Space-time bock coding for wireless communications: performance results" IEEE J. Sel. Areas Commun., vol. 17, no. 3, pp. 451–460, 1999.

[24] F. H. Gregorio, "Space Time Coding for MIMO Systems," Helsinki University of Technology, Signal Processing Laboratory, POB 3000, FIN-02015 HUT, Finland.

[25] X. Shi, C. Siriteanu, S. Yoshizawa, Y. Miyanaga, "Realistic Rician Fading Channel based Optimal Linear MIMO Precoding Evaluation," Communications Control and Signal Processing (ISCCSP), 2012.

Cebrail ÇiFTLiKLi was born in K. Maras, Turkey, in 1961. He received the Ph.D. degree in electronics engineering from Erciyes University in 1990. In 2004, he joined Erciyes University Kayseri Vocational College as Professor where he is now principal. Prof. Dr. Ciftlikli's current research interests include spread spectrum communications, wireless ATM/LAN, signal processing, DSCDMA system engineering, RF power amplifier linearization for wireless communication systems. Department of Electrical and Electronics Engineering, Erciyes University, Kayseri, Turkey.

Musaab AL-OBAIDI was born in Bagdad, Iraq, in 1981. 2000-2004 B.Sc. in department of Electrical engineering / Al-Mustanseria University / Iraq. 2010-2013 M.Sc. in Electrical Engineering / Universiti Tenaga Nasional / Malaysia. Since 2014 he is PhD student in Department of Electrical and Electronics Engineering, Erciyes University, Kayseri, Turkey.

Cost Function based Soft Feedback Iterative Channel Estimation in OFDM Underwater Acoustic Communication

Gang QIAO, Zeeshan Babar, Lu Ma and Xue LI

Abstract— **Underwater Acoustic (UWA) communication is mainly characterized by bandwidth limited complex UWA channels. Orthogonal Frequency Division Multiplexing (OFDM) solves the bandwidth problem and an efficient channel estimation scheme estimates the channel parameters. Iterative channel estimation refines the channel estimation by reducing the number of pilots and coupling the channel estimator with channel decoder. This paper proposes an iterative receiver for OFDM UWA communication, based on a novel cost function threshold driven soft decision feedback iterative channel estimation technique. The receiver exploits orthogonal matching pursuit (OMP) channel estimation and low density parity check (LDPC) coding techniques after comparing different channel estimation and coding schemes. The performance of the proposed receiver is verified by simulations as well as sea experiments. Furthermore, the proposed iterative receiver is compared with other non-iterative and soft decision feedback iterative receivers.**

Index Terms— **Channel Estimation, Equalization, Iterative Receiver, OFDM, Underwater Communication.**

I. INTRODUCTION

U NDERWATER Acoustic (UWA) communication is challenging because of the extremely limited bandwidth, slow speed of sound, multipath, delay spread, signal attenuation and ambient noise. The UWA channel makes it different from terrestrial communication. . Inter-symbol interference (ISI) and Inter-carrier interference (ICI) are introduced into the transmitted signal by the channel. Channel estimation estimates the channel parameters and equalization removes the effects of the channel on the received signal [1]. The role of channel estimation is of prime importance in designing any communication model. Different channel estimation schemes were applied to OFDM UWA

Gang Qiao and Lu Ma are with the College of Underwater Acoustic Engineering, Harbin Engineering University, Harbin 150001, China, and also with the Science and Technology on Underwater Acoustic Antagonizing Laboratory, Beijing, China.

Zeeshan Babar and Xue Li are with the College of Underwater Acoustic Engineering, Harbin Engineering University, Harbin 150001, China, and also with the Acoustic Science and Technology Laboratory and Key Laboratory of Marine Information Acquisition and Security, Harbin Engineering University, Harbin 150001, China (e-mail: babar_zeeshan; qiaogang; malu; xueli @hrbeu.edu.cn).

communication depending upon the requirement of the model [2]. Many such scheme are summarized and compared with each other in our review article previously [3]. Least Square (LS) is one of commonly used channel estimation scheme, where pilot tones are used for channel estimation [4]. In this case many subcarriers need to be assigned to pilot subcarriers and therefore the data rate is affected. To increase the efficiency, many iterative/adaptive channel estimation schemes were introduced and were proved to be more efficient as it reduces the number of pilots [5, 6]. Furthermore the performance of the iterative channel estimation depends on the type of decision feedback used; feedback methods like hard decision and soft decision feedback methods were introduced [7, 8]. Compressed sensing based channel estimation was introduced for sparse channels where a dictionary was used to formulate the channel coefficient vector [9]. Orthogonal Matching Pursuit is one such algorithm widely used for OFDM UWA communication [10].

Channel coding adds some redundancy in the useful bits in order to protect the data in noisy channel. Trellis Coded Modulation (TCM), convolutional codes, Reed Solomon (RS) codes, turbo codes, Space time trellis codes and low density parity check codes (LDPC) are the commonly used coding schemes used for UWA communication. LDPC code is preferred for noisy channels as its check matrix is sparse and the threshold can be set very near to Shannon capacity limit [11].

In this paper we propose an iterative receiver which exploits cost function based soft decision feedback orthogonal matching pursuit (OMP) channel estimation and LDPC coding /decoding schemes. The performance of the receiver is analyzed via simulations as well as experiments. The performance of the proposed receiver is compared with non-iterative and others soft and hard decision feedback iterative receivers. Furthermore in the experimental analysis, different combinations of channel estimation techniques and coding techniques are compared using the proposed feedback method.

The rest of the paper is organized as: section 2 gives the system model, section 3 proposes the receiver design and explains cost function based soft decision feedback method, the OMP channel estimation for UWA communication and LDPC coding scheme. Section 4 gives the results including simulation and experimental results, while section 5 concludes our work.

II. SYSTEM AND CHANNEL MODEL

Consider an OFDM system with symbol duration T and cyclic prefix interval T_{cp}, so that the total OFDM block duration is $T' = T + T_{cp}$. The subcarrier spacing is given by $\Delta f = 1/T$ and for total number of K subcarriers, the bandwidth can be given by $B = K/T$. The frequency of mth subcarrier is given by:

$$f_m = f_c + m/T, \quad m = -K/2,...,K/2-1 \qquad (1)$$

Where f_c denotes the center frequency. The passband signal transmitted is given by:

$$x(t) = 2\,\mathrm{Re}\left\{ \left[\sum_{m=-K/2}^{m=K/2} s[m]\mathrm{e}^{j2\pi f_m t} \right] \right\}, \quad t \in [0,T] \qquad (2)$$

Assume that the channel is time-invariant channel within each OFDM symbol, and the channel impulse response of the multipath channel with L number of paths can be given by:

$$h(\tau) = \sum_{l=1}^{L} \xi_l \delta(\tau - \tau_l) \qquad (3)$$

Where ξ_l and τ_l respectively denote the amplitude and delay of lth path, and the received signal $\tilde{y}(t)$ with additive noise $w(t)$ can be given by:

$$\tilde{y}(t) = \sum_{l=1}^{L} \xi_l \tilde{x}(t - \tau_l) + w(t) \qquad (4)$$

III. ITERATIVE RECEIVER DESIGN

An iterative receiver is proposed here, which uses cost function based soft decision feedback OMP channel estimation and LDPC coding /decoding algorithm as shown in Figure 1. In the preprocessing block, the value of I is taken as zero, which will make the receiver similar to non-iterative receiver, where the pilot symbols will be used for channel estimation. After the decoding, the cost function based soft information will be compared with the previous iteration value, which serves as threshold and value of I is incremented for next iteration. The cost function based soft decision feedback method, OMP channel estimation and LDPC decoding are explained in detail as follows.
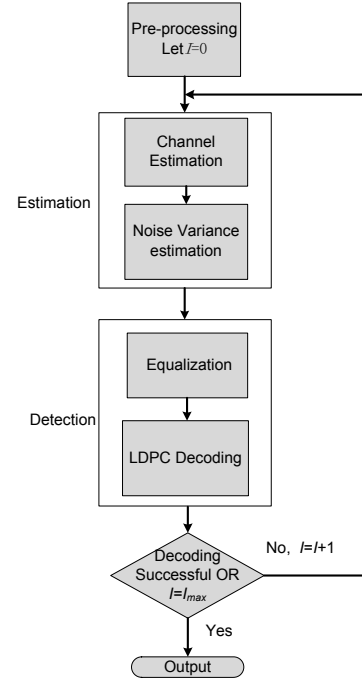

Figure 1: Iterative Receiver Block Diagram

A. Cost Function Based Soft Decision Feedback

Threshold controlled and uncontrolled soft and hard decision feedback methods are already in practice in iterative receiver systems [12, 13]. The soft symbol estimates are claimed to be better than hard symbol estimates especially for iterative channel estimation as they provide more statistical information about the transmitted data [14, 15]. We propose a new feedback method that uses cost function as decision condition threshold. Based on the cost function threshold, it decides whether to select the current iterative channel estimation result or to use the pilot-aided initial channel estimation value. This design is based on the idea given in detail in [15], where a cost function was used for decision feedback for coded OFDM wireless communication system. However the cost function of the channel estimation for the current iteration was always compared with the initial channel cost function $\varsigma\left(H_m^{(0)}\right)$, whereas we compare the cost function of the current iteration with the cost function of the previous iteration of channel estimation $\varsigma\left(\hat{H}_m^{(J-1)}\right)$. The advantage of this change is that the cost function keeps updating in comparison to the previous iteration, therefore the performance of channel estimation improves. Furthermore in [15], pilot-assisted channel estimation was performed based on the hard feedback method. We use soft feedback and OMP channel estimation, which obviously improves the channel estimation performance [3]. Furthermore we also compare LS channel estimation with OMP channel estimation using the same feedback method. This improved decision feedback method based on the cost function is given by:

$$H_m^{(j)} = \begin{cases} \dfrac{Y_m}{\hat{X}_m^{(j)}} & \text{if } \varsigma\left(\dfrac{Y_m}{\hat{X}_m^{(j)}}\right) \le \varsigma\left(\hat{H}_m^{(j-1)}\right) \\ \hat{H}_m^{(j-1)} & \text{otherwise} \end{cases}, \qquad (5)$$

where j indicates the number of iterations, $\varsigma\left(\dfrac{Y_m}{\hat{X}_m^{(j)}}\right)$ and

$\varsigma\left(\hat{H}_m^{(j-1)}\right)$ represents the signal detection cost function and channel estimation cost function for mth subcarrier respectively. Instead of using the soft symbols directly as feedback, soft information on the reliability of $\hat{X}_m^{(j)}$ in the form of Log likelihood rations (LLRs) is exploited by the threshold test in equation (5). To derive the cost function $\varsigma\left(\dfrac{Y_m}{\hat{X}_m^{(j)}}\right)$, the iterative receiver input is taken from the demodulated received symbols, that serves as auxiliary pilots. The modified signal model at the iterative receiver is given by:

$$Y_m = H_m \hat{X}_m + \eta_m, \qquad (6)$$

where η_m is given by:

$$\eta_m = \left(X_m - \hat{X}_m\right) \cdot H_m + \omega_m, \qquad (7)$$

The decision feedback induces this additional noise component, that can be approximated as Additive White Gaussian Noise with zero mean and its variance is given by:

$$\sigma_{\eta_m}^2 = E\left\{|\eta_m|^2\right\} = N_0 + \sigma_{\hat{X}_m}^2. \qquad (8)$$

where N_0 is the variance of AWGN signal and $\sigma_{\hat{X}_m}^2$ can be generated from the LLR of the decoder output [15].

In the first iteration, the cost function $\varsigma\left(\dfrac{Y_m}{\hat{X}_m^{(j)}}\right)$ is compared with the initial cost function $\varsigma\left(\hat{H}_m^{(0)}\right)$, which can be derived by using the initial estimates based on pilot symbols. The channel estimation error can be given by $\varepsilon_m = H_m - \hat{H}_m$. Assuming ε_m to be zero mean with variance equal to the mean square error, denoted by MSE $\sigma_{v_m}^2 = E\left\{|\varepsilon m|^2\right\}$,which depends on the FIR filter $\mathbf{v}$, therefore the variance of the effective noise term can be given by:

$$\sigma_{\eta_m}^2 = E\left\{|\eta_m|^2\right\} = N_0 + E_s \sigma_{v_m}^2. \qquad (9)$$

Where E_s is the energy per information bit of the mapped

symbol X_m. To carry out the threshold test, only the computation of $\sigma_{\hat{X}_m}^2$ is required, as the soft LLR information is available at the decoder output.

B. OMP Channel Estimation

The OMP algorithm is a kind of greedy algorithm. It first searches the dictionary for elements that match the received signal, orthogonalizes the selected element, removes the effect of the element from the signal and the dictionary and obtains the signal residual. Then in the remaining dictionary, it continues to search for the element that has the best match with the signal residual, and the above process is repeated until the residual satisfies the set threshold.

Considering that the multipath UWA channel is linearly time invariant for each OFDM block, the channel estimation needs to determine the corresponding delay τ_p for each path. The estimation problem can be reformulated by constructing a so-called dictionary, made of the signals parameterized by a representative selection of possible values of parameter τ_p. The path delay τ_p depends on these factors as given by:

$\tau_p \in \left\{0, \dfrac{1}{\lambda B}, \dfrac{2}{\lambda B}, ..., \dfrac{N_\tau - 1}{\lambda B}\right\}$, where λ is the time oversampling factor and there are a total of $N_\tau = T_g / \lambda B$ delays, where T_g is the length of the guard interval. The pilots subcarriers are indexed as the set $S_P = \left\{q_1, ... , q_{K_P}\right\}$ with $K_P = |S_P|$ pilot subcarriers in total. With these path delays, the dictionary based formulation is given as:

$$\underbrace{\begin{bmatrix} z[q_1] \\ \vdots \\ z[q_{K_P}] \end{bmatrix}}_{:=\mathbf{z}_p} = \underbrace{\begin{bmatrix} s[q_1] & & \\ & \ddots & \\ & & s[q_{K_P}] \end{bmatrix} \begin{bmatrix} 1 & \cdots & e^{-j2\pi\frac{q_1}{K}\frac{(N_\tau-1)}{\lambda}} \\ \vdots & \ddots & \vdots \\ 1 & \cdots & e^{-j2\pi\frac{q_{K_P}}{K}\frac{(N_\tau-1)}{\lambda}} \end{bmatrix}}_{:=\mathbf{A}}$$
$$\underbrace{\begin{bmatrix} \xi_0 \\ \vdots \\ \xi_{N_\tau-1} \end{bmatrix}}_{:=\xi} + \underbrace{\begin{bmatrix} \eta[q_1] \\ \vdots \\ \eta[q_{K_P}] \end{bmatrix}}_{:=\eta} \qquad (10)$$

which can be put in vector-matrix form as:

$$\mathbf{z}_p = \begin{bmatrix} \mathbf{a}_0 \cdots \mathbf{a}_{p-1} \cdots \mathbf{a}_{N_\tau-1} \end{bmatrix} \xi + \eta \qquad (11)$$

$$\mathbf{z}_p = \mathbf{A}\xi + \eta \qquad (12)$$

where $\mathbf{a}_{p-1}$ denotes the pth dictionary element and is of size $K_P \times 1$, $\mathbf{z}_p$ shows the received pilot information, η is the noise vector, ξ shows the channel information to be estimated and $\mathbf{A}$ is the constructed dictionary vector of size $K_P \times N_\tau$.

Let $\mathbf{r}_p$ be the residual after p iterations with initial value $\mathbf{r}_0 = \mathbf{z}_p$, search for the elements in the dictionary that have the largest inner product of residuals and get the index of the matching element in the dictionary:

$$s_p = \arg \max_{j=1,..,N_\tau - 1, j \notin I_{p-1}} \frac{\left| \mathbf{a}_j^H \mathbf{r}_{p-1} \right|^2}{\left\| \mathbf{a}_j \right\|_2^2} \tag{13}$$

where $I_{p-1} = \{s_1, s_2, \cdots, s_{p-1}\}$ is the index of the previous $p-1$ iterations. Schmidt orthogonalization of the selected elements is given by:

$$\mathbf{u}_{s_p} = \mathbf{a}_{s_p} - \sum_{i=1}^{p-1} \frac{\langle \mathbf{a}_{s_p}, \mathbf{u}_i \rangle}{\langle \mathbf{u}_i, \mathbf{u}_i \rangle} \mathbf{u}_i \tag{14}$$

Where $\mathbf{u}_i$ is the value of the orthogonalized element chosen for the first time and the estimated values of elements in signal $\boldsymbol{\xi}$ is given by:

$$\hat{\xi} = \frac{\langle \mathbf{u}_{s_j}, \mathbf{r}_{p-1} \rangle}{\left\| \mathbf{u}_{s_p} \right\|_2^2} \tag{15}$$

And the residual signal is calculated as:

$$\mathbf{r}_p = \mathbf{r}_{p-1} - \hat{\xi} \mathbf{a}_{s_p} \tag{16}$$

Stop the iterations when $\left\| r_p \right\|_2^2 < \varepsilon$ (where ε is the residual threshold). Finally the channel coefficients at all subcarriers can be constructed as:

$$\hat{H}[m] = \sum_{p=0}^{N_\tau - 1} \hat{\xi} e^{-j2\pi \frac{mp}{\lambda K}} \tag{17}$$

C. LDPC Coding

Low-density parity-check (LDPC) code is a linear block error correcting code, used for transmitting a message over a noisy transmission channel. Its check matrix is sparse and the codes are capacity-approaching codes, means that the threshold can be set very much close to Shannon capacity limit. The description format of LDPC codes is relatively simple and has strong error correction capability and excellent flexibility, which makes LDPC codes suitable for almost all channels. The amount of computation does not increase dramatically with the increase in code length, therefore keeping the complexity low. There are many design approaches to construct LDPC code check matrix, such as Gallager's construction method, MacKay construction method, repeated accumulation design construction method, -

rotation matrix construction method, etc. We used the regular LPDC Gallager codes here with ½ code rate and block size of 851.

IV. RESULTS

A. Simulation Results

A shallow water channel is modeled using Bellhop and the channel impulse response is given in Figure 2, while the simulation parameters for the OFDM system are given in Table 1 below. First of all the iterative and non-iterative receivers are compared, then different feedback methods are compared. The soft feedback method is analyzed for reduced number of pilots and the proposed design is then compared with other soft decision feedback methods.
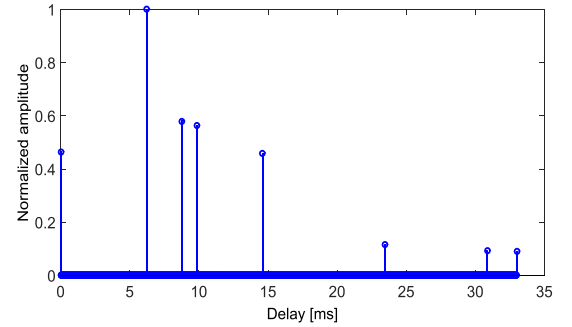

Figure 2: Simulated Channel Impulse response

Table 1
OFDM Simulation Parameters

Serial #	Parameter	Value
01	Sampling frequency	48 kHz
02	Communication bandwidth	6 kHz-12 kHz
03	Total number of subcarriers	1024
04	Number of data carriers	851
05	Number of pilots	125
06	Number of Null carriers	48
07	OFDM symbol period	170.67 ms
08	Cyclic prefix length	40 ms
09	Spectrum utilization	0.67 b/s/Hz
10	Communication rate	4.04 kb/s

The performance comparison is done by comparing the BER performance as well as normalized mean square error (NMSE) performance. The NMSE is defined as:

$$\text{NMSE} = E\left(\left\| \mathbf{H} - \hat{\mathbf{H}} \right\|^2 / \left\| \mathbf{H} \right\|^2 \right) \tag{18}$$

First of all we compare the BER and NMSE of the iterative receiver with non-iterative receiver in Figure 3. The non-iterative receiver is similar to the iterative receiver with single iteration. The performance of iterative receiver even after the second iteration is far better than that of non-iterative receiver We use soft information feedback in our design, as the overall

performance of soft-decision feedback is better than that of hard-decision feedback, because soft information feedback can generally make more use of symbol statistics than hard information feedback [14, 15] .
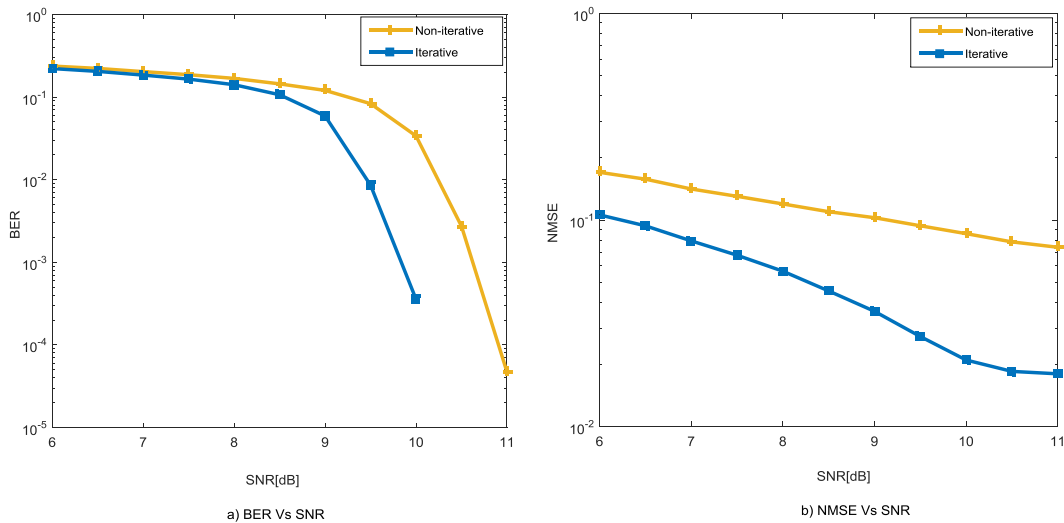

a) BER Vs SNR

b) NMSE Vs SNR

Figure 3: Iterative Vs Non-iterative receiver

Next, we compare the performance of iterative channel estimation at different pilot intervals by changing the pilot interval from 4 to 8 and 12 while using soft decision feedback method with 4 iterations, as shown in Figure 4. The curves in figure 4 (a), (b) and (c) show the comparison between iterative and non-iterative channel estimation for the pilot intervals 12, 8 and 4 respectively. It can be seen that when the pilot interval increases, the channel estimation performance decreases, i.e., smaller number of pilots cause a decrease in channel estimation performance. Furthermore, when the pilot interval is large, the performance gap between the iterative and non-iterative channel estimations is more obvious, whereas, the difference is less obvious in case of smaller pilot interval. This shows that the additional pilot information feedback when the number of pilots is small is more important for the channel estimation.

In the Figure 4(d), the comparison of pilot spacing 4, 8 and 12 shows a significant difference in the performance of the iterative channel estimation and the performance degrades for the larger pilot interval. This Figure 4 further shows that the performance of pilot spacing 4 and 8 is very close in case of iterative channel estimation, which shows that the use of iterative method can easily reduce the number of pilots used.

(a) BER Vs SNR of iterative vs non-iterative with pilot Interval =12

(b) BER Vs SNR of iterative vs non-iterative with pilot Interval =8

(c) BER Vs SNR of iterative vs non-iterative with pilot Interval =4

(d) BER Vs SNR of iterative channel estimation with different pilot intervals
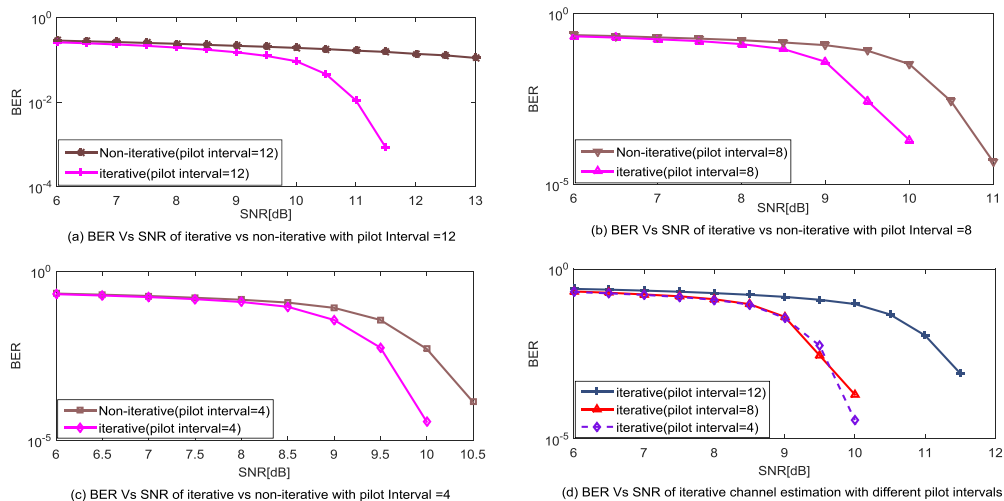
Figure 4: Comparison of Iterative Channel Estimation Performance at different Pilot intervals using Soft feedback method

Cost Function based Soft Feedback Iterative Channel
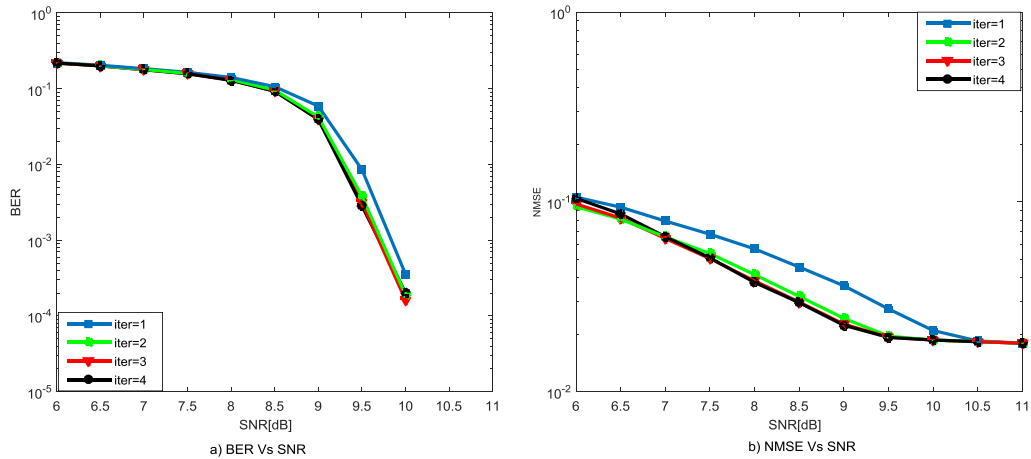Estimation in OFDM Underwater Acoustic Communication

Figure 5: Performance Comparison of cost based soft feedback method at different number of iterations

Figure 5 compares the BER and NMSE the performances of
the proposed feedback method based on the cost function for
different number of iterations. It can be seen from the figure
that system's BER and NMSE is significantly reduced with the
increase in number of iterations and the system's performance
is gradually improved until it reaches stability.

Next we compare the BER performance of the proposed
feedback method with soft decision feedback for every
iteration as shown in Figure 6. It can be seen that the
performance of the proposed method is better than the soft

decision feedback in each iteration. The performance gap
decreases with the increase in iterations as can be seen in the
figures that the gap is more in the first iteration and is reduced
in the fourth iteration when the system stabilizes, however the
performance of soft feedback based on cost function is still
better than soft feedback method. It is also concluded that as
the proposed method performs better even in the first and
second iterations, the processing time and complexity can be
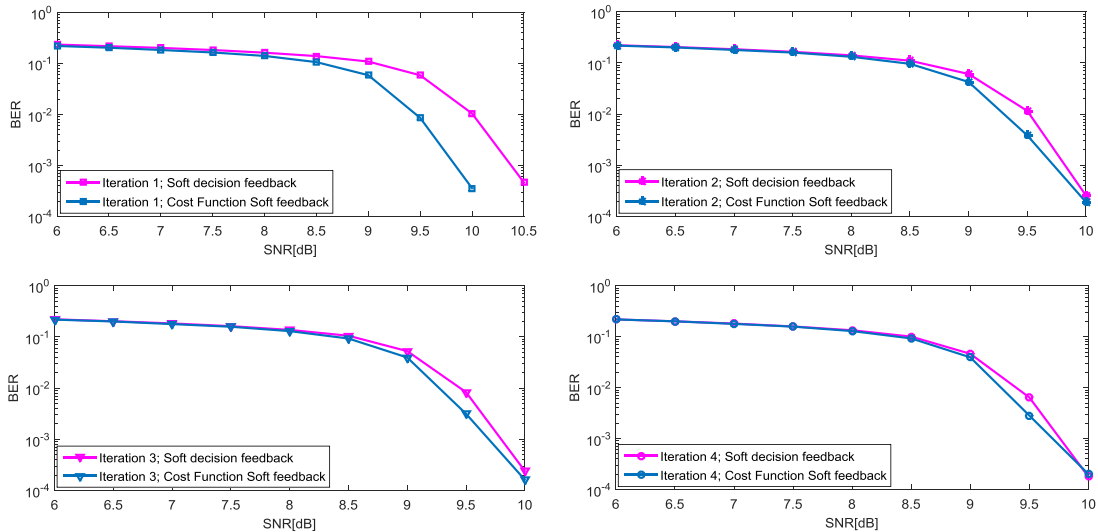reduced if we reduce the number of iterations for this method.

Figure 6: Comparison of soft decision feedback with cost based soft decision feedback

B. Experimental Results

The performance of the proposed iterative receiver
algorithm in underwater acoustic SISO OFDM
communication system is verified via sea trials. The
experimental data was collected in experiments conducted in

South China sea. The OFDM system experimental parameters
are shown in Table 2. The depth of sea water was 60 to 70
meters with good sea conditions. Two ships were used to
verify the communication performance. The receiving vessel
was anchored and four hydrophones were deployed 30m deep;
the transmitter was deployed 27m below the launching ship.

The launching ship was moving towards the receiving ship at a speed of 2 knots and kept moving from a position 3km away to 1km and was continuously sending test signals.

Table 2
Sea Experiment OFDM System Parameters

Serial #	Parameter	Value
01	Sampling frequency	48 kHz
02	Communication bandwidth	6 kHz-10 kHz
03	Total number of subcarriers per transmitter	681
04	Number of data carriers per transmitter	595
05	The number of pilots at each transmitter	86
06	OFDM symbol period	170.25 ms
07	Cyclic prefix length	20 ms
08	Cyclic Suffix Length	5 ms
09	Spectrum utilization	0.76 b/s/Hz
10	Communication rate	3.05 kb/s

Each frame of data contains 8 OFDM symbols, while QPSK mapping is used. Two encoding methods are used: 1/2 code rate convolutional code and 1/2 code rate LDPC, both with the same information sequence length.

The performance of the convolutional code and LDPC code, and the performance of the LS channel estimation algorithm and the OMP algorithm are compared and analyzed. The signals of the second receiver and fourth receiver are processed respectively, as shown in Figure 7.

Comparing the two upper curves in Figure 7 (a) & (b), it can be observed that with the same channel coding scheme, the performance of OMP channel estimation is better than the traditional LS channel estimation. Comparing the second and third curves, we can see that when the same channel estimation algorithm is used, the LDPC code performs better than the convolutional code. Therefore it is concluded that a combination of LDPC code and OMP channel estimation gives the best performance.

Next we verify the performance of the iterative reception algorithm. Taking 7 frames of data from the hydrophone 4 for the analysis. The number of bits transmitted in each frame of data is $595 \times 8 \times 2 = 9520$, as there are 8 OFDM symbols in each frame and each symbol has 595 data carriers, while the modulation is QPSK so there are two bits in each symbol. Table 3 lists the number of error bits for different data frames at different iterations.

It can be observed from Table 3 that the performance of different data frames after receiver's initial processing (without iterations) is quite different. The relative movements of the transmitter and receiver during the experiment and the different interference of frames with the background noise and the channel conditions can be the reasons for these large differences. Let us take the first frame and the fourth frame of the received data that are widely different in performance, as an example for analysis.

Figure 8 (a) &(b) shows the data signal received for these two frames, normalization is performed and the frame header LFM signal is used to measure the channel impulse response experienced by the two frames of data, as shown in Figure 9. It can be seen that the data of the first frame is more affected by noise than the data of the fourth frame, furthermore the experienced channel for the first frame is more complicated than the fourth frame. This is the reason why the bit error rate of the first frame data is high.
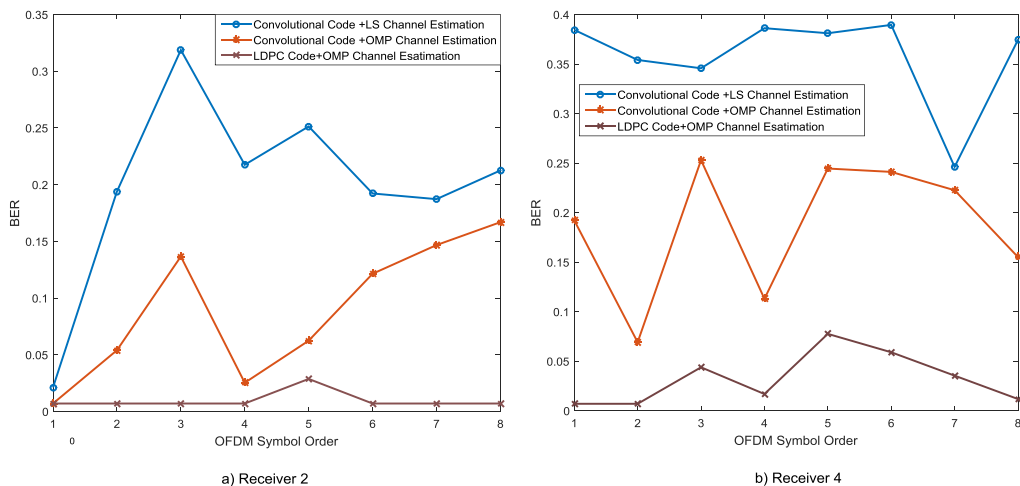

a) Receiver 2

b) Receiver 4

Figure 7: Comparison of different channel estimation methods with different channel coding schemes

Table 3
Statistics of the number of bit errors at different iteration times for different data frames

Frame No.	No iteration	1st Iteration	2nd Iteration	3rd Iteration	4th Iteration	5th Iteration
01	1086	526	270	162	36	0
02	512	228	48	0	0	0
03	881	346	150	4	0	0
04	0	0	0	0	0	0
05	116	0	0	0	0	0
06	184	0	0	0	0	0
07	2146	2146	2262	2476	2684	2904

a)   Data Frame 1

b) Data Frame 4
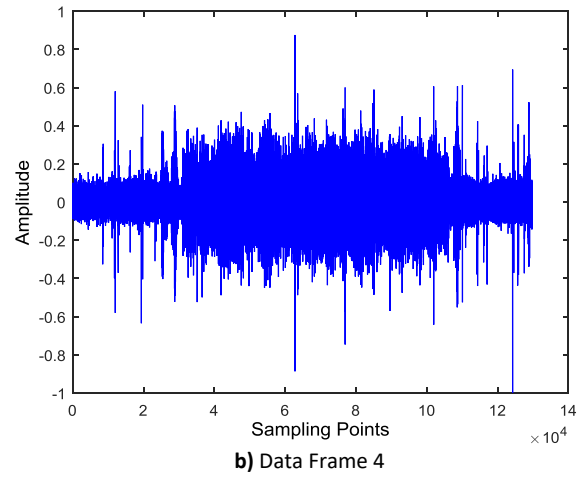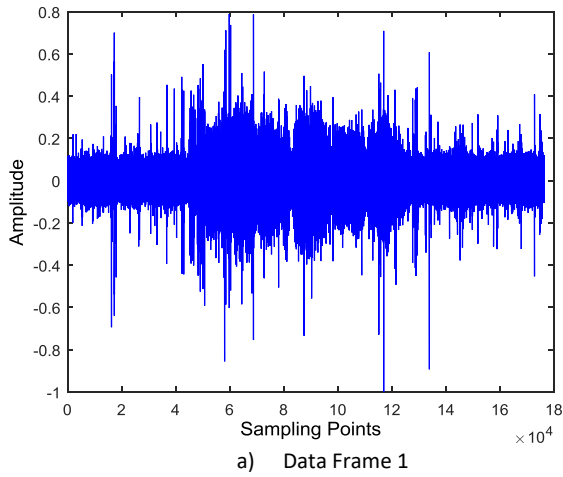
Figure 8 : Received signal in the sea experiment

a)   Channel experienced by Data Frame 1

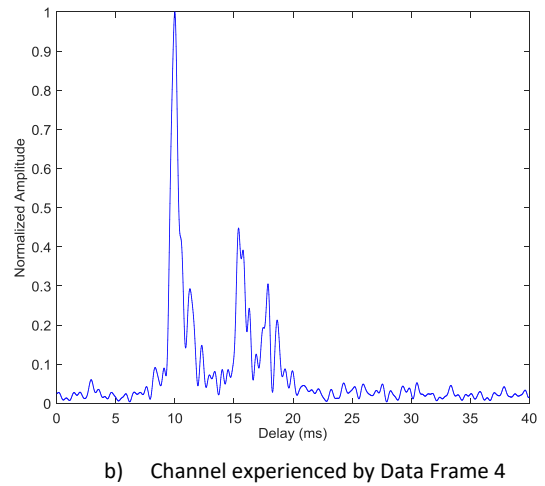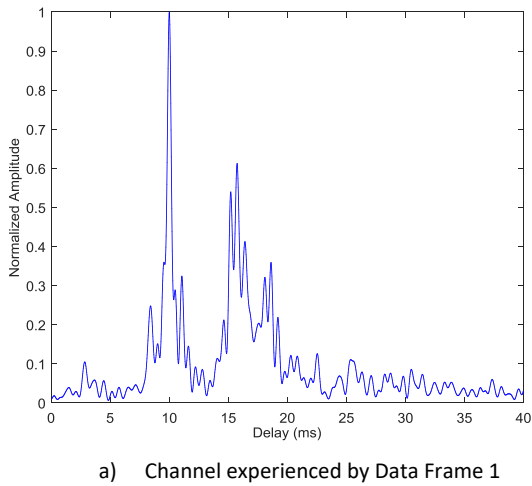b)   Channel experienced by Data Frame 4

Figure 9: Measurement of CIRs in sea experiment

Further analysis of table 3 shows that with the increase in the number of iterations, the number of errors in the decoded bits gradually reduces and with each increase in iteration, the number of erroneous bits almost halves. If the number of erroneous bits is more, it needs multiple iterations to reduce this number to 0 as obvious for the first frame, whereas the number of the initial erroneous bits of the 5th and 6th frames is less; therefore the number of erroneous bits is reduced to 0 right after the first iteration.

The effectiveness of the iterative reception algorithm is

verified, however the iterative reception algorithm also has its limitations. For the case where the initial bit error rate is very high, such as the seventh frame (the number of error bits is 2146, the corresponding bit error rate is about 0.23), the number of bit errors increases after the iteration instead. The reason is that there may exist some error propagation in the iterative process and the processing capability of the iterative reception algorithm has a certain range or threshold. Just like the error correction code, it may be not be effective after a certain error correction threshold is exceeded.

V. CONCLUSION

This paper proposes a receiver based on cost function threshold driven soft decision feedback iterative channel estimation technique for OFDM UWA communication. The receiver exploits OMP channel estimation and LDPC coding schemes. The performance of the proposed receiver is verified by simulations as well as sea experiments. The proposed receiver is compared with other non-iterative and soft and hard decision feedback iterative receivers and it outperforms them in terms of BER and NMSE performance. During the sea trials, combinations of different channel estimation schemes and coding schemes are compared and LDPC coding with OMP channel estimation outperformed the LS estimation and convolutional codes. Furthermore the better performance of the proposed receiver is proved in the sea experiment.

VI. REFERENCES

[1] Mandal, A. and R. Mishra, *Design of Pipelined Adaptive DFE Architecture For High Speed Channel Equalization* INFOCOMMUNICATIONS JOURNAL, 2015. **7**(3).

[2] Horvath, B. and P. Horvath, *Establishing Lower Bounds on the Peak-to-Average-Power Ratio in Filter Bank Multicarrier Systems.* INFOCOMMUNICATIONS JOURNAL, 2015. **7**(3).

[3] Qiao, G., et al., *MIMO-OFDM underwater acoustic communication systems—A review.* Physical Communication, 2017. **23**: p. 56-64.

[4] Li, B., et al. *MIMO-OFDM Over An Underwater Acoustic Channel*. in *OCEANS 2007*. 2007.

[5] Stojanovic, M. *Low Complexity OFDM Detector for Underwater Acoustic Channels*. in *OCEANS 2006*. 2006.

[6] Carrascosa, P.C. and M. Stojanovic. *Adaptive MIMO detection of OFDM signals in an underwater acoustic channel*. in *OCEANS '08*. 2008.

[7] Stojanovic, M. *OFDM for underwater acoustic communications: Adaptive synchronization and sparse channel estimation*. in *2008 IEEE International Conference on Acoustics, Speech and Signal Processing*. 2008.

[8] Stojanovic, M. *Adaptive Channel Estimation for Underwater Acoustic MIMO OFDM Systems*. in *Digital Signal Processing Workshop and 5th IEEE Signal Processing Education Workshop, 2009. DSP/SPE 2009. IEEE 13th*. 2009.

[9] Huang, J., et al. *Iterative sparse channel estimation and decoding for underwater MIMO-OFDM*. in *OCEANS 2009*. 2009.

[10] Huang, J., C.R. Berger, and S. Zhou. *Comparison of basis pursuit algorithms for sparse channel estimation in underwater acoustic OFDM*. in *OCEANS 2010 IEEE - Sydney*. 2010.

[11] Upadhyay, N., M. Tiwari, and J. Singh, *LDPC Based MIMO-OFDM System for Shallow Water Communication using BPSK*. International Journal of Electronics & Communication Technology (IJECT) 2015. **Vol. 6** (Issue 4).

[12] Niu, H. and J.A. Ritcey. *Iterative channel estimation and decoding of pilot symbol assisted LDPC coded QAM over flat fading channels*. in *The Thrity-Seventh Asilomar Conference on Signals, Systems & Computers, 2003*. 2003.

[13] Valenti, M.C. and B.D. Woerner, *Iterative channel estimation and decoding of pilot symbol assisted turbo codes over flat-fading channels*. IEEE Journal on Selected Areas in Communications, 2001. **19**(9): p. 1697-1705.

[14] Laot, C., A. Glavieux, and J. Labat, *Turbo equalization: adaptive equalization and channel decoding jointly optimized*. IEEE Journal on Selected Areas in Communications, 2001. **19**(9): p. 1744-1752.

[15] Auer, G. and J. Bonnet. *Threshold Controlled Iterative Channel Estimation for Coded OFDM*. in *2007 IEEE 65th Vehicular Technology Conference - VTC2007-Spring*. 2007.

Gang Qiao received the B.S., M.S., and Ph.D. degrees in underwater acoustic engineering from the Harbin Engineering University (HEU), Harbin, China, in 1996, 1999, and 2004, respectively. He visited the Department of Electrical Engineering, University of Washington, Seattle, WA, USA, as a Senior Visiting Scholar in 2015. He has been a full Professor with HEU since 2007. His research interests lie in the areas of underwater acoustic communication and networking, and underwater acoustic target detection and localization.

Zeeshan Babar received the B.S. and M.S. degrees from National University of Science and Technology (NUST) and University of Engineering and Technology Taxila Pakistan in 2008 and 2012 respectively. Currently he is pursuing his Ph.D. in Underwater Acoustic Engineering from Harbin Engineering University (HEU), Harbin, China. His research interests lie in the areas of underwater acoustic communication and networking.

Lu Ma received the B.S. and Ph.D. degrees in signal and information processing from the Harbin Engineering University (HEU), Harbin, China, in 2010 and 2016, respectively. She visited the University of Connecticut, Storrs, CT, USA, from October 2014 to October 2015. She has been an Assistant Professor with the College of Underwater Acoustic Engineering, HEU, since November 2016. Her research interests lie in the areas of multicarrier and multiuser communications for underwater acoustic channels.

Xue Li received her B.S. and M.S. degrees in 2015 and 2018 respectively from Harbin Engineering University, Harbin, China and is currently involved in active research in the field of underwater acoustics. Her research interests lie in the areas of underwater acoustic communication andnetworking.

Minimum BER Criterion Based Robust Blind Separation for MIMO Systems

Zhongqiang Luo, Wei Zhang, Lidong Zhu and Chengjie Li

Abstract—In this paper, a robust blind source separation (BSS) algorithm is investigated based on a new cost function for noise suppression. This new cost function is established according to the criterion of minimum bit error rate (BER) incorporated into maximum likelihood (ML) principle based independent component analysis (ICA). With the help of natural gradient search, the blind separation work is carried out through optimizing this constructed cost function. Simulation results and analysis corroborate that the proposed blind separation algorithm can realize better performance in speed of convergence and separation accuracy as opposed to the conventional ML-based BSS.

Index Terms—Blind Source Separation; Cost Function; Bit Error Rate; Maximum Likelihood; Natural Gradient

I. INTRODUCTION

In the past few years, as a paradigm of unsupervised learning in machine learning, blind source separation (BSS) has played an increasingly important role in wireless communication systems for performance enhancement and intelligent information processing [1-14]. It contributes significantly to achieve high spectral efficiency, adaptive signal processing and anti-interference requirements due to its blind feature and statistical information utilization. By virtue of BSS technique, on the one hand, frequently used pilot sequences can be eliminated for enhancing spectral efficiency. On the other hand, it can improve the capacity of the source recovery and resist unpredictable interference in spite of little prior information acquired in advance. In wireless communication systems, a number of received models can be structured as a BSS framework, such as CDMA (code division multiple access) [4-6], OFDM (orthogonal frequency division multiplexing) [7-10] and MIMO (Multiple Input Multiple Output) [11-14], and so on. Generally speaking, those received models can be considered as mixtures of independent source and unknown channel. The expected signals can be separated or extracted from the received mixed signals by using the independent component analysis (ICA) algorithm based BSS technique.

In a general way, the ICA algorithms are composed of two steps. First, the cost function is built based on an independent principle. Second, the cost function is optimized for blind separation. Therefore, it is vital for constructing the cost function and implementing optimizing scheme. There are three popular independent principles based cost function, which includes maximum likelihood (ML), minimum mutual information (MMI) and non-Gaussian maximization [1, 3]，respectively. So far, there has been proposed some famous algorithms based on those independent principles, such as FastICA, JADE, Infomax, and so on. Those algorithms are always directly used to carry out blind separation work in the communication system. They always take no account of the performance criterion of the communication system. In fact, those ignored criteria may be combined with independent principles based cost function to propose a more suitable algorithm for executing blind separation of communication mixed signals.

Taking into account of the communication system, the bit error rate (BER) is a significant performance criterion. In this paper, the idea of a minimum BER criterion incorporated into ML or MMI principle is motivated to build the cost function, and then the natural gradient is used to optimize the built new cost function. Simulation results show the proposed new cost function based blind separation algorithm can lead to better performance in speed of convergence and separation accuracy compared with the original one.

The remainder of the paper is organized as follows. In the Section II, the system model of blind source separation is reviewed. The new cost function of ICA and the proposed blind separation algorithm are both described in Section III. Simulation results and discussion are presented in Section IV. Section V draws the conclusions.
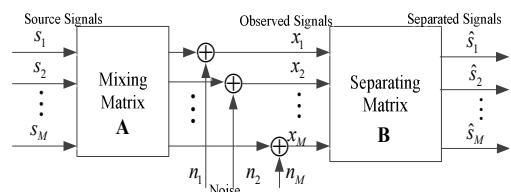
Zhongqiang Luo is with the Artificial Intelligence of Key Laboratory of Sichuan Province, Sichuan University of Science and Engineering, Yibin, Sichuan, China, e-mail: zhongqiangluo@gmail.com.

Wei Zhang is with the with the Artificial Intelligence of Key Laboratory of Sichuan Province, Sichuan University of Science and Engineering, Yibin, Sichuan, China

Lidong Zhu is the National Key Laboratory of Science and Technology on Communications, University of Electronic Science and Technology of China, Chengdu, Sichuan, China, e-mail: zld@uestc.edu.cn

Chengjie Li is the School of Computer Science and Technology, Southwest Minzu University, Chengdu, Sichuan, China, e-mail: junhongabc@126.com.

II. SYSTEM MODEL

Fig.1 The basic BSS model block diagram

In this section, the basic BSS model is reviewed. As shown in Fig. 1, the BSS model has a close relationship to MIMO system [1, 14]. Considering the determined BSS model, that is to say, the number of transmitting antennas and receiving antenna is the same in MIMO system. The mutually independent source vector is denoted as $\mathbf{s} = (s_1, s_2, \ldots s_M)^T$. The mixing matrix is $\mathbf{A}$, which describes a MIMO channel condition. $\mathbf{n} = (n_1, n_2, \ldots, n_M)^T$ is the noise vectors. The observed mixed signal is $\mathbf{x} = (x_1, x_2, \ldots, x_M)^T$, in other words, the received signals in MIMO. The received mixed signals can be described as follows,

$$\mathbf{x} = \mathbf{As} + \mathbf{n} \tag{1}$$

The goal of BSS is to separate or extract source signals only from observed mixed signals. The source signal estimation can be obtained after the separating operation is executed,

$$\hat{\mathbf{s}} = \mathbf{BAs} + \mathbf{Bn}$$
$$= \mathbf{s} + \mathbf{Bn} \tag{2}$$

Ideally, $\mathbf{C} = \mathbf{BA}$ is an identity matrix, i.e., the separating matrix $\mathbf{B}$ is the inverse of the mixing matrix. In fact, the matrix $\mathbf{C}$ is a generalized permutation matrix due to inherent indeterminacy in BSS. However, this problem has no effect into the separation work.

III. NEW COST FUNCTION FOR BSS

A. ML principle based cost function

The cost function of the ICA problem is usually derived via the maximum likelihood (ML) approach under the independence assumption. Suppose that sources $\mathbf{s}$ are independent with marginal distribution $f_i(s_i)$.

$$f_{\mathbf{s}}(\mathbf{s}) = \prod_i^M f_{s_i}(s_i) \tag{3}$$

In the linear model, $\mathbf{x} = \mathbf{As}$, the joint density of the observation vector is related to the joint density of the source vector as follows:

$$f_{\mathbf{x}}(\mathbf{x}) = \frac{1}{|\det \mathbf{A}|} f_{\mathbf{s}}(\mathbf{A}^{-1}\mathbf{x}) = |\det \mathbf{A}^{-1}| f_{\mathbf{s}}(\mathbf{A}^{-1}\mathbf{x}) \tag{4}$$

Then our goal is to find a maximum likelihood estimation of $\mathbf{A}$ (or $\mathbf{B}$ where $\mathbf{B} = \mathbf{A}^{-1}$) to maximize (4). Noting that $\mathbf{y} = \mathbf{A}^{-1}\mathbf{x} = \mathbf{Bx}$, the ML cost function can be derived from the log likelihood of (4) as

$$\log f_{\mathbf{x}}(\mathbf{x}) = -\log|\det \mathbf{A}| + \log f_{\mathbf{s}}(\mathbf{A}^{-1}\mathbf{x}) \tag{5}$$

which can be also written as

$$\log f_{\mathbf{x}}(\mathbf{x}) = \log|\det \mathbf{B}| + \log f_{\mathbf{y}}(\mathbf{y}) \tag{6}$$

$\mathbf{y}$ is the estimation of $\mathbf{s}$ with the actual distribution $f_{\mathbf{s}}(\mathbf{s})$

replaced by a hypothesized distribution $f_{\mathbf{y}}(\mathbf{y})$. Since sources are assumed to be statistically independent, the cost function is written as

$$J(\mathbf{B}) = -\log|\det \mathbf{B}| - \sum_{i=1}^M \log f_{y_i}(y_i) \tag{7}$$

The separating matrix $\mathbf{B}$ is determined by

$$\hat{\mathbf{B}} = \arg\min_{\mathbf{B}} \left\{ -\log|\det \mathbf{B}| - \sum_{i=1}^M \log f_{y_i}(y_i) \right\} \tag{8}$$

B. Minimum BER constrained ML principle based cost function

In this subsection, the minimum BER criterion is derived firstly. Then the minimum BER criterion incorporated into ML principle based cost function is built. The BSS problem in MIMO is a blind equalization one. Taking into account communication signals in a MIMO system model, the transmitted symbols are equiprobable antipodal symbols (i.e., ± 1, BSPK) uncorrelated with each other, i.e.,

$$E\left\{\mathbf{ss}^T\right\} = \mathbf{I} \tag{9}$$

The antipodal assumption is made for simplicity, and other constellations can also be used to extend, such as 4-QAM/QPSK. The noise vector $\mathbf{n}$ is zero-mean, white and Gaussian, with covariance matrix

$$E\left\{\mathbf{nn}^T\right\} = \sigma^2 \mathbf{I} \tag{10}$$

When $\mathbf{s}$ is transmitted, $\hat{\mathbf{s}}$, as given by (2), will be the received signal vector. The elements of this vector are then quantized by a threshold detector to obtain $\hat{\mathbf{s}}_q$, whose elements will be ± 1. The average BER of the detected signal is the average of the probability of error of each element of the block, i.e.,

$$P_e = \frac{1}{M} \sum_{m=1}^M P_{em} \tag{11}$$

In which P_{em} denotes the BER of the mth source symbol. Since the signal power of each data symbol is unity and the covariance matrix of the received noise is $\sigma^2 \mathbf{BB}^T$, by following standard steps, it can be shown that the probability of the mth source symbol in $\hat{\mathbf{s}}_q$ being in error can be written as

$$P_{em} = \frac{1}{2} erfc\left(\frac{1}{\sqrt{2\sigma^2 \left[\mathbf{BB}^T\right]_{mm}}} \right) \tag{12}$$

Where, $erfc(\varsigma) \triangleq \left(2/\sqrt{\pi}\right) \int_{\varsigma}^{\infty} e^{-z^2} dz$, and $\left[\mathbf{BB}^T\right]_{mm}$ denotes the $(m, m)^{th}$ element of the matrix $\mathbf{BB}^T$. The term

$\sigma^2 \left[\mathbf{BB}^T \right]_{mm}$ represents the noise variance in the receiver's estimation of the mth source symbol of the transmitted signal vector. Substituting (12) into (11), yielding

$$P_e = \frac{1}{2M} \sum_{m=1}^{M} erfc \left(\frac{1}{\sqrt{2\sigma^2 \left[\mathbf{BB}^T \right]_{mm}}} \right) \quad (13)$$

If we assume $\phi(z) = erfc \left(1/\sqrt{2\sigma^2 z} \right)$ for $z > 0$, then

$$\frac{d^2\phi}{dz^2} = \frac{1}{\sqrt{\pi}} \left(2\sigma^2 \right)^{-(1/2)} \exp \left(-\frac{1}{2\sigma^2 z} \right) \left(-\frac{3}{2} + \frac{1}{2\sigma^2 z} \right) z^{-(5/2)}$$
$$(14)$$

Therefore, if $z < 1/3\sigma^2$, then $d^2\phi/dz^2 > 0$. Applying this fact to (13), $\phi\left(\left[\mathbf{BB}^T \right]_{mm} \right)$ is a convex function if the noise power σ^2 is less than $1/3 \left[\mathbf{BB}^T \right]_{mm}$. If this condition is satisfied for all m (i.e., if there is sufficiently large SNR at the receiver), the average block BER P_e is also convex [15].

Since P_e is convex at moderate-to-high SNRs, the Jensen's inequality can be applied to obtain the following lower bound on P_e:

$$P_e = \frac{1}{2M} \sum_{m=1}^{M} erfc \left(\frac{1}{\sqrt{2\sigma^2 \left[\mathbf{BB}^T \right]_{mm}}} \right)$$

$$\geq \frac{1}{2} erfc \left(\frac{1}{\sqrt{\frac{2\sigma^2}{M} \sum_{m=1}^{M} \left[\mathbf{BB}^T \right]_{mm}}} \right) \quad (15)$$

$$= \frac{1}{2} erfc \left(\sqrt{\frac{M}{2\sigma^2 tr \left(\mathbf{BB}^T \right)}} \right) = P_{e,LB}$$

Equality in (15) holds if and only if $\left[\mathbf{BB}^T \right]_{mm}$ are equal $\forall m \in [1, M]$. The inequality of (15) is valid only when P_e is convex, i.e., when

$$\left[\mathbf{BB}^T \right]_{mm} < \frac{1}{3\sigma^2}, \forall m \in [1, M]$$

The quantity $P_{e,LB}$ in (15) defines a lower bound on the BER P_e. Note that since $erfc(\cdot)$ is a monotonically

decreasing function, to minimize $P_{e,LB}$ in (15), we need only minimize $tr\left(\mathbf{BB}^T \right)$. That is to say, the minimum BER criterion can be described as follows:

$$\min_{\mathbf{B}} tr\left(\mathbf{BB}^T \right)$$
$$subject~to~\left[\mathbf{BB}^T \right]_{mm} < \frac{1}{3\sigma^2} \quad (16)$$

Combined with (7), the new cost function with minimum BER criterion can be obtained,

$$\begin{cases} \arg\min_{\mathbf{B}} \left\{ -\log|\det \mathbf{B}| - \sum_{i=1}^{M} \log f_{y_i}(y_i) \right\} \\ \min_{\mathbf{B}} tr\left(\mathbf{BB}^T \right) \\ subject~to~tr\left[\mathbf{BB}^T \right] < \frac{M}{3\sigma^2} \end{cases} \quad (17)$$

In order to simplify the above constrained optimization problem (17), considering (7), the new cost function with minimum BER criterion in condition of the moderate-to-high SNRs can be described as a unconstrained optimization problem, i.e.,

$$\hat{\mathbf{B}} = \arg\min_{\mathbf{B}} \left\{ -\log|\det \mathbf{B}| - \sum_{i=1}^{M} \log f_{y_i}(y_i) + \lambda tr\left(\mathbf{BB}^T \right) \right\}$$
$$(18)$$

Where λ is a regulation parameter. Then the natural gradient search for optimizing the cost function (18) can be realized for BSS.

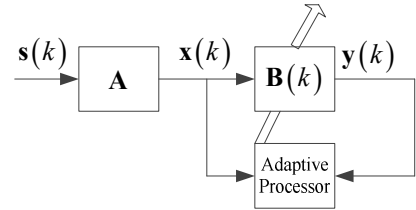C. *Optimizing cost function by natural gradient*

Fig.2 Adaptive processor block diagram

As the previous illustration, the ICA-based blind separation algorithms include a two-step process. The first step is to choose a principle, based on which a cost function is obtained. Next, a suitable method for optimizing the cost function needs to be adopted. In other words, using a cost function converts the blind separation problem into an optimization problem. In this paper, the separation processing is implemented by the adaptive BSS based on the natural gradient for its fast and accurate adaptation behavior. The adaptive processor block diagram for BSS is shown in Fig. 2. For any suitable smooth

gradient-searchable the cost function $J(\mathbf{B})$, the natural adaptation is defined as:

$$\mathbf{B} \leftarrow \mathbf{B} - \mu \nabla J(\mathbf{B}) \mathbf{B}^T \mathbf{B} \qquad (19)$$

The new built cost function in (18), since the probability density function (PDF) of sources are supposed to be unknown, and $f_{y_i}(y_i)$ is also unknown. Therefore, the activation or score function need be used to approximate probability density function of separation source signals. The function $\varphi_i(y_i)$ denotes the activation or score function in ML approach, which is defined as

$$\varphi_i(y_i) = -\frac{d \log f_{y_i}(y_i)}{dy_i} = -\frac{f'_{y_i}(y_i)}{f_{y_i}(y_i)} \qquad (20)$$

Since sources in digital communication are always subgaussian signal, this activation function can be chose as follows [3],

$$\varphi_i(y_i) = -y_i^3 \qquad (21)$$

Furthermore we can obtain the gradient of the cost function as follows:

$$\nabla J(\mathbf{B}) = \frac{\partial J(\mathbf{B})}{\partial \mathbf{B}} = -\mathbf{B}^{-T} + \boldsymbol{\varphi}(\mathbf{y})\mathbf{x}^T + 2\lambda\mathbf{B} \quad (22)$$

The natural gradient learning law now yields

$$\mathbf{B} \leftarrow \mathbf{B} - \mu\left(\mathbf{I} - \boldsymbol{\varphi}(\mathbf{y})\mathbf{y}^T - 2\lambda\mathbf{B}\mathbf{B}^T\right)\mathbf{B} \qquad (23)$$

IV. SIMULATIONS AND DISCUSSIONS

To demonstrate the effectiveness of the proposed algorithm in this paper, we conduct simulation experiments to evaluate the performance of the proposed ML based cost function with minimum BER criterion by nature gradient (called ML-BER-NG). For comparison, the only ML based cost function by nature gradient (ML-NG) is also illustrated for highlighting the proposed algorithm mechanism by comparative experiments. Considering a MIMO system, the number of transmitting antennas and receiving antennas is 5, the source symbols are from BPSK, the sample size is 4000. The mixing matrix is generated randomly. The performance index is cross talk error. The smaller is this performance index, the better performance is acquired. The cross talk error is defined as following[1, 3]

$$E_{ct} = \sum_{i=1}^{M}\left(\sum_{j=1}^{M}\frac{|c_{ij}|}{\max_k|c_{ik}|}-1\right)+\sum_{j=1}^{M}\left(\sum_{i=1}^{M}\frac{|c_{ij}|}{\max_k|c_{kj}|}-1\right)$$

where $\mathbf{C} = \mathbf{BA}$, c_{ij} is element in matrix $\mathbf{C}$. The moderate SNR condition is considered and other parameters setting are same for two methods.

The simulation results are demonstrated in Fig. 3 and Fig. 4, respectively. We can conclude that the proposed cost function by nature gradient can lead to better performance in speed of convergence and separation accuracy. In Fig. 3, we can see

that the proposed ML-BER-NG algorithm has low cross talk error and fast convergence rate compared with the original ML-NG algorithm. It is noteworthy that the initial value of a separation matrix is randomly generated, so that the number of iterations is a bit larger. However, the computation complexity is low. It takes just 2-4 seconds to achieve the algorithm convergence from time complexity. From Fig. 4, we can see that BER performance of the ML-BER-NG is better than the ML-NG in moderate SNR condition.
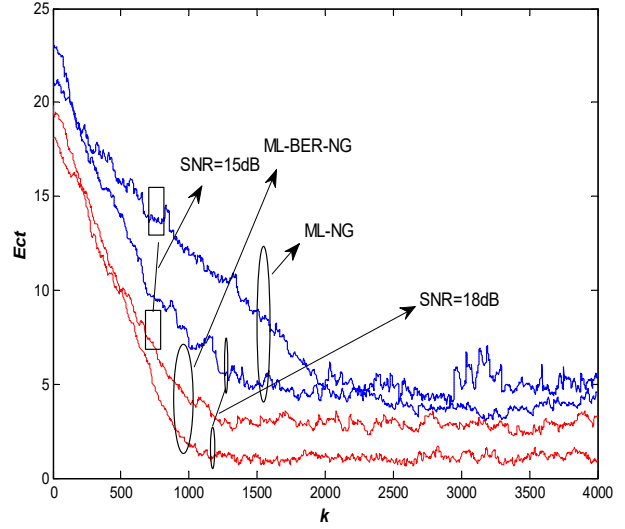

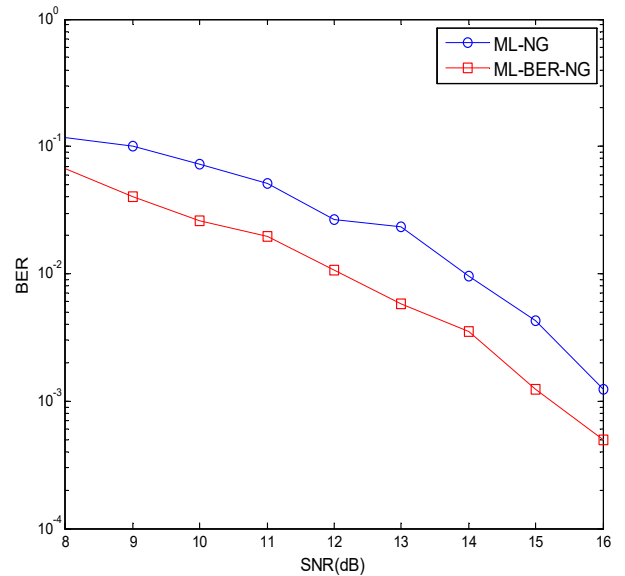Fig.3 The cross talk error as a function of iterations

Fig.4 BER performance as a function of SNR

In Fig.5, the further performance comparison of the representative methods is conducted 100 experiments for highlighting the proposed algorithm when the moderate SNR=10dB. In Fig.5(a), the statistical analysis of BER

Minimum BER Criterion Based Robust Blind
Separation for MIMO Systems

performance is given in a boxplot form, and in Fig.5(b) the BER performance with error bar is drawn to exhibit the performance enhancement of the proposed method compared with other representative algorithms. We can safely obtain that the proposed method achieve the performance refinement in contrast with that of some representative BSS methods for MIMO signals detection.
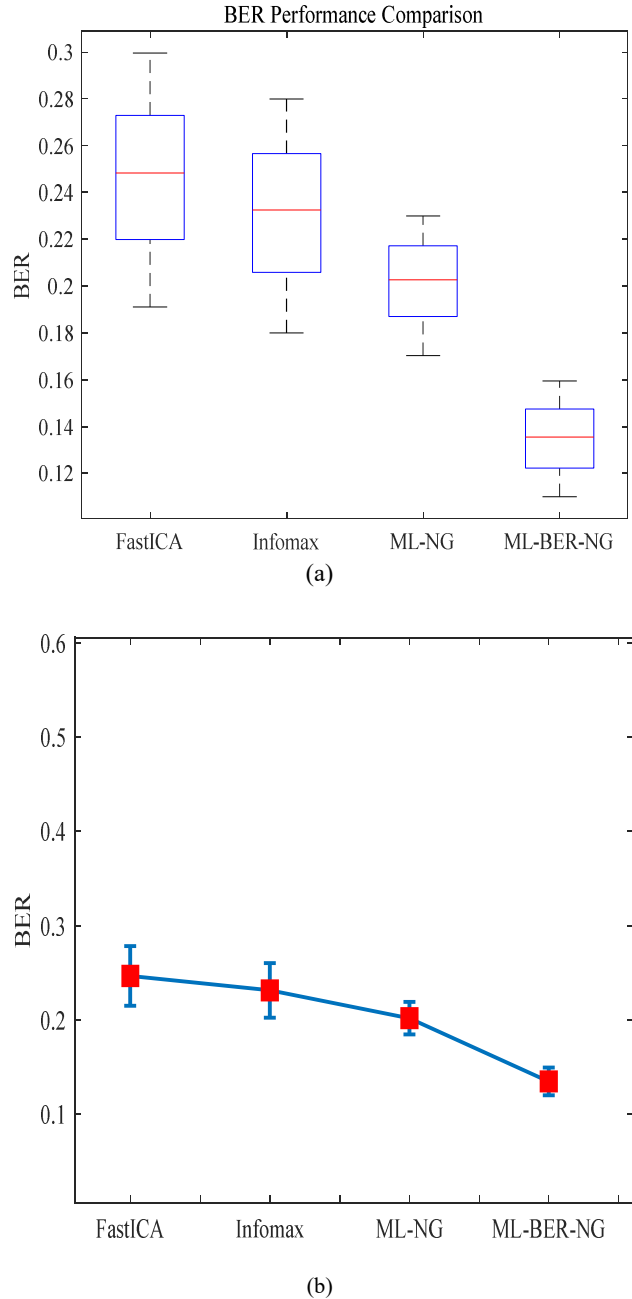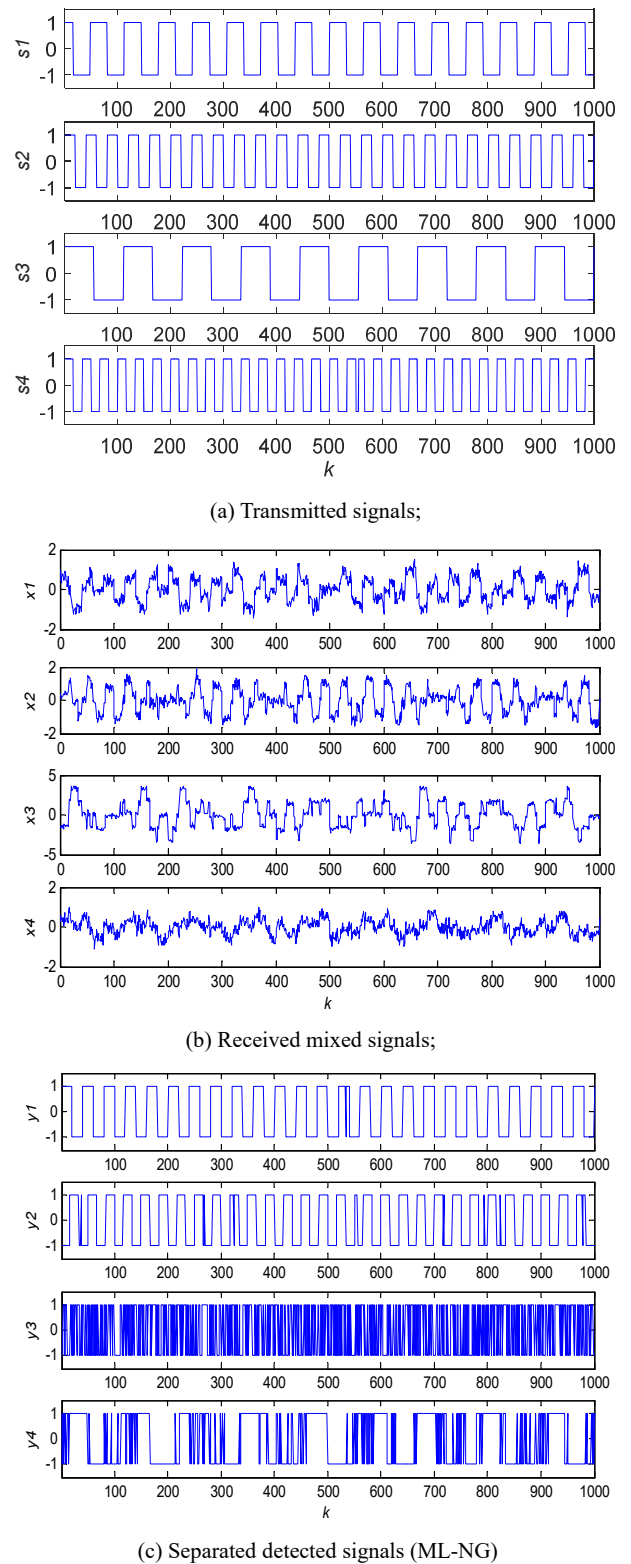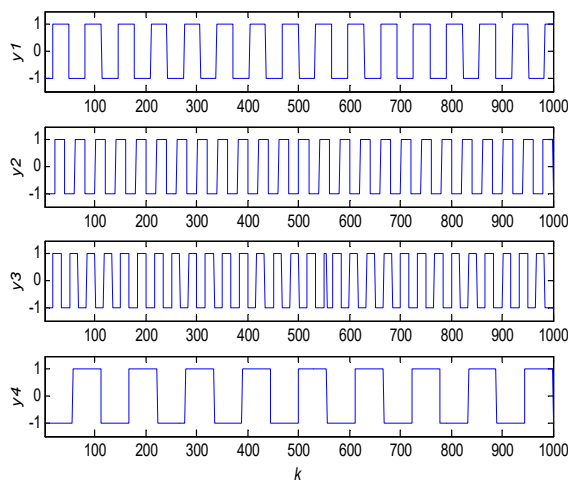

(a)

(b)

Fig. 5 BER performance comparisons of different representative methods

(a) Transmitted signals;

(b) Received mixed signals;

(c) Separated detected signals (ML-NG)

(d) Separated detected signals (ML-BER-NG)

Fig.6 4×4 MIMO；(a) Transmitted signals; (b) Received mixed signals; (c) Separated detected signals (ML-NG) (d) Separated detected signals (ML-BER-NG)

In the next simulation, the direct separation graphs are exhibited for illustration. As shown in Fig.6, it shows the results of blind separation of 4×4 MIMO in SNR=15dB. From the separated results of Fig.6, we can verify that the incorporation of minimum BER criterion in BSS improves the separation performance.

Remarks: The ML principle with minimum BER criterion considers the effect of noise term in the model of the cost function. It is fit for communication signals circumstance. The original ML principle neglects the effect of noise. However, noise is inevitable in a wireless communication environment. Furthermore, the computation complexity of the proposed algorithm (ML-BER-NG) is nearly similar to the ML-NG algorithm with low computation.

V. CONCLUSIONS

In this paper, a minimum BER criterion is considered in combination with the ML independent principle for blind separation problem in MIMO signal detection. The effect of the noise term is taken into account in the process of constructing cost function. The proposed algorithm can lead to better performance in speed of convergence and separation accuracy in moderate SNR condition. It is strongly encouraged to investigate the constrained cost function for BSS problem in low SNR in the future work. It is promising idea for thinking over other communication performance criteria for developing advanced BSS algorithms.

ACKNOWLEDGMENT

REFERENCES

[1] Tülay Adali, Simon Haykin, "Adaptive Signal Processing: Next Generation Solution", Hoboken, NJ: Wiley-IEEE Press, 2010.

[2] Zhongqiang Luo, Chengjie Li, Lidong Zhu, "A Comprehensive Survey on Blind Source Separation for Wireless Adaptive Processing: Principles, Perspectives, Challenges and New Research Directions, " *IEEE Access*, vol. 6, pp. 1-24, 2018

[3] X. Yu, D. Hu, J. Xu, "Blind Source Separation: Theory and Applications", Singapore: John Wiley & Sons, 2014.

[4] Jiang Zhang, Hang Zhang and Zhifu Cui, "Dual-antenna-based blind joint hostile jamming cancellation and multi-user detection for uplink of asynchronous direct-sequence code-division multiple access systems," *IET Commun.*, Vol. 7, No. 10, pp. 911-921, 2013

[5] Zhongqiang Luo, Lidong Zhu, "A Charrelation Matrix-Based Blind Adaptive Detector for DS-CDMA Sytsems,"*Sensors*, vol. 15, no. 8, pp. 20152–68, 2015.

[6] FU Wei-hong, YANG Xiao-niu, LIU Nai-an, "The Multi-User Detection and Chip Sequence Estimation for CDMA System Based on the Blind Source Separation,"*ACTA ELECTRONICA SINICA*, Vol. 36, No. 7, pp.1319-1323, 2008.

[7] Zhongqiang Luo, Lidong Zhu, Chengjie Li, "Employing ICA for Inter-Carrier Interference Cancellation and Symbol Recovery in OFDM Systems", *in Proc. IEEE Global Communications Conference (GLOBECOM 2014)*, Austin, USA, pp. 3501-3505, Dec. 2014.

[8] Zhongqiang Luo, Lidong Zhu, Chengjie Li, "Independent Component Analysis based Blind Adaptive Interference Reduction and Symbol Recovery for OFDM Systems", *China Communications*, vol. 13, no.2, pp. 41-54, 2016

[9] M.G.S. Sriyananda, Jyrki Joutsensalo, Timo Hämäläinen, "Blind Source Separation for OFDM with Filtering Colored Noise and Jamming Signal,"*Journal of Communications and Networks*, Vol. 14, No. 4, pp. 410-417, 2012.

[10] Zhongqiang Luo, Lidong Zhu, Chengjie Li, "Vandermonde Constrained Tensor Decomposition Based Blind Carrier Frequency Synchronization for OFDM Transmissions", *Wireless Personal Communications*, Vol. 95, No. 3, pp.3499-3508, 2017.

[11] Iman Moazzen, "*Array Signal Processing for Beamforming and Blind Source Separation*," University of Victoria, Doctoral Dissertation, 2013.

[12] Zhongqiang Luo, Lidong Zhu, Chengjie Li, "Exploiting Large Scale BSS Technique for Source Recovery in Massive MIMO Systems", in *Proc. IEEE/CIC ICCC*, 2014, pp. 391-395.

[13] Zhongqiang Luo, Chengjie Li, Lidong Zhu, "Robust Blind Separation for MIMO Systems against Channel Mismatch Using Second-Order Cone Programming", *China Communications*, vol. 14, no. 6, pp. 168-178, 2017.

[14] Zhongqiang Luo, Chengjie Li, "Robust Wireless Statistic Division Multiplexing and Its Performance Analysis", *International Journal of Distributed Sensor Network*, vol. 14, no. 12, pp. 1-13, 2018

[15] Yanwu Ding, Timothy N. Davidson, Zhi-Quan Luo, *et al.*, "Minmum BER Block for Zero-Forcing Equalization", *IEEE Trans. on Signal Processing*, vol.51, no.9, pp. 2410-2423, 2003

Minimum BER Criterion Based Robust Blind
Separation for MIMO Systems

Zhongqiang Luo received the B.S. and M.S. degrees in communication engineering and pattern recognition and intelligent systems from Sichuan University of Science and Engineering, Zigong, China, in 2009 and 2012, respectively. He received the Ph.D. degree in communication and information systems from University of Electronic Science and Technology of China (UESTC), in 2016. Since 2017, he has been with the Sichuan University of Science and Engineering, where he is currently a lecturer. From December 2018-December 2019, he is a visiting scholar with Department of Computer Science and Electrical Engineering in University of Maryland Baltimore County (UMBC). His research interests include machine learning, blind source separation, signal processing for wireless communication system and intelligent signal processing.

Wei Zhang received her bachelor's degree in electrical engineering and automation from Sichuan University of Science and Engineering(SUSE), Zigong, China, in 2017. Now she is studying at the Sichuan University of Science and Engineering master's degree. Her research interests include blind source separation, signal processing for power line communication and intelligent information processing.

Lidong Zhu received the B.S and M.S from Sichuan University, Chengdu, China, in 1990 and 1999, respectively, and the Ph.D. degree in Communication and Information Systems from Electronic Science and Technology of China (UESTC), Chengdu, China, in 2003. From July 2009 to June 2010, he was a visiting scholar with Department of Electronic Engineering of The University of Hong Kong. His research interests include satellite communications, blind source separation, and communication countermeasure.
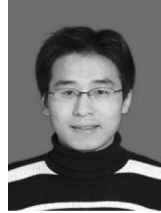
Chengjie Li received the B.Sc. degree in Shandong Normal University, Qufu (Confucius's hometown), China, 2004, the M.Sc. degree in computer software and theory in Xihua University, Chengdu, China, 2009. He received the Ph.D. degree in Communication and Information System in University of Electronic Science and Technology of China (UESTC), Chengdu, China, in 2017. Since 2017, he has been with the Southwest Minzu University, where he is currently a lecturer. His research interests include blind source separation, data mining and intelligent information processing.

Opto-Electronic Oscillator with Mach-Zender Modulator

Alexander A. Bortsov and Sergey M. Smolskiy, *Member IEEE*

Abstract. **The non-standard opto-electronic oscillator (OEO) operation is discussed in the generation mode of a single-side optical harmonic on the base of external and internal modulation of the laser signal. The OEO mathematical model is formed basing on laser differential equations for the closed radiofrequency network. With the help of the model offered, the phase noise of OEO radiofrequency oscillations is analyzed. It is shown that phase noise reduction in the circuit with external modulation depends not only on the increased laser power and growth of the geometric length of the optical fiber, but on reduction of the laser phase noise.**

Keywords: opto-electronic oscillator, phase noise, optical fiber, QW laser, microwave oscillator.

I. INTRODUCTION. THE OPTO-ELECTRONIC OSCILLATOR STRUCTURE

Development and creation of the compact ultra-low-noise microwave signal sources, which would be impact-resistant, is an important problem of modern radio-physics and radio engineering. Levels of the phase noise spectral density at the microwave source output must be for most of the applications -120…-170 dB/Hz at generation frequency 8…12 GHz for 1-kHz offset from a carrier. Constructions of these oscillators must sustain the strong mechanical impact loads in 200…2000 N/cm and high accelerations up to 2…10g. Geometrical dimensions of the modern signal sources should often be approximately 10x10x10 cubic mm, especially for the satellite applications.

Development and implementation of new compact microwave and millimeter-wave oscillators with improved performance would lead to revolutionary jump in radio electronics, perhaps, comparable to discovery of the quantum-dimensional lasers or (as in radio engineering) at arriving of the high-stability quartz crystal resonator. The new type of oscillators called as opto-electronic oscillator (OEO) described in this paper will permit to use in the mobile communications and in Internet systems of new radiofrequency channels for information transmission, including 30…75-GHz ranges at the low power of transmitters. A number of publications devoted to OEO experimental investigations grows each year [1-8].

Opto-electronic oscillators will undoubtedly find wide application in the fiber-optical communication lines as well as in on-board radar systems on millimeter- and centimeter

[1]Alexander A. Bortsov is with Moscow Power Engineering Institute (National Research University), Russia (e-mail: laseroeo5@gmail.com).

Sergey M. Smolskiy is with Moscow Power Engineering Institute (National Research University), Russia (e-mail: SmolskiySM@mail.ru).

ranges, in communication systems as low-noise local oscillators in receivers and as a master clock in transmitters, in an optical lidar technology, as sensors of different physical quantities and in many other systems [8-11].

Let us consider the OEO structural diagram with *external modulation* of optical emission, which is often called as an opto-electronic oscillator with the Max–Zender modulator (OEO MZ) presented in Figure 1a.
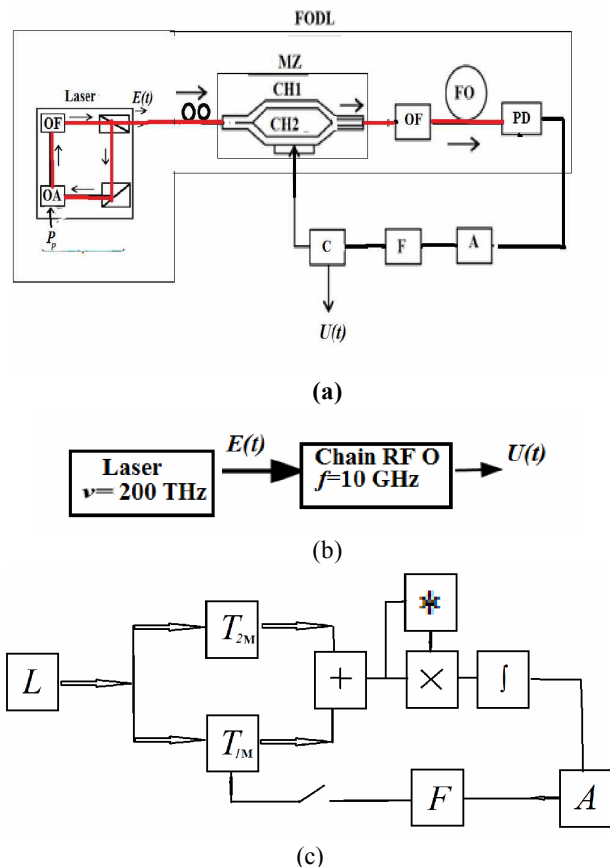

(a)

(b)

(c)

Figure 1. (a) Structural diagram of OEO with external MZ modulator; (b) OEO circuit, a laser is the energy pump; (c) Equivalent OEO circuit with a correlator.

OEO is formed by the following principal units: a laser, the Mach-Zender (MZ) modulator, which is connected serially into a ring, the fiber-optical system (FOS) containing an optical filter (OF) and the single-mode optical fiber (FO), a photo-detector (PD), for instance, the quantum-dimension photo-diode, a narrowband radiofrequency filter (F), a

nonlinear amplifier (A), and a directional coupler (C). Serially connected Laser, MZ, OF, FO, and PD constitute the unit of fiber-optical delay line (FODL), which electrical input is the MZ modulator input (the MZ input signal), and its electrical output coincides with PD electrical output i.e., the output voltage on the PD load resistor).

As we see, OEO contains the feedback loop of radiofrequency and it results in double generation: laser on the optical frequency and RF feedback circuit with RF modulation of the optical oscillation.

The opto-electronic oscillator implemented according to the *scheme of external modulation* can be considered as an oscillator with delayed feedback in which FODL of the radiofrequency oscillation is active. The FODL has its own amplitude and phase noises which are the laser noises reduced to the FODL output (or passed from the Laser output through MZ, OF, FO).

We can use the quantum-dimension laser diode or the fiber-optical laser with activated erbium dope etc. as the OEO laser. In the diagram in Figure 1, the Laser is presented by closed into a loop the optical amplifier (OA), the optical filter (OF), which corresponds to the "traveling-wave" laser or the fiber-optical laser. The optical pump power P_P acts at the active amplifier. If the excitation conditions are met, the laser generates optical oscillations which pass from its output into MZ, then pass via two optical channels with different delays, combine together and through OF and FO acts to the light-sensitive PD area. An effective modulation by MZ is possible in microwave range only for single-mode single-frequency and linear-polarized emission of the highly-coherent laser. Quantum-Well (QW) laser diodes and the fiber-optical lasers with polarizers at their outputs are such emission sources.

The laser is the pump source for the radiofrequency network (Figure 1b) closed into a loop and formed by a modulator, an optical fiber, a photo-detector, an electronic amplifier, an electric filter, and a coupler.

As a result of oscillation processes, the spectra are formed with fluctuations having the various nature, but the spectral line width of radiofrequency oscillations is defined by parameters of two oscillating system: the laser and the radiofrequency oscillator.

II PROBLEM STATEMENT

At present, in large-dimension models of laser OEO (Figure 1) with the fiber-optical delay line the low phase noise level of -157 dB/Hz [5,6] is achieved on the 10 GHz generation frequency at 1 kHz offset from a carrier.

Experimental and theoretical investigations of the power spectral density of the laser oscillator phase noise described in [13], show that reduction of the phase noise level of OEO in many respects depends on the laser phase noise level. At oscillation frequency 8…10 GHz at standard offsets from 1 to 10 kHz, the power spectral density of the phase noise is -120 dB/Hz…-140 dB/Hz.

Appearance on the commercial market of nano-dimension optical fibers with low losses (down to 0.001 dB per one bend, at small bend radii up to 2…5 mm) becomes the stimulus for improvement of OEO radiofrequency generation methods. This allows implementation of comparably small (by

geometric linear maximal dimensions) fiber-optical 5-μs delay lines of 10…30 mm.

In spite of the growth of publications devoted to OEO experimental investigations, the theoretical analysis and systematization of main mechanisms of the phase noise suppression in the low-noise laser OEO was not yet described in known literature. The laser phase noise influence on the OEO radiofrequency phase noise was not researched yet.

The aim of this paper is to analyze of the main mechanisms of the phase noise suppression in the ultra-low-noise laser OEO and research of OEO phase noise influence from the laser phase noise, the time constant of the laser resonator, the geometric length of the optical fiber, and optical power.

Following to an approach described in [13], for OEO noise analysis, we consider the system in Figure 1, in which two different oscillation processes are developed: laser oscillations with the generation frequency of approximately 200 THz and 10-GHz oscillations in the radiofrequency network closed into a loop. At that, the frequency multiplicity is approximately 20,000.

III LASER IN OEO

We consider that our laser is highly-coherent device, i.e., the spectral line is much less than 100 MHz and the mean generation frequency is 200 THz. We assume that oscillations of the normalized electromagnetic field (EMF) at the laser output are close to sinusoidal with the phase noise component $\varphi_{Lm}(t)$ and normalized amplitude noises $m_{Lm}(t)$:

$$E_L(t) = [E_{0L} + m_{Lm}(t)]\cos[2\pi\nu_{0L}t + \varphi_{0L} + \varphi_{Lm}(t)]. \quad (1)$$

Here $E_L(t)$, E_{0L}, $m_{Lm}(t)$ are normalized non-dimensional quantities, respectively: the instantaneous intensity, the EMF intensity amplitude, and the EMF amplitude noise, ν_{0L} is the average laser oscillation frequency, φ_{0L} is the initial constant phase shift, t is the current time.

In the opto-electronic oscillator system, under fulfillment of excitation conditions in the electronic part of such an oscillator, the radiofrequency oscillations $u = u_g(t)$ give rise. At that, the radiofrequency signal passes to the electric MZ input from the output of a nonlinear amplifier through the C coupler during oscillation generation. The instantaneous voltage of this signal is

$$u_g(t) = [U_{10MZ} + m_{em}(t)]\cos[2\pi ft + \phi_{0e} + \varphi_{em}(t)], \quad (2)$$

where $U_{01MZ} = U_{01C}$ is the amplitude of fundamental oscillation at the electric input of the MZ modulator or at the C output, f is the oscillation radiofrequency, ϕ_{0e} is the constant phase shift, $\varphi_{em}(t)$ are electronic phase fluctuations, $m_{em}(t)$ are electronic amplitude fluctuations.

The low-noise single-mode and single-frequency quantum-dimension laser diodes or the fiber optical lasers are used as the light sources in OEO.

The laser included in the OEO structure (Figure 1) is formed by (closed in the loop) the nonlinear OA, the narrowband optical filter (OF), and the optical delay line. The

optical oscillation frequency ν_{0L}, which is generated by the quantum-dimension laser diodes in the autonomous steady-state, can be found (under excitation condition fulfillment) on the basis of the phase balance equations solution for the steady-state optical intensity oscillations in the optical resonator and in the laser active element.

To reveal the main mechanisms of the laser noise influence on the OEO radiofrequency noise, the laser can be described by a system of semi-classical equation with the Langevin's sources of the white noise (ξ_E, ξ_P, ξ_N), relatively, for the EMF intensity E_L, a polarization of the laser active material P_n, a population difference N. We studied the laser equation system under its operation in the single-frequency single-mode regime. At that, oscillation are linear-polarized. The main assumption for utilization of semi-classical equations is that the carrier life time on the upper operation level and the time constant T_{0F} of the laser optical filter (OF) are much larger than the relaxation time of polarization T_2. At that, the equation system with the Langevin's sources for the laser can be written as:

$$\begin{cases} \dfrac{d^2 E_L}{dt^2} + \dfrac{1}{T_{0F}}\dfrac{dE_L}{dt} + (2\pi\nu_{0F})^2 E_L = \dfrac{d^2 P_n}{\varepsilon_0 dt^2} + \xi_E; \\[2mm] \dfrac{d^2 P_n}{dt^2} + \dfrac{1}{T_2}\dfrac{dP_n}{dt} + (2\pi\nu_{12})^2 P_n = \dfrac{p_e^2}{h} N E_L + \xi_P; \\[2mm] \dfrac{dN}{dt} = \alpha_{N0}\cdot J_{0N} - \dfrac{N}{T_1} - G_0\cdot P_n E_L + \xi_N; \end{cases} \qquad (3)$$

In (3) T_2 is the polarization time constant, the excited particles at the upper energy level, T_1 is the lifetime of the excited particles at the upper energy level, T_{0F} is the time constant of the optical resonator, p_e is the combined dipole moment, h is the Planck constant, ν_{0F} is the natural frequency of the optical resonator on the specific n-th longitudinal mode, ν_{12} is the optical frequency of the transition, J_0 is the constant pump current, $\alpha_{N0}\cdot J_0 = (N_{02} - N_{01})/(N_{02}T_1)$ is the constant pump, ε_0 is the electrical constant, ν_{0F} is the intrinsic optical frequency of the resonator, P_n is the polarization of the active material, $N = (N_{02} - N_{01})$ is the population difference between the excited and unexcited levels produced by the pumping, G_0 - gain factor .

It should be noted that equations (3) are similar to well-studied equations in the oscillator theory for the double-circuit autonomous oscillator with the inertial auto-bias chain with fluctuations.

IV MACH-ZENDER MODULATOR IN OEO: THE EMF CORRELATOR

An effect of the $u_g(t)$ voltage in the one from two MZ optical channels (Figure 1) on the refraction index of the electric-optical material (the lithium niobate) from which the MZ optical channels are made, leads to phase modulation of optical oscillation. Adding of two emission on the PD area, which passed through different optical MZ channels, leads to intensity modulation of the laser emission.

Retarded output emissions of the first and second channels of the MZ modulator E_{1L} and E_{2L} pass to the input of PD. If the fiber-optical system (FOS) is formed by single OF, the delay difference is determined as $\Delta T_M = T_{M20} - T_{M10}$.

We considered OEO with the Mach-Zender interferometer, which perform a role of optical emission modulator as a correlator of two optical oscillations $E_L = E_L(t)$ and delayed by some time Δt oscillation $E_{Lx} = E_L(t - \Delta t)$:

$$R_E(\tau) = \left\langle E_L(t) E_{Lx}^*(t - \Delta t) \right\rangle = \frac{1}{\tau}\int_0^\tau E_L E_{Lx}^* dt,$$

where τ - the time of observation. To the PD area in OEO occurs at high optical power (in contrast to fiber optic systems), so the law of random distribution (amplitude m_{Lm} and phase φ_{Lm} of the laser oscillation) are considered normal.

Figure 1c shows an equivalent circuit of OEO. Here the following blocks are introduced: «+» (adding), «x» (multiplication), «*» (conjugate) «∫» (integration). Blocks L, A, F designate a laser, an electronic amplifier and an electronic filter, relatively. Blocks «T_{1M}» and «T_{2M}» are delays in optical channels MZ and OF and equal to: $T_{1M} = T_{M10} + T_{BC}$ and $T_{2M} = T_{M20} + T_{BC}$. At open switch, the PD photo-current is $S_{PD}R_E(\tau)$, where S_{PD} is the PD sensitivity. When this switch is open, there is a strong correlation between random quantities of m_{Lm} and φ_{Lm} of different optical MZ channels due to a small delay difference of optical oscillations (tens picosecond)). At closed switch in Figure 1c), the electric oscillation affecting on the second optical MZ channel is delayed with respect to the optical oscillation of the first channel by the delay time in the optical fiber (the delay 1…20 μs). Interchannel correlation of random quantities becomes weak. Therefore, requirements to phase noise smallness are essentially increased.

The normalized correlation function of oscillation $E_L = E_L(t)$ at the MZ output depends on time, and it unambiguously determines the frequency spectrum of oscillation power.

We take into account that oscillations $E_{1L} = k_{01}E_{0L}$ and $E_{2L} = k_{02}E_{0L}$ are propagated through the different MZ optical channels, where k_{01} and k_{02} are excitation coefficients ($k_{01} + k_{02} \approx 1$). We introduce the excitation irregularity

coefficient of MZ optical channels $\gamma = (k_{02}/k_{01}) \approx 1$ (in the experiment $k_{01} \approx k_{02} \approx 0.5$), then the result on interferencing oscillations after MZ is E_{12L}. Let us extract the modulus and the argument of E_{12L}:

$$\left|E_{12L}\right|^2 = E_{0L}^2 \{k_{01}^2 + k_{02}^2 - 2k_{01}k_{02}\cos(\varphi_{0L1}(u_g) - \varphi_{0L2})\}$$

$$= \frac{E_{0L}^2}{2}\gamma\{\frac{(1+\gamma^2)}{2\gamma} - \cos(\varphi_{0L1}(u_g) - \varphi_{0L2})\}. \tag{4}$$

$$\arg E_{12L} = \arctan\{\frac{k_{01}\sin\varphi_1 + k_{02}\sin\varphi_2}{k_{01}\cos\varphi_1 + k_{02}\cos\varphi_2}\}, \tag{5}$$

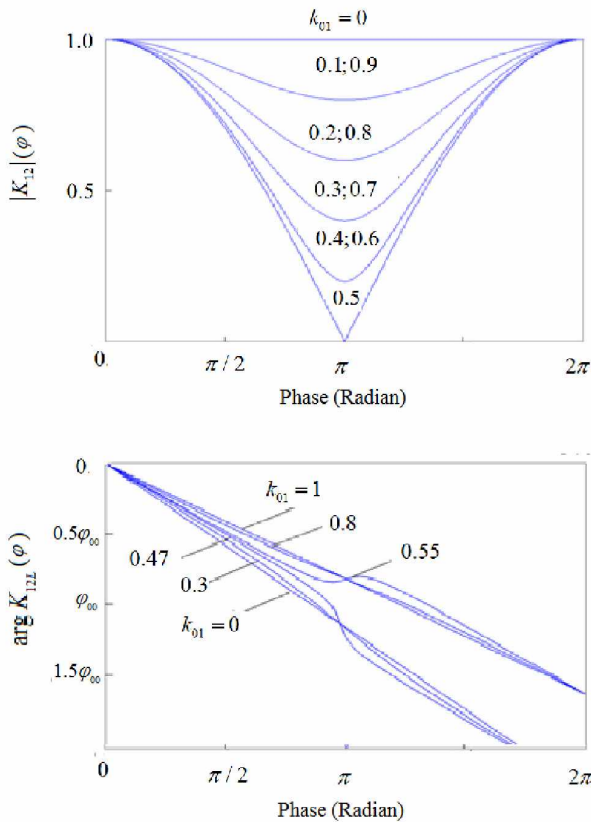where $\varphi_1 = 2\pi T_{M10}\cdot\nu$, $\varphi_2 = 2\pi T_{M20}\cdot\nu$.

Figure 2. The magnitude and argument plots of the transfer function of the MZ modulator versus frequency.

Plots of the modulus $\left|K_{12L}\right|$ and the argument $\arg K_{12L}(\varphi)$ are presented in Figure 2, where $K_{12L} = E_{12L}^2 / E_{0L}^2$, $\varphi = 4\pi\nu(T_{M20} - T_{M10})$. On the y-axis of argument we use $\varphi_{00} = -\pi\nu(T_{M20} + T_{M10})$. Noteworthy, the smoothing degree of optical channels according to the excited optical power influences on the modulus and argument of the MZ transfer function.

We attract your attention to the fact that in expression for $\left|E_{12L}\right|^2$ the phase $\varphi_{0L1}(u_g)$ is modulated by the harmonic oscillation $u_g(t) = U_{1MZ}\cos[2\pi f_0 t + \phi_{0e} + \varphi_{em}(t)]$. The expression for the function $(E_{12L})^2$ versus the oscillation amplitude U_{0M} and the choice of MZ operation point φ_{0L2}.
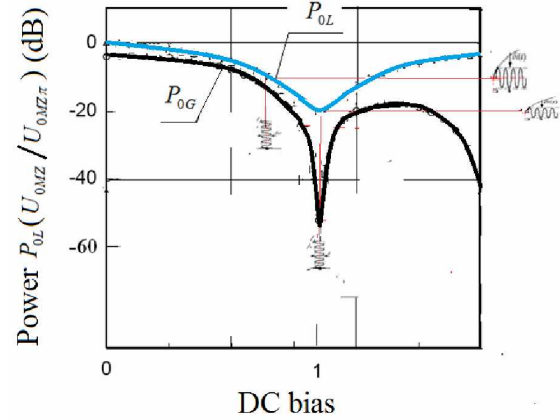

Figure 3. Plots of the power DC bias component of the optical emission P_{0L} and power AC fundamental component P_{0G} of OEO in the PD photo-current (at MZ output)
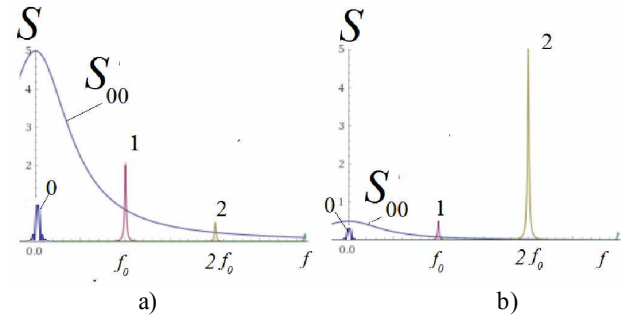

Figure 4. The spectrum structure (qualitative picture) of the PD photo-current of the OEO (Figure 1,c) at $\varphi_{0MZ} = m\pi/2$ (a) and $\varphi_{0MZ} = m\pi$ (b). Designations: DC component - 0, enlarged noise spectrum of DC component - S_{00}, fundamental harmonic - 1, second harmonic - 2

The MZ operation point varies by the DC bias voltage (Figure 3). We introduce the constant half-wave MZ bias voltage $U_{0MZ\pi}$, which provides the phase difference φ_{0L2} of 180 degrees between optical oscillations of the first and second MZ channels. Let us suppose for designation convenience that

$$x = \frac{U_{1MZ}}{U_{0MZ\pi}}; \qquad \varphi_{0MZ} = \frac{\pi U_{0MZ}}{2U_{0MZ\pi}}.$$

In OEO we use the optical filter, which effectively suppress optical harmonics of carries higher than second $\nu_2 = \nu_0 - 2f$, and in the OEO circuit with the single-side band

harmonics from the "left" are suppressed. Then we may present the simplified expression for E_{12L}.

The expression for $(E_{12L})^2$ can be rewritten using an expansion on even J_{2k} and odd J_{2k-1} Bessel functions. Using the trigonometric formula for cosine of the two angles sum, we keep the first and second harmonics in the record of the carrier expression only from the "left of the carrier". Now we can write expressions without fluctuations as:

$$(E_{L12})^2 = \frac{E_{0L}^2}{2}\gamma \{\frac{(1+\gamma^2)}{2\gamma} \cdot \cos(2\pi\nu\, t + \phi_{0e})$$
$$- \cos(\varphi_{0MZ})J_0(x) \cdot \cos(2\pi\nu\, t + \phi_{0e}) \qquad (6)$$
$$- \sin(\varphi_{0MZ})J_1(x) \cdot \cos(2\pi\nu\, t - 2\pi f - \phi_{0e}) - \cos(\varphi_{0MZ})$$
$$\times J_2(x) \cdot \cos(2\pi\nu\, t - 2 \cdot 2\pi f t - 2 \cdot \phi_{0e})\}.$$

At spectrum calculation for Bessel functions we use the approximation for $x \in [0;1]$, where $x = U_{1MZ}/U_{0MZ\pi}$:

$$J_0(x) \approx 1 - \frac{x^2}{4};\ J_1(x) \approx \frac{x}{2} - \frac{x^3}{16}, \text{ and }\ J_0(x) \approx \frac{x^2}{8}.$$

Now we introduce coefficients a_0, a_1, a_2:

$$a_0 = \frac{E_{0L}^2}{2}\gamma \{\frac{(1+\gamma^2)}{2\gamma} - \cos(\varphi_{0MZ}) \cdot (1 - \frac{x^2}{4})\};$$

$$a_1 = -\frac{E_{0L}^2}{4}\gamma \sin(\varphi_{0MZ});\ a_2 = -\frac{E_{0L}^2}{8}\gamma \cos(\varphi_{0MZ}).$$

The PD transfer function (or sensitivity) we define as S_{PD}, then taking a noise into account, the expression for PD photo-current is:

$$I_{PD} = S_{PD} \cdot \left\langle E_{12L}(t)E_{12Lx}^*(t - \Delta t)\right\rangle_T.$$

Having introduced the total phase incursion ϕ_{0eMZ}, we obtain following equations for PD photo-current harmonics not taking a noise into account:

$$I_{0PD} = S_{PD}a_0 - S_{PD}(a_2/2)x^2;$$

$$I_{1PD} = S_{PD}a_1(\frac{x}{2} - \frac{x^3}{16}) \cdot \cos(2\pi f t + \phi_{0eMZ}); \qquad (7)$$

$$I_{2PD} = S_{PD}a_2x^2 \cos^2(\pi f t + \phi_{0eMZ}).$$

Calculations are presented according to the approach accepted in statistic radio engineering. After obtaining of the correlation function, we determine obtain the normalized (by S_{PD}) spectrum of first and second harmonics and noise contributions as:

$$S_{\eta MZ}/S_{PD} = a_1^2 \frac{U_{1MZ}^2}{2}\delta(f - f_0) + a_2^2 \frac{U_{1MZ}^4}{8}\delta(f - 2f_0)$$

$$+ 4(a_1^2 \sigma_{Le}^2 + a_2^2 \sigma_{Le}^4) \cdot S_{Lm}(f) + a_1^2 \frac{U_{1MZ}^2}{2}S_{L\varphi1}(f - f_0) \qquad (8)$$

$$+ a_2^2 \frac{U_{1MZ}^4}{8}S_{L\varphi2}(f - 2f_0) + 4a_2^2 U_{1MZ}^2 \sigma_{Le}^2 \sigma_{L\varphi e}^2 S_{Lm\varphi}(f - f_0).$$

In (8) δ is the delta-function, and two first terms define powers of the first and second harmonics of the photo-current. From these expressions, we can see that levels of first and second harmonics depends on squared coefficients a_1^2, a_2^2, which in turn are defined by a choice of the MZ operation point and normalized power of optical emission. The third equation in (8) determines the noise spectrum of the constant component, while the fourth one – relatively, the noise spectrum of the fundamental harmonic, while the fifth one – the second harmonic.

From this research we can make the following conclusion. The photo-reception, at relatively high optical power arriving on the PD area, is nonlinear and is accompanied by appropriate interaction of the constant intensity component with its alternate component. The level of the constant component of the optical emission of the PD area affects of the noise spectrum of the photo-current of the alternate component of the fundamental photo-current harmonic. To decrease this influence, we can transfer into MZ operation mode with 180^0-difference of phase incursions in MZ optical channels. Figure 3 shows PSD and harmonics, which qualitatively illustrates the formula (8) at different choices of φ_{0MZ}.

V SYMBOLIC EQUATIONS of OEO

If we introduce into equation system (3) and (11) the operator $p = d/dt$ and take into consideration the total delay time T_{BC} in the open circuit "MZ-C" introducing the FOLD transfer function K_{BZ}, we obtain the system of symbolic equations with fluctuating noise sources in the compact form for Laser and OEO:

$$\begin{cases} Q_o(p)E_L = \alpha_{00}E_L - \beta_{00}E_L|E_L|^2 + \xi_{SN}, \\ i = 0.5\left\langle E_L \cdot E_L^*\right\rangle\gamma \cos[\varphi_{0MZ} + u_{MZ}/U_{0MZ}], \\ [p^2 + (1/T_{eF})p + (2\pi f_{eF0})^2]u_{MZ} \\ = (K_{BZ}/S_{PD})pS_A(i_{PD})\exp(-pT_{BC}) + \xi_U. \end{cases} \qquad (9)$$

where K_{BZ} is the FOLD transfer function, T_{eF} is the time constant of the electronic filter (EF), f_{eF0} is the EF natural frequency, ξ_U is the Langevinian noise of the electronic amplifier, which is defined by shot noises. In (9), the nonlinear function $S_A(i_{PD})$ is introduced, which connects the instantaneous current i_{PD} value at the A amplifier input (or the PD photo-current) with the u_{MZ} voltage at the A amplifier output (or MZ voltage). Equations (9) describe oscillations in the opto-electronic part: closed into a loop of MZ, OF, PD, A, F, C.

Here in (9), we introduce the operator $Q_0(p) = Q_{0F}Q_{0P}$, where

$$Q_{0OF} = (p^2 + (1/T_{0F})p + (2\pi\nu_{0F})^2)/(2\pi\nu_{0F})^2;$$

$$Q_{0P} = (p^2 + (1/T_2)p + (2\pi\nu_{12})^2)/(2\pi\nu_{12})^2.$$

The total noise component ξ_{SN} is determined as

$$\xi_{SN} = (\xi_N \cdot E_n\eta_{00} + Q_P^{-1}\xi_P + \xi_E)/((2\pi\nu_{0F})^2(2\pi\nu_{12})^2).$$

Coefficients α_{00} and β_{00} have a sense of amplification and laser saturation, relatively, and are calculated as

$$\alpha_{00} = \frac{(N_{02} - N_{01})p_e^2 T_2}{2\varepsilon_0 h}\eta_{00};$$

$$\beta_{00} = N_{02}T_1 \cdot G_0 \frac{p_e^2 T_2}{2\varepsilon_0 h}(\eta_{00})^2.$$

The η_{00} parameter defines the laser inertia and connects with a life time of T_1:

$$\eta_{00} = \frac{\exp(-j2\pi\nu_0 T_1)}{(1 + (2\pi\nu_0 T_1)^2)^{1/2}}.$$

The first equation of the (9) system has a feature that it is similar by its form to well-studied equations in radio engineering for the double-circuit autonomous oscillator with the arcwise-cubic function of the nonlinear inertial element of the AC voltage versus current. But coefficients included into equations (9) are expressed via AC components of the laser physical quantities: a population, a dipole moment, a life-time on the upper operation level, a time constant of the laser optical filter, Langevinian noise sources of optical emission, population and polarization.

A transfer from (9) to differential abbreviated equations allows not only determination the laser power $|E_{0L}|^2$ in steady-state, but to write abbreviated equations with fluctuations, from which we below obtain expressions for power spectral density (PSD) of the phase and amplitude noises. At that, the laser emission intensity is determined by the expression:

$$|E_{0L}|^2 = \frac{\alpha_{00}}{\beta_{00}}(1 - \frac{1}{\alpha_{00}\beta_{00}}), \qquad (10)$$

in which the (α_{00}/β_{00}) coefficient is equal to

$$(\alpha_{00}/\beta_{00}) = \frac{(N_{02} - N_{01})}{N_{02}G_0 T_1}.$$

Thus, the coefficient ratio of (α_{00}/β_{00}) has got the clear physical sense for lasers. The larger an amplitude of the laser output optical oscillation, the higher a ratio of relative population excess on the level under excitation, and inversely proportional gain factor and lifetime $G_0 \cdot T_1$.

To derive a formula for the noise PSD, we expand the truncated representation $Q_0(p)$, denoted as $Q(p)$, into the real and imaginary parts:

$$Q(p) = Q_{Re}(p) + jQ_{Im}(p),$$
where

$$Q_{FRe} = (1 + FT_F)\cos(FT_L)/(P_{00L}|K_{0L}|),$$

$$Q_{F Im} = (1 + FT_{0F})\cos(FT_L)/(P_{00L}|K_{0L}|).$$

The T_L is delay in the cavity, $|K_{0L}|$ is the coefficient of a total loss of optical power in the laser feedback loop. Now we present of the total complex noise component by a sum of real and imaginary parts as:

$$\xi_{SN} = \xi_{SN Re} + j\xi_{SN Im}.$$

Using the standard approach to abbreviation of differential equations with fluctuating sources, the Fourier transform, the Wiener-Khinchin theorem, we obtain single sideband (SSB) PSD of the laser amplitude and phase noise. The $\xi_{SN Re}$ real part has in spectral representation a view of $S_{SL Re}$, while the imaginary part $\xi_{SN Im}$ has a view $S_{SL Im}$.

SSB PSD equations obtained from (12) for the laser phase noise, which operates in quasi-stationary mode (single-mode and single-frequency) have the following form:

$$S_{PL} = \frac{(Q_{F Re} - \sigma_{EL})^2 \cdot S_{SL Im} + (Q_{F Im})^2 S_{SL Re}}{\{(Q_{F Re} - \sigma_{EL}) \cdot (Q_{F Re} - S_{0E}) + [Q_{F Im}]^2\}^2}; \qquad (11)$$

where $S_{0E} = \alpha_{00} - \beta_{00}|E_{0L}|^2$, $\sigma_{EL} = \beta_{00}|E_{0L}|^2$. If for (11) we examine a case when the imaginary part $Q_{F Im} = 0$, $P_{0L}K_{0L} \approx 1$, and there is a small delay, i.e., $\cos^2(FT_L) \approx 1$, $\sin^2(FT_L) \approx 0$, then expression (11) for PSD gets the classical form:

$$S_{PL} = \frac{S_{SL Im}}{(1 + T_{0F}F - \alpha_{00} + \beta_{00}P_{0L})^2} \approx \frac{S_{SL Im}}{P_{0L}(T_{0F}F)^2}; \qquad (12)$$

where $P_{0L} = E_{0L}^2$ is the optical emission power on the PD light-sensitive area.

The (11) expression defines that the power growth and increase of the laser resonator time constant T_{0F} (or resonator Q-factor increase) leads to reduction of the laser phase noise.

Expressions (11),(12) for SSB PSD of the laser phase noise do not reflect the important property of the laser oscillating system: a presence of the relaxation resonance on the frequency ν_{00L} at the offset from a carrier ν_{0L}, i.e., at $F_{00L} = 2\pi(\nu_{00L} - \nu_{0L})$. We can take this "resonance peak" into account at linearization of (3) system with account of the population equation. At that, the expression for SSB PSD of the laser phase noise take a form:

$$S_{PL}/P_{0L} \approx \frac{S_{SL Im}}{(FT_{0F})^2} + \frac{S_{LE}D_{11}^2 + S_{LN}D_{22}^2}{(F^2 - F_{00L}^2)^2 + (F\alpha_{00I})^2} \qquad (13)$$

where $F_{00L} = (1/T_{1L})((T_{0F}/T_1)\alpha_0 - 1)^{1/2}$, α_0 is an excess of DC laser pumping over its threshold value, α_{00I} is a damping decrement, D_{11} and D_{22} are the constant coefficients, and S_{LE}, S_{LN} are. Relatively, spectral densities of impacts in (3) ξ_E, ξ_N. Figure 5 shows the plot 1 of PSD of the laser phase noise calculated by formula (13) for

$$S_{SL\,Im} \approx S_{LE}D_{11}{}^2 + S_{LN}D_{22}{}^2 \approx -105 \text{ dB/Hz}, F_{00L} \approx 14 \text{ kHz},$$
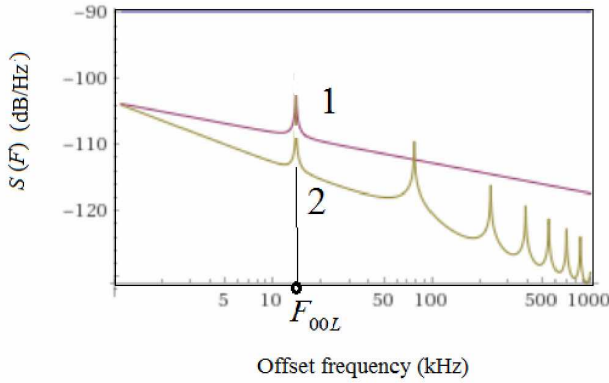
$$T_{0F} = 10^{-7} \text{ s}.$$

Figure 5. Laser phase noise SSB PSD (curve 1), calculated by (13), and OEO phase noise SSB PSD (curve 2).

VI OEO PHASE NOISE SSB PSD

From equations (9) with account of (10) for nonlinear characteristic of the A amplifier (Figure 1) as a cubic polynomial $i_A(u) = \alpha_{e0}u - \beta_{e0}u^3$ (where u is the instantaneous voltage at the amplifier input, and the average slope of this characteristics is $\sigma_U = \alpha_{e00} - (3/4)\beta_{e00}P_{0G})$ and we can obtain through laser and delay line parameters the power of the opto-Electronic oscillator radiofrequency generation P_{0G}:

$$P_{0G} = \frac{\alpha_{e00}}{\beta_{e00}}(1 - \frac{1}{P_{0L}\left|K_{BZ}\right|\alpha_{e00}\beta_{e00}}).$$

Similarly to (11) for laser PSD, we obtain from the general symbolic equations (9) the equation for PSD S_Ψ of the OEO phase noise. PSD S_Ψ reduced to the radiofrequency oscillation power P_{0G} is determined by expression derived in [12] according to the Evtianov-Kuleshov approach:

$$S = \frac{S_\Psi}{P_{0G}} = \frac{(Y_{a\,Re} - \sigma_U)^2 \cdot S_{Im\,FDNY} + Y_{a\,Im}^2 \cdot S_{Re\,FDNY}}{U_0^2\{[Y_{a\,Re} - \sigma_U]\cdot[Y_{a\,Re} - 1] + [Y_{a\,Im}]^2\}^2} \quad (14)$$

where $S_{Im\,FDNY} = S_{Im\,FDNY}(F)$, $S_{Re\,FDNY} = S_{Re\,FDNY}(F)$ are the in-phase and quadrature components of fluctuations determining by the joint noises of a laser, a photodiode, and in the amplifier the OEO closed loop; F is the analysis frequency ω offset from the generation frequency ω_0, $(F = \omega - \omega_0)$; $Y_{a\,Re} = Y_{a\,Re}(F)$, $Y_{a\,Im} = Y_{a\,Im}(F)$ the in-phase and quadrature components of the OEO control conductance (abbreviated representations) $Y_a = Y_{a\,Re} + jY_{a\,Im}$:

$$Y_{a\,Re} = y_M \frac{(1 + FT_F)\cos(FT_{BC})}{P_{0L}\left|K_{BZ}\right|}, \quad (15)$$

$$Y_{a\,Im} = y_M \frac{(1 + FT_F)\sin(FT_{BC})}{P_{0L}\left|K_{BZ}\right|}, \quad (16)$$

where $\left|K_{BZ}\right|$ the modulus of the transfer function of the open circuit OEO, T_{BC} is the total delay time of oscillations in the OEO open loop including a delay in the OF fiber, y_M is the input normalized conductivity of the MZ modulator.

Let us consider the case of large delay and we take into account the laser SSB PSD as in (13). Let in (14) $S_{Im\,FDNY} = S_{Re\,FDNY} = N_{sp}h\nu$, where the N_{sp} is a number of spontaneous photons received by PD, while $Y_{a\,Re}$ and $Y_{a\,Im}$ are defined as (18) and (19). Then the function of OEO phase noise PSD (17) can be represented as

$$S = \frac{S_\Psi}{P_{0G}} = \frac{K_2 C_A h\nu N_{sp}}{P_{0G}}, \quad (17)$$

where C_A - the constant coefficient, the K_2 coefficient depends on the delay time in the optical fiber and on the laser optical power and it is equal

$$K_2 = \frac{\sigma_U^{-2}}{\frac{(1 + FT_F)^2}{(P_{0L}\left|K_{BZ}\right|\sigma_U)^2} - 2\frac{(1 + FT_F)\cos(FT_{BC})}{P_{0L}\left|K_{BZ}\right|\sigma_U} + 1} \quad (18)$$

From (17), (18) we see that the laser phase noise are suppressed with OF length growth, increase of the total transfer function in the OEO loop, the laser power as well as α_{e00} and β_{e00} choice.

Figure 5 shows plots of (13), (18) which are limited functions of OEO of the phase noise PSD with account of small noises of PD and the A amplifier, at laser phase noise for the offset frequency 1 kHz equaled to about -120 dB/Hz, at laser power 20 mW, the delay of $T_{BC} = 5 \cdot 10^{-6}$ s (the OF length is 100 m), $\sigma_U = 1$. We see that the first peak is defined by the laser phase noise PSD, and average suppression of the phase noise for 50 kHz offset is more, that -10 dB/Hz.

Figure 6 shows the OEO phase noise PSD versus delay time T_{BC} (or the length of the optical fiber). This calculation is fulfilled on the basis of formulas (17), (18) with about the same assumptions and values of the laser phase noise and main OEO parameters as in Figure 5. It should be noted that at the optical fiber length of 2 km the uniform suppression of the laser phase noise is achieved in the offset range 1…50 kHz. Calculation of the phase noise suppression factor $K_2(F)$ suppression factor according to (18) is presented in Figure 7 $\sigma_U = 1$: $\sigma_U = 1$: $T_{BC}/T_F = 1$, $P_{0L}\left|K_{BZ}\right| = 2$ (curve 1); $T_{BC}/T_F = 10$, $P_{0L}\left|K_{BZ}\right| = 2$ (curve 2); $T_{BC}/T_F = 10$, $P_{0L}\left|K_{BZ}\right| = 4$ (3 curve). It can be seen that increase of delay time from $T_{BC}/T_F = 1$ (curve 1) to $T_{BC}/T_F = 10$ (curve 2) results in reduction of K_2 factor more than 10 times in the rated offset frequency $F \cdot T_F$ range 0.05…0.5. For example, $P_{0L}\left|K_{BZ}\right| = 2$, $T_{BC}/T_F = 10$, $T_{BC} = 10^{-5}$ s, $T_F = 10^{-6}$ s. It is shown that at OF length, the further reduction of the OEO phase noise is possible using the PLL (phase-locked loop) system.

Calculation results are well-agreed with experimental dependences of OEO phase noise SSB PSD, which can be found in [14]. Here, we should remind that first publications on research of frequency stability in OEO with the help of FOLD were fulfilled in 1987-1989 at Radio Transmitter Dept. of Moscow Power Engineering Institute (now ТКГ MPEI) while the OEO circuit was offered in [15].
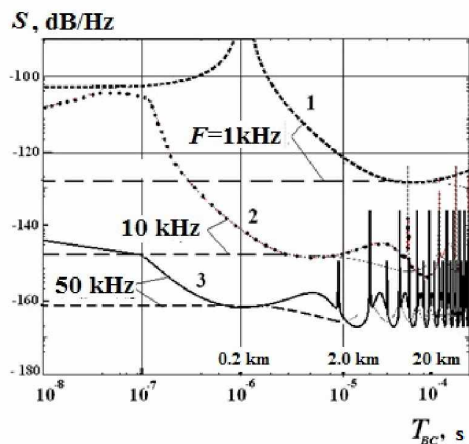

Figure 6. OEO phase noise SSB PSD of MZ modulator depending upon the delay time in OF at various offsets from the radiofrequency of 10 GHz.
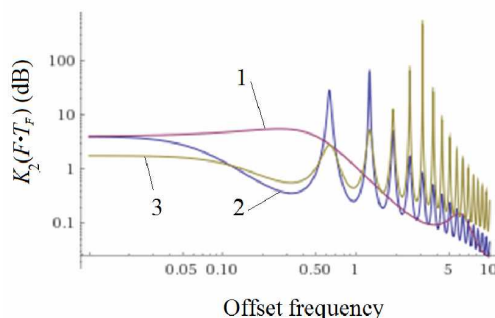

Figure 7. The phase noise suppression factor K_2 (equation (18)) versus the rated offset frequency $F \cdot T_F$ from the OEO generation frequency f_0 at different delays in the optical fiber of delay time T_{BC}/T_F and the power of the laser optical emission P_{OL}, $|K_{BZ}|$ and $\sigma_U = 1$: $T_{BC}/T_F = 1$, $P_{0L}|K_{BZ}| = 2$ (curve 1); $T_{BC}/T_F = 10$, $P_{0L}|K_{BZ}| = 2$ (curve 2); $T_{BC}/T_F = 10$, $P_{0L}|K_{BZ}| = 4$ (3 curve).

VII EXPERIMENTAL INVESTIGATIONS

Experimental researches were devoted for several experimental OEO of microwave range with various pumping laser diodes, which emit at wavelengths of 1310 nm or 1550 nm. The maximal output power of optical emission for used laser diodes formed about 10…20 mW. Figure 8 shows the photo picture of one piece assembled on the base of the circuit in Figure 1(a). As the photo-detector, we applied the FD on

the base of InGaAs. The radiofrequency filter represented the dielectric resonator of microwave range with the loaded Q-factor of 1000. This resonator was made on ceramics and had a natural frequency 8.2 GHz. This breadboard model used the wideband (up to 12 GHz) modulation of laser emission, which was performed by the Mach-Zender modulator from Hitachi Co. The single-mode light guiders with lengths from 60 m to 4640 m were used for experiments. The stable generation of single-frequency oscillation at frequency close to 8.2 GHz was observed in OEO system for various OF lengths.

The delay of OEO signal was performed with the help of additional fiber-optical light guider with the 10km-length and the additional photo-diode. The phase noise level at usage of different lasers formed the value −100… −127 dB/Hz, for offsets 1…10 kHz from the microwave sub-carrier frequency under generation and it depends on the spectral line width of laser emission.

Essential reduction of the phase noise by 15 dB was observed in OEO using the differential delay line on the base of two optical fibers of different length. These experimental functions are well-agreed with theoretical at account of the stabilization effect at OF lengths more than 2000 m.
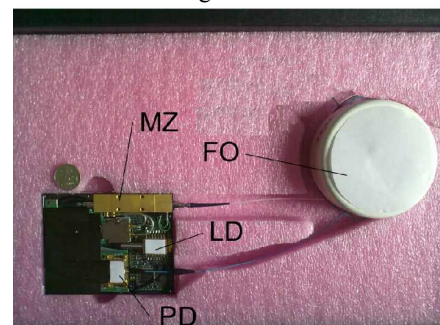

Figure 8. General view of the experimental breadboard of low-noise laser opto-electronic oscillator of microwave range. The mean oscillation frequency is 8…10 GHz.

VIII CONCLUSION

Under assumption of the small and large oscillation amplitude at the modulator electrical input, we study OEO as a system in which two oscillation processes are developed on the optical frequency and in radiofrequency. The relatively simple expressions for phase noise PSD of the radiofrequency generation in optoelectronic generator in the mode with the single-side carrier with an account of the laser phase noise. The analysis fulfilled shows that under condition of predominance of laser noises being detected over v noises of the electronic amplifier and the OEO photo-detector of the filtering system.

For reduction of spurious influence of DC intensity component on the photo-detector we offer to use the modulator operation mode with an offset of the optical channels «pi».

The suppression factor of the OEO laser phase noise at optical fiber lengths from 2 to 10 km is about -8…-10 dB/Hz at offset of $F = 1$ kHz. Utilization in OEO of the highly-coherent laser with the phase noise less than $S(F) = -100$

dB/Hz (at the same offset) is the condition of OEO small phase noises less than $S(F) = -130$ dB/Hz at the $F = 1$ kHz offset. The value of the OEO power spectral density is proportional to the spectral line width of the laser optical emission.

REFERENCES

[1.] Aliou Ly, Vincent Auroux, Ramin Khayatzadeh « Highly Spectrally Pure 90-GHz Signal Synthesis Using a Coupled Optoelectronic Oscillator », IEEE Photonics Technology Letters, vol. 30, no.14, pp. 1313-1316, 2018.

[2.] Dan Zhu, Tianhua Du, Shilong Pan « A Coupled Optoelectronic Oscillator with Performance Improved by Enhanced Spatial Hole Burning in an Erbium-doped Fiber », Journal of Lightwave Technology, pp. 3726-3732, (2018).

[3.] Zhuansun Xiaobo and etc, « Low phase noise frequencymultiplied optoelectronic oscillator using a dual-parallel Mach–Zehnder modulator », Optical Engineering 57(08), p. 086101, (2018).

[4.] A. G. Correa-Mena and etc « Performance Evaluation of an Optoelectronic Oscillator Based on a Band-Pass Microwave Photonic Filter Architecture », Radioengineering, 26(3), pp. 642-646, (2017).

[5.] C. X. Li et al., « A Novel Optoelectronic Oscillator with Series-Coupled Double Recirculating Delay Lines », Advanced Materials Research, Vols. 986-987, pp. 1730-1733, (2014).

[6.] Xihua Zou, Xinkai Liu, et al., « Optoelectronic Oscillators (OEOs) to Sensing, Measurement, and Detection », IEEE Journal of Quantum Electronics 52(1):0601116, (2016).

[8.] X. S. Yao and L. Maleki, « Optoelectronic microwave oscillator », J. Opt. Soc. Amer. B, Opt. Phys., vol. 13, no. 8, pp. 1725–1735, (1996).

[9.] A. A. Savchenkov, A. B. Matsko, V. S. Ilchenko, and L. Maleki, "Optical resonators with ten million finesse," Opt. Express 15, 6768-6773 (2007).

[10.] J. J. McFerran, E. N. Ivanov, A. Bartels, G. Wilpers, C. W. Oates, S. A. Diddams, and Hollberg, "Low-noise synthesis of microwave signals from an optical source," Electron. Lett. 41, pp. 650-651 (2005).

[11.] Russian patent on invention №2282302 RU, МПК³ 7 H03 C3/00. « Former (generator) of frequency-modulated signal / Bortsov A. A., Il'in Yu.B. – 10 p. 2004г. (in Russian)

[12.] Zhalud V., Kuleshov V. N. « Noise in semiconductor devices. Under edition of A.K. Naryshkin. – Moscow: Soietskoe Radio, 1977. -416 p. (in Russian)

[13.] Bortsov A. A., Il'in Yu. B. « Laser Spectral Line Effect on RF Phase and Amplitude Noise of an Opto-Electronic Oscillator// Radiotekhnika. No. 2, 2010. - pp. 21-31. (in Russian)

[14.] C.W. Nelson and etc. // Microwave optoelectronic oscillator with optical gain, IEEE, №12, v. 31, pp.152-157, 2007.

[15.] V.V. Grigor'yants, Yu. B. Il'in, « Laser optical fibre heterodyne interferometer with frequency indicating of the phase shift of a light signal in an optical waveguide », Quantum and Quantum Electronics, 21(5), pp. 423-427, (1989).

Alexander A. Bortsov, born in 1959, in Moscow, Ph.D. in Engineering, Graduated from MPEI in 1982. PhD thesis was on the theme "Opto-electronic oscillator with the QW laser diode". Author of more 40 scientific publications, among them 30 scientific papers, one book «Quantum Opto-Electronic Oscillator», three USSR copyright certificates on invention, 4 Russian patents, more than 20 technological reports on various conferences, including international. Field of current research: the theory and technique of the opto-electronic oscillator, lasers, QW lasers, phase noise in such oscillators.

Sergey M. Smolskiy, born in 1946, Ph.D. in Engineering, Dr.Sc. in Engineering, full professor of Department of Radio Signals Formation and Processing of the National Research University "MPEI". He was engaged in theoretical and practical problems concerning the development of modern transmitting cascades including the short-range radar. In 1993 he defended the Doctor of Science thesis and now he works as a professor of Radio Signals Formation and Processing Dept. Academic experience - over forty years. The list of scientific works and inventions contains over three hundreds of scientific papers, 15 books, more than 100 technological reports on various conferences, including international. The active member of International Academy of Informatization, International Academy of Electrotechnical Sciences, International Academy of Sciences of Higher Educational Institutions. The active member of IEEE. The scientific work for the latter fifteen years is connected with conversion directions of short-range radar systems, radio measuring systems for fuel and energy complex, radio monitoring system etc.

Sun Tracker Robotic Arm Optical Distance Measurement Evaluation at Different Positions Using Six Sigma Tools

Roland Szabo and Aurel Gontean, *Member, IEEE*

Abstract—**This paper presents an optical distance evaluation solution, for a sun tracker robotic arm, with the help of Six Sigma. With the help of statistical tools any measurement system can be evaluated and a measurement system analysis (MSA) can be easily made. Like every measurement system, optical distance measurement can have errors. Six Sigma tools can evaluate the measurement system and can give useful data about its accuracy. Sometimes measurement system evaluation is done twice. First, initial tests are done, after some fine tuning and error correction is performed, and finally a repeated test is done, to show that the measurement errors were corrected.**

Index Terms—**cameras, databases, distance measurement, data processing, stereo vision.**

I. INTRODUCTION

THIS paper presents an evaluation tool of an optical distance measurement system. Optical distance measurement can have errors, apparently larger than traditional systems [1, 2]. Using the Six Sigma (6σ) tools, we can ensure that optical distance measurement is accurate, having high precision at smaller and bigger distances too [18].

In today's industrialized world, robots are the key elements which makes possible to build products in big volume and with a high-quality standard to cover the needs of today's consumer world [3, 4, 14, 15]. Robots need to measure distances to know their position in space and the distance to the manipulated object [5]. They must use optical distance measurement methods to ensure flexibility [6]. Optical distance measurement with the usage of stereo cameras [16] is one of the most common ways to achieve high precision distance measurement for industrial robots [7].

Measurement system analysis (MSA) is often performed to ensure that the system behaves as desired [10]. First, a pre-test is done, where the measurement system errors are measured [11]. After, some corrections are made, and is checked if the changes really reduced the measurement errors [12].

II. PROBLEM FORMULATION

In the laboratory we had access to an educational/industrial robotic arm (Fig. 1), which we needed to program to track the sun [18]. The demand was to know its position in space and the distance to the manipulated object to implement automated software which can control it to move autonomously [18]. The optical distance measurement was the best solution to obtain the position of the key parts of the robotic arm in space [8]. We evaluated the optical distance measurement against the distances measured with laser. The optical distance measurement had some errors. We had to measure somehow if these errors are acceptable, if some corrections are needed, or if we need to use another distance measurement method [9].
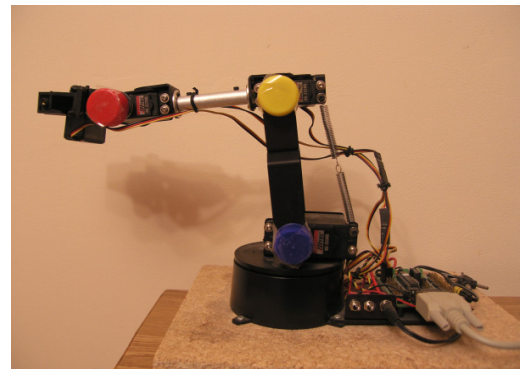

Fig. 1. The normal probability plot, for the actual real distance and the distance computed, by the system using the cameras.

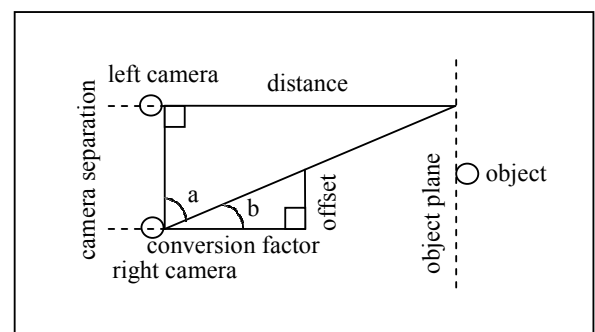On Fig. 2 there can be seen the optical distance measurement method with two cameras (stereo cameras).

Fig. 2. Distance computation using two video cameras (stereo cameras).

The camera separation and initial distance from the base of the robotic arm is measured previously with laser. These values are hardcoded in the automated distance measurement software, made by the authors, in C++ programming language, for the robotic arm. The automated distance measurement system can compute the distances to each colored bottle cap (blue, yellow and red) at the robotic arm's joints. The colored bottle caps are recognized using color filtering.

On the *0x* and *0y* axes the distance can be computed easily based on a 2D coordinate system based on the pixels from one camera. To compute the distance on the *0z* axis (in 3D) the following formulas were used.

On equation (1) can be seen the tangent of the *a* and *b* angles.

$$\begin{cases} tg(a) = \dfrac{distance}{camera\ separation} \\ tg(b) = \dfrac{offset}{conversion\ factor} \end{cases} \qquad (1)$$

The initial offset can be computed from the *x* coordinates of the left and right camera, as shown on equation (2).

$$initial\ offset = |x_{i_R} - x_{i_L}| \qquad (2)$$

The conversion factor can be computed as shown on equation (3).

$$conversion\ factor = \frac{initial\ offset \times initial\ distance}{camera\ separation} \qquad (3)$$

The final offset can be computed from the *x* coordinates of the left and right camera, as shown on equation (4).

$$final\ offset = |x_{f_R} - x_{f_L}| \qquad (4)$$

The final distance can be computed as shown on equation (5).

$$final\ distance = \frac{converison\ factor \times camera\ separation}{final\ offset} \qquad (5)$$

The novelty of the paper is measuring movement distances for a robotic arm's gripper, during movement (dynamically), with the usage of two cameras (stereo cameras) in real-time.

To have a robotic arm which can move freely, to execute any given task, as it was programmed previously (statically), the optical distance measurement must be very precise. To test the robustness of the optical distance measurement, the system must be tested as any industrial process. The best way to test this is to create a measurement system analysis (MSA) using Six Sigma tools.

III. Problem Solution

The optical distance measurement method was tested using Six Sigma tools [17]. Six Sigma represents a set of methods and tools which are used to improve the process. Six Sigma methods try to improve the quality of a process by finding and eliminating the root causes of defects. It uses a set of quality management tools, mainly statistical tools. The Six Sigma tools were implemented using graphs in Minitab statistical software [18].

These tools can show if the measurements are accurate enough and if some fine tuning is needed [13].

As shown on Table I., the system was tested with measurements at different distances. The range of values used for the measurements is between 100 mm and 3000 mm, with 100 mm step. The real values, measured by laser, and the distance measured and computed by the system with the cameras are very close. There are two cameras, they are placed near each other, and the distance is computed with stereo triangulation. We computed also an error delta, the difference between the actual distance value and the value measured by the camera system. The low sample size is not a problem for the Six Sigma tools, because it can be used always normal probability plot instead of histograms.

TABLE I
DISTANCE MEASUREMENT USING CAMERAS AT DIFFERENT DISTANCES [MM]
AND THE MEASUREMENT ERROR DELTA [MM]

Real Distance [mm]	Computed Distance [mm]	Error Delta [mm]
100	99	1
200	202	-2
300	303	-3
400	395	5
500	502	-2
600	598	2
700	699	1
800	797	3
900	904	-4
1000	1005	-5
1100	1101	-1
1200	1204	-4
1300	1298	2
1400	1402	-2
1500	1494	6
1600	1599	1
1700	1701	-1
1800	1802	-2
1900	1905	-5
2000	2005	-5
2100	2105	-5
2200	2202	-2
2300	2302	-2
2400	2404	-4
2500	2496	4
2600	2598	2
2700	2697	3
2800	2796	4
2900	2902	-2
3000	3006	-6

IV. Evaluation

In Fig. 3 we present a normal probability plot with a 95% confidence interval of the two measurements, the real distance and the measured distance with the camera system. Please note that these graphs overlap almost perfectly, so the measured distance, does not differ very much from the actual distance. The Anderson-Darling (AD)value is 0.321, and the p-value (the p-value or probability value is the probability for a specific statistical model, when the null hypothesis is true) is

0.514, so it is higher than α = 0.05 (the significance level α is the probability of making the wrong decision, when the null hypothesis is true), so the null hypothesis is not rejected; thus, we can say that the measured distance values do not differ too much from each other.
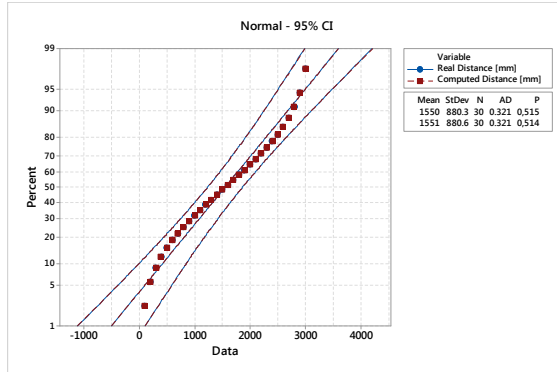

Fig. 3. The normal probability plot, for the actual real distance and the distance computed, by the system using the cameras.

In Fig. 4 we see the normal probability plot for absolute error delta with a confidence interval of 95%. The mean for the absolute error delta is 3.033 mm. The standard deviation is 1.586 mm. The AD value is 1.261, and the value is p <0.005, which is lower than 0.05, so the null hypothesis is rejected. This means that the absolute error delta values differ from each other, which could be expected, because for absolute error delta is a computed value, not a measured one. Each value is transformed to a positive error, all errors are added and stacked, and all errors are over 0, even if the computed distance is higher or lower than the real distance. The mean of the absolute error has the value just over 3 mm.
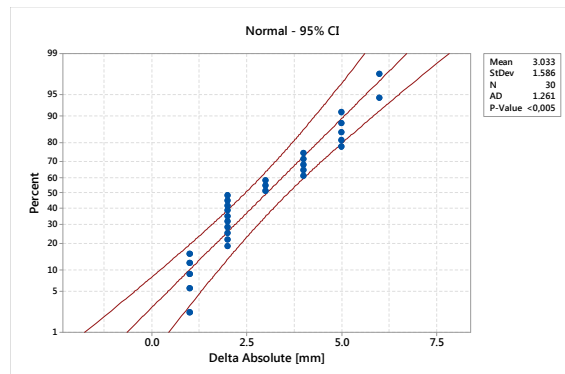

Fig. 4. The normal probability plot created for the absolute error delta.

In Fig. 5 we can see the fitted line plot, which is a method of the regression analysis. The computed distance is presented as a function of the actual real distance. The values are obtained first from the actual real distance values and then from the computed distance values. The standard deviation of these values is 3.42693 mm. The R-Square (R-Sq) and R-Square adjusted (R-Sq (adj)) values are 100%, which shows that the responses can be perfectly predicted by knowing the input values. This means that if we know the actual real distance, we can obtain the distance computed by the

algorithm using video cameras. For regression analysis we obtained an empirical formula presented in the graph and shown in equation (6).

$$computed\ distance\ [mm] = 0.246 + real\ distance\ [mm]$$
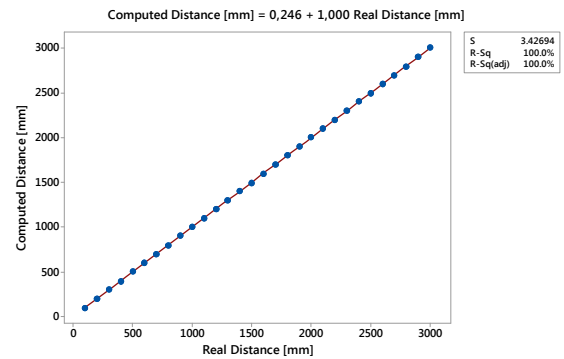$$\text{or} \qquad\qquad (6)$$
$$Y = 0.246 + X$$

Fig. 5. Regression analysis, for actual real distance and the distance computed, by the system using cameras.

In Fig. 6 we show a more detailed analysis of regression, where, versus graphs are observed, indicating that there are no problems with the regression model, because the values are spread randomly above and below 0. Also, on the graph we can see a red dot, representing a high residual value, at the (-6, 1500) coordinate. This means that for the measurement of 1500 mm, the largest error delta is 6 mm.
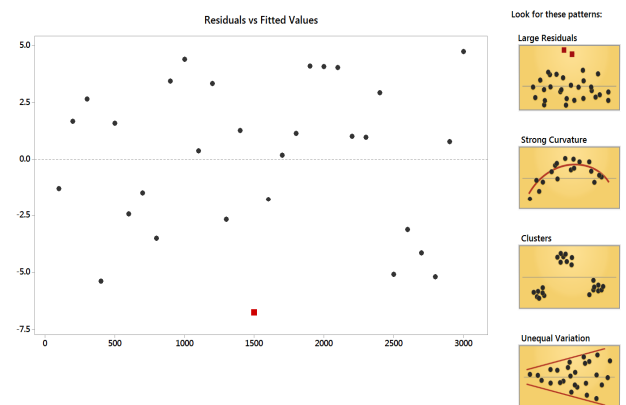
Fig. 6. The graph of residuals versus fitted values, for the actual real distance and the distance computed, by the system using cameras.

In Fig. 7 we show the residual values obtained after the fitted line plot. We can see that the AD value is 0.549, and the p-value is 0.145, this is higher than α = 0.05, the null hypothesis is not rejected. Thus, we can say that the residual values do not differ too much from each other. The histogram does not look like a Gaussian distribution, but for such a small number of values it cannot be expected a better result. The versus graphs (versus fits and versus order) show a large distribution of the values, which is normal and expected.

Fig. 7. Analysis of the residual values, for the distance computed, by the system using cameras.

In Fig. 8 we continue the regression analysis between the actual real distance and the distance computed by the algorithm for measuring distances using cameras. For each input value x (actual real distance) there is a prediction of y (the computed distance) using a prediction interval of 95% for $\alpha = 0.05$.
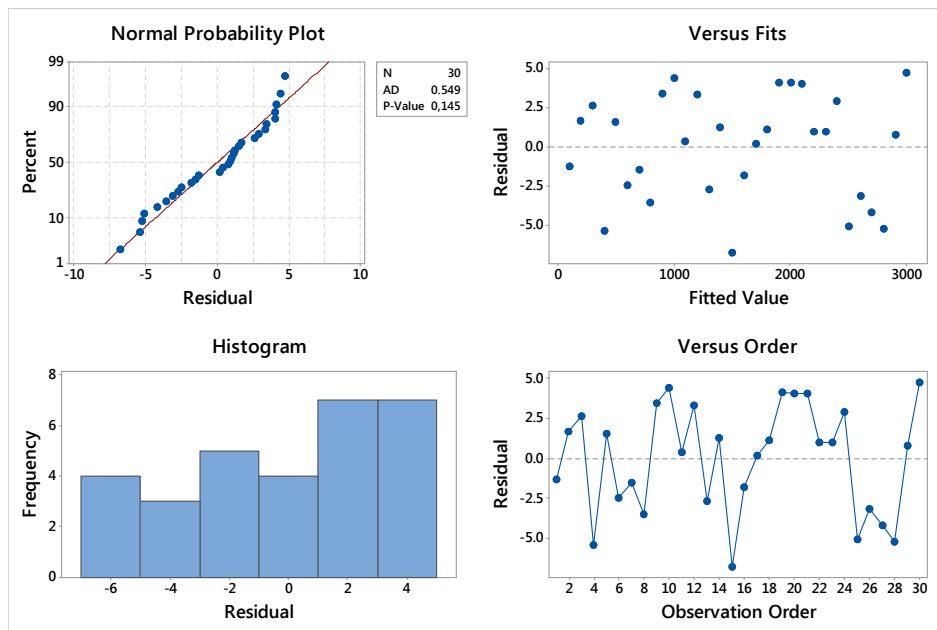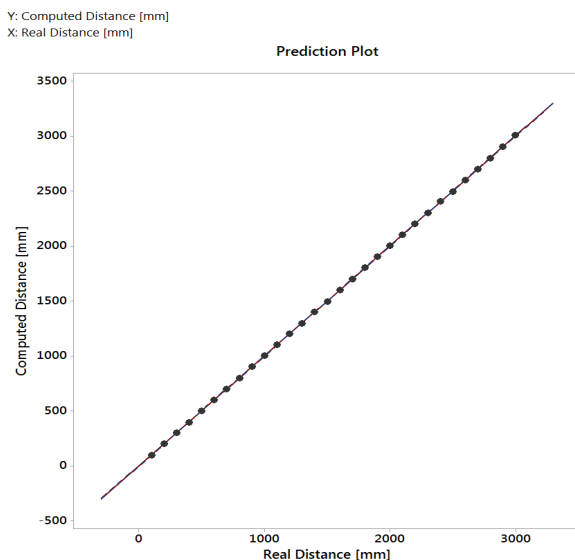

Fig. 8. The prediction plot, for the actual real distance and the distance computed, by the system using cameras.

In Fig. 9 we continue again the regression analysis, highlighting certain important values. We can see the R-Square (R-Sq) value adjusted to 100%, which shows that the output values (computed distance) can be predicted 100% from the input values (actual real distance). The residual standard deviation is 3.427 mm in the linear model and in the

alternative quadratic model is 3.468 mm; these values are very good and there were expected. On the graph we can observe the empirical formula obtained by the regression analysis and the highest residual value of 6 mm when measuring the distance of 1500 mm.
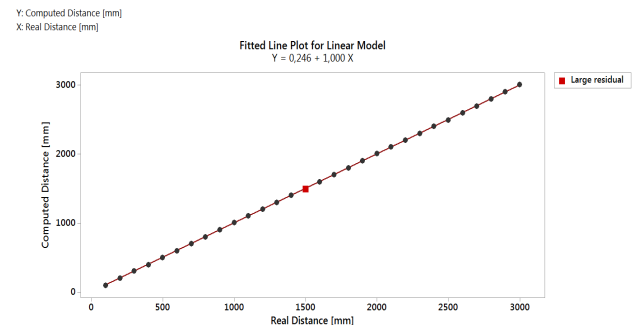
Fig. 9. The fitted line plot for linear model, for the actual real distance and the distance computed, by the system using cameras.

In Fig. 10 we present the summary report of the regression analysis. We can see that p <0.001, which is lower than $\alpha = 0.05$, so the null hypothesis is rejected: This means that the measured values differ enough from each other, to form a mathematical relationship between the computed distance (Y) and the actual real distance (X). The model variation, the R-Square (R-Sq) is 100%, therefore the output values (computed distance) can be predicted 100% from the input values (actual real distance), in other words the variation of the model is very small or non-existent, or the computed values with the camera system are very close to the actual real values measured with laser. There is a perfect correlation between the computed distance (Y) and the actual real distance (X) using the empirical equation obtained by the regression analysis.

Sun Tracker Robotic Arm Optical Distance Measurement
Evaluation at Different Positions Using Six Sigma Tools

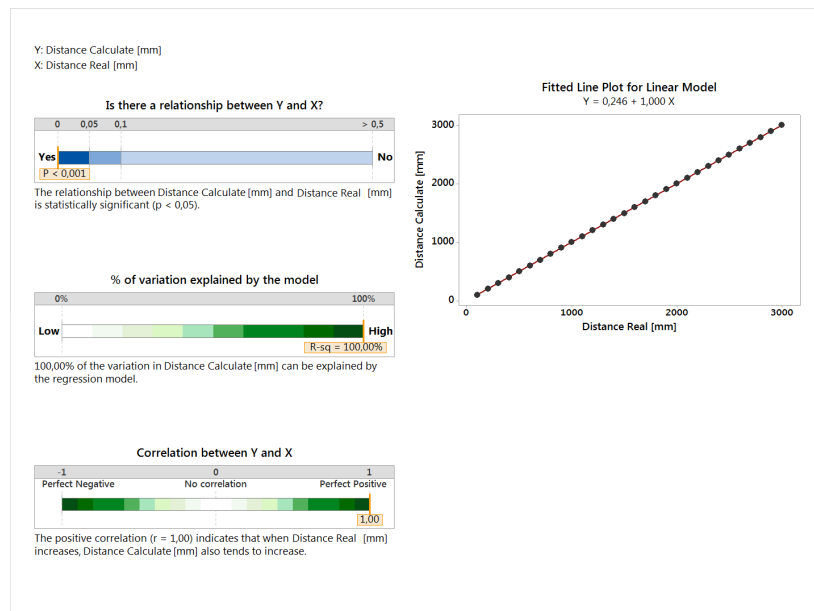Fig. 10. Summary report of the regression analysis, for the actual real distance and the distance computed, by the system using cameras.

In Fig. 11 we show the capability analysis for 30 error deltas. The individual value and moving range (I-MR) charts are within limits. The histogram has somehow a Gaussian tendency but for a histogram, 30 values are not enough (better use normal probability plot). On the histogram we observe that there are no values where the error delta is 0, which means there is no measurement without error, but the errors are not too high. On the normal probability plot, the AD value is 0.643 and the p-value is 0.084, so this is higher than α = 0.05, so the null hypothesis is not rejected. This means that the error deltas do not differ too much between each other. The most important values are at the conclusions: the standard deviation is 2.965 mm for the subgroup and 3.38 mm for all the measurements. The process capability index for subgroup: C_{pk} = 1.38, over 4σ (where C_{pk} = 1.33), which is a very good result in a system of this kind. The performance for subgroup: C_p = 1.46, the performance overall the data: P_p = 1.28 and the process capability index overall the data: P_{pk} = 1.21, all values are very close 4σ, which is a very good result for a system running under normal conditions. For parts per million (PPM), or the reported error to one million measurements is 20.21 for the subgroup and 171.11 for all the measurements, these values are also very good.
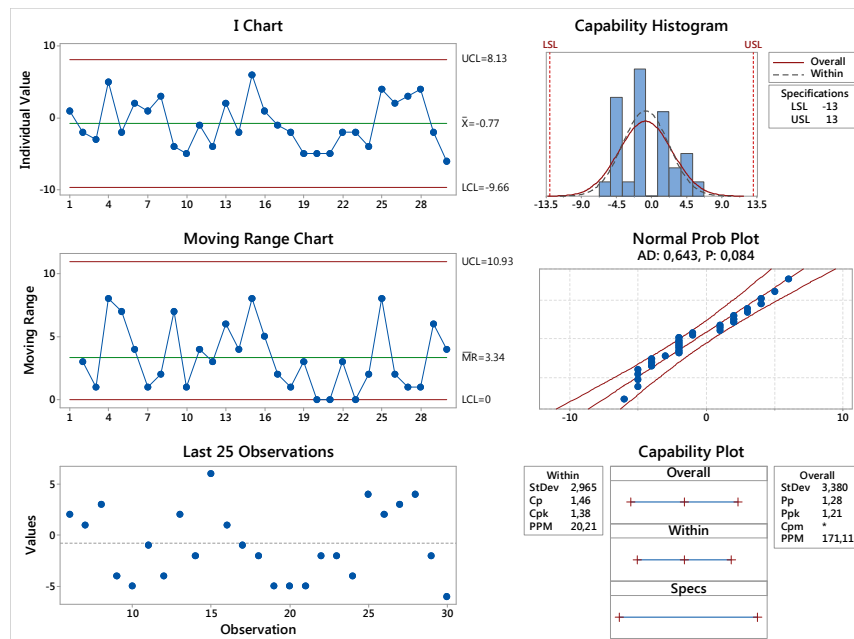

Fig. 11. The process capability analysis made for the error delta.

In Fig. 12 we continue the capability analysis for the error delta. We can see the individual value and moving range (I-MR) charts which are in limits. The normality (Anderson-Darling) test is passed with the p-value of 0.084, which is greater than $\alpha = 0.05$, so the null hypothesis is not rejected. Thus, we can say that the error delta values do not differ too much between each other.
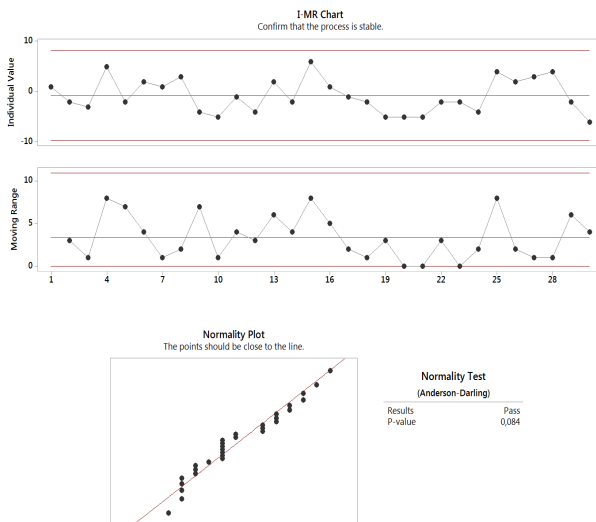

Fig. 12. The I-MR (individual value - moving range) analysis and the normality test made for the error delta.

In Fig. 13 we observe the fluctuation of the error delta, measured in mm, as a function of the actual real distance, measured with laser in m. We can see a tendency of fluctuation of higher values, for the small distances, under 1 m, a tendency of fluctuation of proportional values, for the average distances, between 1 m and 2 m, and a tendency of fluctuation of lower values, for the higher distances, between 2 m and 3 m. This was expected, as this chart represents proportionality, so after this graph it can be said that the error deltas are mostly constant throughout all the distance ranges. This graph is a qualitative rather than a quantitative one; it shows the errors as the measurement distance is increased.
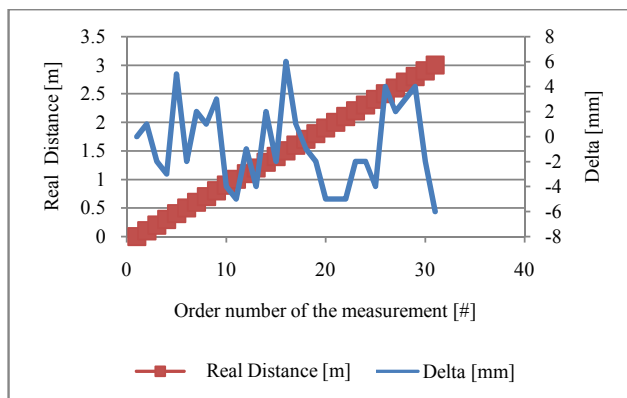

Fig. 13. Graphic representation of the actual real distance [m] and the error of measurement (error delta) [mm] on the same graph.

V. CONCLUSION

As it was seen an optical distance measurement system, with stereo cameras, used for a sun tracker robotic arm, was evaluated using Six Sigma tools.

The Six Sigma tools materialized by the graphs in Minitab showed that the optical distance measurement with video cameras is accurate enough and there is no need for fine tuning or replacing with other distance measurement method. This means that the measurement system analysis (MSA) has good results, 4σ accuracy which for real processes is very good (6σ is the theoretically ideal process, not existent in real life). Knowing that the MSA had good results we can say that the industrial robots can precisely detect their position in space and the distance to the manipulated object just by using optical distance measurement using video cameras.

REFERENCES

[1] Wong Guan Hao, Yap Yee Leck, Lim Chot Hun, "6-DOF PC-Based Robotic Arm (PC-ROBOARM) with efficient trajectory planning and speed control," in *Proc. 4th International Conference On Mechatronics*, Kuala Lumpur, Malaysia, May 17–19, 2011, pp. 1–7.

[2] Woosung Yang, Ji-Hun Bae, Yonghwan Oh, Nak Young Chong, Bum-Jae You, Sang-Rok Oh, "CPG based self-adapting multi-DOF robotic arm control," in *Proc. International Conference on International Conference on Intelligent Robots and Systems*, Taipei, Taiwan, October 18–22, 2010, pp. 4236–4243.

[3] E. Oyama, T. Maeda, J. Q. Gan, E. M. Rosales, K. F. MacDorman, S. Tachi, A. Agah, "Inverse kinematics learning for robotic arms with fewer degrees of freedom by modular neural network systems," in *Proc. International Conference on International Conference on Intelligent Robots and Systems*, August 2–6, 2005, pp. 1791–1798.

[4] N. Ahuja, U. S. Banerjee, V. A. Darbhe, T. N. Mapara, A. D. Matkar, R.K. Nirmal, S. Balagopalan, "Computer controlled robotic arm," in *Proc. 16th IEEE Symposium on Computer-Based Medical Systems*, New York, NY, USA, June 26–27, 2003, pp. 361–366.

[5] M. H. Liyanage, N. Krouglicof, R. Gosine, "Design and control of a high performance SCARA type robotic arm with rotary hydraulic actuators," in *Proc. Canadian Conference on Electrical and Computer Engineering*, St. John's, NL, USA, May 3–6, 2009, pp. 827–832.

[6] M. Mariappan, T. Ganesan, M. Iftikhar, V. Ramu, B. Khoo, "A design methodology of a flexible robotic arm vision system for OTOROB," in *Proc. 2nd International Conference on Mechanical and Electrical Technology*, Singapore, September 10–12, 2010, pp. 161–164.

[7] Guo-Shing Huang, Xi-Sheng Chen, Chung-Liang Chang, "Development of dual robotic arm system based on binocular vision," in *Proc. International Automatic Control Conference*, Nantou, Taiwan, December 2–4, 2013, pp. 97–102.

[8] N. C. Orger, T. B. Karyot, "A symmetrical robotic arm design approach with stereo-vision ability for CubeSats," in *Proc. 6th International Conference on Recent Advances in Space Technologies*, Istanbul, Turkey, June 12–14, 2013, pp. 961–965.

[9] F. Medina, B. Nono, H. Banda, A. Rosales, "Classification of Solid Objects with Defined Shapes Using Stereoscopic Vision and a Robotic Arm," in *Proc. Andean Region International Conference*, Cuenca, Spain, 2012, p. 226.

[10] M. Puheim, M. Bundzel, L. Madarasz, "Forward control of robotic arm using the information from stereo-vision tracking system," in *Proc. 14th International Symposium on Computational Intelligence and Informatics*, Budapest, Hungary, November 19–21, 2013, pp. 57–62.

Sun Tracker Robotic Arm Optical Distance Measurement
Evaluation at Different Positions Using Six Sigma Tools

[11] T. P. Cabre, M. T. Cairol, D. F. Calafell, M. T. Ribes, J. P. Roca, "Project-Based Learning Example: Controlling an Educational Robotic Arm with Computer Vision," IEEE Revista Iberoamericana de Tecnologias del Aprendizaje, vol. 8, issue 3, 2013, pp. 135–142.

[12] G. S. Gupta, S. C. Mukhopadhyay, M. Finnie, "WiFi-based control of a robotic arm with remote vision," in *Proc. IEEE Instrumentation and Measurement Technology Conference*, Singapore, May 5–7, 2009, pp. 557–562.

[13] Haoting Liu, Wei Wang, FengGao, Zhaoyang Liu, Yuan Sun, Zhenlin Liu, "Development of Space Photographic Robotic Arm based on binocular vision servo," in *Proc. Sixth International Conference on Advanced Computational Intelligence*, Hangzhou, China, October 19–21, 2013, pp. 345–349.

[14] Wen-Chung Chang, Chih-Wei Cho, "Automatic Mobile Robotic Manipulation with Active Eye-to-Hand Binocular Vision," in *Proc. 33rd Annual Conference of the IEEE Industrial Electronics Society*, Taipei, Taiwan, November 5–8 2007, 2007, pp. 2944–2949.

[15] P. C. Nunnally, J. M. Weiss, "An inexpensive robot arm for computer vision applications," in. *Proc. IEEE Energy and Information Technologies in the Southeast*, Columbia, SC, USA, vol. 1, April 9–12, 1989, pp. 1–6.

[16] T. Kizaki, A. Namiki, "Two ball juggling with high-speed hand-arm and high-speed vision system," in *Proc. IEEE International Conference on Robotics and Automation*, Saint Paul, MN, USA, May 14–18, 2012, pp. 1372–1377.

[17] Atarod Goudarzlou, Tan Kay Chuan "Using six sigma in new service development," in *Proc. International Conference on Service Systems and Service Management*, 2008, pp. 1–6.

[18] R. Szabo, A. Gontean, "Sun tracker robotic arm optical distance measuring algorithm evaluation using Six Sigma methods," *in Proc. International Conference on Environment and Electrical Engineering*, Milan, Italy, June 6–9, 2017, pp. 1439–1444.

Roland Szabo was born in Timisoara, Romania on April 14, 1986. He received the B.Sc., M.Sc. and Ph.D. degrees from the Politehnica University Timisoara in 2009, 2011 and 2015, respectively.

In 2009 he joined the Applied Electronics Department of the Politehnica University Timisoara where he is now a Lecturer. He is a hardware engineer, mainly with software tasks, developing test system software, at Continental Automotive Romania, located in Timisoara, since 2009. He is a LabWindows/CVI (ANSI C programming language) and NI TestStand (test sequencer language) industrial test software design trainer at Honeywell Life Safety, located in Lugoj, Romania since 2012.He got a Design for Six Sigma Green Belt (DfSS) certificate from Innovensys Germany in 2015, a LabVIEW Basics I & II certificate from National Instruments Hungary in 2009.He is the author of 4 books, has 67 papers, 3 patent proposals and is a team member in 5 research grants.

His research interests are: robotics, computer communication interfaces, measuring equipment, software drivers, servers, mobile programming, web programming, programming languages, operating systems, communication systems, and embedded systems.

Aurel Gontean (M'05) was born in Petrosani, Romania on June 27, 1961. He received the Eng. and Ph.D. degrees from the Politehnica University Timisoara in 1986 and 1998, respectively.

He is a professor since 2005 in the Applied Electronics Department of the Politehnica University Timisoara. He is a PhD Advisor since 2008 (field: Electronics and Telecommunications). From 2004 till 2012 he was vice dean of the Electronics and Telecommunications Faculty, Timisoara, Romania. He is the author of 8 books, has over 150 papers, 3 patent proposals and has over 30 research grants and contracts. His research interests are in renewable energies, smart cities and memristors. He is also a visiting professor at the Loerrach University, Germany since 2009.He has been appointed as EU expert for evaluating project proposals for the Scientific Research Fund, Sofia, Bulgaria, from 2008 to 2009. He was recipient of the IEEE International Conference on Intelligent Data Acquisition and Advanced Computing Systems Best Paper Award in 2011.

IEEE/IFIP Network Operations and Management Symposium Networking

20-24 April 2020 // Budapest, Hungary

◆IEEE IEEE ComSoc IEEE Communications Society

CALL FOR PAPERS

The 17th IEEE/IFIP Network Operations and Management Symposium (NOMS 2020) will be held 20-24 April 2020 at Budapest, Hungary. Held in even-numbered years since 1988, NOMS 2020 will follow the 32 years tradition of NOMS and IM as the primary IEEE Communications Society's forum for technical exchange on management of information and communication technology focusing on research, development, integration, standards, service provisioning, and user communities. The theme of NOMS 2020 will be Management in the Age of Softwarization and Artificial Intelligence presenting recent, emerging approaches and technical solutions for dealing with management of Fixed Networks, Mobile Networks, Clouds, and Vertical Systems (e.g., smart cities and smart transportations, etc.) in order to enable convergence of the networked services. NOMS 2020 will offer various types of sessions: keynotes, technical, experience, demo, tutorial, poster, panel, and dissertation. Topics of interest include, but are not limited to, the following:

Management of Smart Vertical Systems in the Industry 4.0 Era
- Smart Cities, Smart Grid, Smart Homes Cyber-Physical Systems
- Internet of Things (IoT)
- 5G
- Social Networks
- Techniques supported with Augmented Reality, Virtual Reality, Mixed Reality
- Applications and case studies

Artificial Intelligence Techniques for Network and Service Management
- Management with AI
- Artificial Neural Networks
- Markov Chains and Management
- Machine Learning, Deep Learning and Management
- Data Mining
- Management with Big Data
- Mobile Agents

Management of SDN and NFV
- Network virtualization
- Control plane programmability
- Data plane programmability
- Management & Orchestration (MANO)
- Service Function Chaining
- Protocols, languages and frameworks
- Open source networking
- Cloud native networking
- Case studies and practical deployments

Management Functional Areas
- Billing, Accounting
- FCAPS: Fault, Configuration, Accounting, Performance and Security Management
- Energy-efficiency/green management
- Service Assurance
- Service Fulfillment
- Service Level Management

Network Management and Operational Experience
- Ad-hoc networks
- Automotive and Vehicular Networks
- Broadband access networks Cognitive Radio networks Data Centers
- e-Maintenance
- Future Internet
- Heterogeneous networks
- Home networks
- M2M networks
- OSS/BSS development
- Overlay networks
- Personal area networks
- Sensor networks
- Wireless and mobile networks

Service Management
- Business management
- Clouds
- Data center management
- Data service management
- Hosting
- Infrastructure as a Service, Management as a Service, Platform as a Service, Software as a Service
- IT service management
- Managed service provisioning
- Multimedia service management
- OTT service management
- Virtualized infrastructure management

Security Management
- Intrusion detection, intrusion prevention, intrusion response
- Network security
- Security for peer-to-peer and overlay networks
- Security for smart X and large systems and critical infrastructures
- Privacy and anonymity
- Vulnerability management
- Early warning

Methodologies for Network Operations and Management
- Control theory
- Data collection and aggregation
- Design and simulation
- Economic/finance theories
- Experimental approaches
- Optimization theory
- Probability and stochastic processes, queuing theory
- Risk management
- Software engineering methodologies Visualization
- Management approaches for Quantum Networking

Management Approaches
- Autonomic and self-management
- Best practices
- Centralized management
- Distributed management
- Integrated management
- Management architectures
- Organizational aspects
- Policy-based management
- Process oriented management
- IT service management (ITSM)
- Process engineering and frameworks (ITIL, CobIT, RiskIT, ValIT)

IMPORTANT DATES
Paper Submission Deadline: 30 August 2019
Notification of Acceptance: 8 November 2019
Camera-Ready Submission: 12 January 2020

GENERAL CO-CHAIRS
Pal Varga, Budapest University of Technology and Economics, Hungary
Doug Zuckerman, Perspecta Labs, USA

TPC CO-CHAIRS
Imen Grida Ben Yahia, Orange Labs, France
Alex Galis, UCL, UK
Istvan Godor, Ericsson, Hungary

For more information, please visit http://noms2020.ieee-noms.org

Call for Papers

10th International Conference on Cognitive Infocommunications

Call for Papers

CogInfoCom 2019

Naples, Italy

23-25 September, 2019

Committees

Chairs
Péter Baranyi, *Széchenyi István University, Hungary*
Anna Esposito, *Università degli Studi della Campania "Luigi Vanvitelli", Italy*
Nelson Mauro Maldonato, *Università di Napoli Federico II, Italy*
Carl Vogel, *Trinity College Dublin, Ireland*

Honorary Chairs
Vilmos Csányi, *MTA, Hungary*
Valéria Csépe, *MTA, Hungary*
József Bokor, *MTA, Hungary*
Helen Meng, *Chinese University of Hong Kong, China*
Junzo Watada, *Petronas University of Technology, Malaysia*

International Scientific Board
Attila Gilányi, *University of Debrecen, Hungary*
György Szaszák, *Budapest University of Technology and Economics, Hungary*
Yeung Yam, *Chinese University of Hong Kong, China*
Miroslav Macik, *Czech Technical University in Prague, Czech Republic*
Maria Koutsombogera, *Trinity College, Dublin*
Katarzyna Chmielewska, *Kazimierz Wielki Universit, Poland*

International Program Committee
Klára Vicsi, *Budapest Univesity of Technology and Economics, Hungary*
Ágoston Török, *MTA, Hungary*
Atsushi Ito, *Utsunomiya University, Japan*
Zsolt Győző Török, *ELTE, Hungary*
Károly Hercegfi, *Budapest Univesity of Technology and Economics, Hungary*
Ildikó Horváth, *Széchenyi István University, Hungary*
Hassan Charaf, *Budapest Univesity of Technology and Economics, Hungary*

Local Organizing Committee Chairs
Silvia Dell'Orco, *Università di Napoli "Federico II", Italy*
Gennaro Cordasco, *Università della Campania "Luigi Vanvitelli", Italy*

Local Organizing Committee
Benedetta Muzii, *Università di Napoli "Federico II", Italy*
Marzia Duval, *Università di Napoli "Federico II", Italy*
Terry Amorese, *Università della Campania "Luigi Vanvitelli", Italy*
Marialucia Cuciniello, *Università della Campania "Luigi Vanvitelli", Italy*
Betul Tolgay, *Università della Campania "Luigi Vanvitelli", Italy*

Technical Program Committee Chair
Ádám Csapó, *Széchenyi István University, Hungary*

Technical Program Committee
to be determined

Publication Chair
Jan Nikodem, *Wroclaw University of Science and Technology, Poland*
Ryszard Klempous, *Wroclaw University of Science and Technology, Poland*

Industrial Relations Chair
Péter Galambos, *Óbuda University, Hungary*

Secretary General
Anna Sudár, *Szechenyi University, Hungary*

Financial Chair
Aniko Szakal, *IEEE Hungary Section, Hungary*

Scope CogInfoCom is a new interdisciplinary field of science defined as follows:

Cognitive infocommunications (CogInfoCom) investigates the link between the research areas of infocommunications and cognitive sciences, as well as the various engineering applications which have emerged as the synergic combination of these sciences. The primary goal of CogInfoCom is to provide a systematic view of how cognitive processes can co-evolve with infocommunications devices so that the capabilities of the human brain may not only be extended through these devices, irrespective of geographical distance, but may also interact with the capabilities of any artificially cognitive system. This merging and extension of cognitive capabilities is targeted towards engineering applications in which artificial and/or natural cognitive systems are enabled to work together more effectively.

For more information on CogInfoCom please visit its official home-site at www.scitope.com/coginfocom19

Contributions are expected from the following areas

Human- computer combo (focusing on the complex mixture of human and artificial cognitive capabilities in human computer interaction processes; HCI, HMI, HRI)

Infocommunication-related aspects of the cognitive sciences

Artificial cognitive capabilities of infocommunication systems

Sensory substitution, sensorimotor extension, sensory augmentation

CogInfoCom channels

Socio-cognitive ICT (including any approach that uses or influences collective knowledge)

Embodied and enactive cognitive systems (based on e.g. cognitive robotics and autonomous mental development)

Cognitive biases: how biases in human perception and high-level reasoning can be put to use in system design

Cognitive control: control theoretical solutions based on or targeting cognitive and other human body related processes

Speechability (based on e.g. cognitive linguistics, verbal/non-verbal social communicative signals, speech technologies)

Augmented interaction capabilities and augmented cognition (based on e.g. multimodal interfaces)

Ethology-inspired engineering / Ethorobotics

Mathability: modeling and understanding mathematical capabilities, developing artificial mathematical capabilities

Cognitive informatics and media

Ergonomics-based aspects of CogInfoCom

Cognitive networks (intelligent capabilities of cognitive networks)

Brain computer interface

Human and bio-interfaces

Affective computing

Intelligent vehicle and transportation systems (based on e.g. enhanced driver awareness, advanced driver assistance systems)

Augmented 3D capabilities (based on e.g. 3D visualization and immersive augmented/virtual interaction)

Human cognitive interfaces-virtual and real avatars (based on e.g. BCI, body area networks, virtual avatars)

Future Internet (Cognitive capabilities of e.g. Internet of Things, 3D Internet)

Virtual Reality (cognitive aspects of immersive 3D spaces, avatars)

Industrial applications of CogInfoCom (production engineering, production management etc.)

CogInfoCom based learning abilities (investigating capabilities for learning through modern informatics based education)

Educoaching (education through online collaborative systems and virtual reality solutions, project based education)

Authors are encouraged to submit full papers describing original, previously unpublished, complete research, not currently under review by another conference or journal, addressing state-of-the-art research and developments. All papers will be reviewed and accepted papers will appear in the conference proceedings. Papers must be submitted electronically via EasyChair in IEEE format (double column A/4, 4-6 pages long).

Just like last year, publications of the 9th IEEE International Conference on Cognitive Infocommunications (CogInfoCom 2018) will be uploaded to the IEEE Xplore database upon consent of IEEE. We reserve the right to exclude any paper from the final proceedings (as well as any official database), if it is not presented at the conference.

Authors' Schedule   First submission: 1 June 2019
Notification of acceptance: 5 August, 2019
Final submission: 23 August, 2019

Journal Publications Authors of selected best papers of the conference shall be invited to publish their previously unpublished research results in special issues of international journals.

Track and Session Organizers: Those who would like to propose a track or session (a set of oral or DEMO presentations) in order to introduce the new scientific results of their fields or large scale international projects are warmly welcome. Please kindly note that the minimum number of sessions is 3 per track and 1 session is of 4 publications.

ieee-sensors2019.org

IEEE SENSORS 2019
Palais des Congrès de Montréal | October 27-30, 2019
Montreal, Canada

CALL FOR PAPERS

Organizers

General co-chairs
Jill Gostin
Georgia Tech Research Institute, USA

Fabrice Labeau
McGill University, Canada

TPC co-chairs
Rudra Pratap
Indian Institute of Science, India

Rolland Vida
Budapest University of Technology and Economics, Hungary

Important Dates

May 6, 2019
Proposals for Tutorials

May 20, 2019
Proposal for Focused Sessions

June 18, 2019
4 pages (max) - 3 pages of text (max) + 1 page of references (max)

August 10, 2019
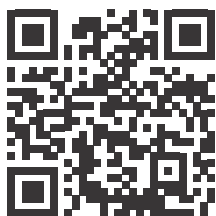Notification of Paper Acceptance

August 31, 2019
Submission of Final Papers

Conference Dates

Palais des Congrès de Montréal

October 27-30, 2019
Conference

Please visit
ieee-sensors2019.org

IEEE SENSORS 2019 is intended to provide a forum for research scientists, engineers, and practitioners throughout the world to present their latest research findings, ideas, and applications in the area of sensors and sensing technology.

IEEE SENSORS 2019 will include keynote addresses and invited presentations by eminent scientists and engineers. The conference solicits original state-of-the-art contributions as well as review papers.

Topics for IEEE SENSORS 2019 include

- Sensor Phenomenology, Modeling and Evaluation
- Sensor Materials, Processing and Fabrication (including Printing)
- Chemical, Electrochemical and Gas Sensors
- Microfluidics and Biosensors
- Optical Sensors
- Physical Sensors - Temperature, Mechanical, Magnetic and Others
- Acoustic and Ultrasonic Sensors
- Sensor Packaging (including on Flexible Materials)
- Sensor Networks (including IoT and related areas)

- Emerging Sensor Applications
- Sensor Systems: Signals, Processing and Interfaces
- Actuators and Sensor Power Systems
- Sensors in Industrial Practices
  This track is for traditional papers where the focus is on the industrial applications of different sensors. This track is only for industry, i.e. first author must be from industry.
- Live Demonstration of Sensors and Sensing Technologies

Focused Sessions

IEEE SENSORS 2019 will have focused sessions on emerging sensor-related topics. Details related to the Call For Focused Sessions is on the conference website.

Publication of Papers

Presented papers will be included in the Proceedings of IEEE SENSORS 2019 and in IEEE Xplore pending author requirements being met. Authors may submit extended versions of their paper to the IEEE Sensors Journal.

Exhibition Opportunities

The Conference exhibit area will provide your company or organization with the opportunity to inform and display your latest products, services, equipment, books, journals, and publications to attendees from around the world.

For further information, contact Rachel Brockhoff, **rbrockhoff@conferencecatalysts.com**

Industry Day

A special track designed to encourage industry participation will include industry showcase, industry networking, and an industry panel discussion. Special flexible one-day registration will be available to facilitate industry participation.

Visit the website for the most up to date information relating to abstract submission, tutorials, and special sessions information and deadlines.

Special Issue in the IEEE Sensors Journal

If your paper is accepted for publication at this conference, you may receive an invitation to submit an extended manuscript to be considered for publication in the IEEE Sensors Journal. Best papers presented at the conference will be invited to participate via the call for papers for this special issue of the journal.

IEEE
Advancing Technology for Humanity

IEEE Sensors Council

Guidelines for our Authors

Format of the manuscripts

Original manuscripts and final versions of papers should be submitted in IEEE format according to the formatting instructions available on
  http://www.ieee.org/publications_standards/
  publications/authors/authors_journals.html#sect2,
"Template and Instructions on How to Create Your Paper".

Length of the manuscripts

The length of papers in the aforementioned format should be 6-8 journal pages.
Wherever appropriate, include 1-2 figures or tables per journal page.

Paper structure

Papers should follow the standard structure, consisting of *Introduction* (the part of paper numbered by "1"), and *Conclusion* (the last numbered part) and several *Sections* in between.
The Introduction should introduce the topic, tell why the subject of the paper is important, summarize the state of the art with references to existing works and underline the main innovative results of the paper. The Introduction should conclude with outlining the structure of the paper.

Accompanying parts

Papers should be accompanied by an *Abstract* and a few *index terms (Keywords)*. For the final version of accepted papers, please send the *short cvs* and *photos* of the authors as well.

Authors

In the title of the paper, authors are listed in the order given in the submitted manuscript. Their full affiliations and e-mail addresses will be given in a footnote on the first page as shown in the template. No degrees or other titles of the authors are given. Memberships of IEEE, HTE and other professional societies will be indicated so please supply this information. When submitting the manuscript, one of the authors should be indicated as corresponding author providing his/her postal address, fax number and telephone number for eventual correspondence and communication with the Editorial Board.

References

References should be listed at the end of the paper in the IEEE format, see below:
  a) Last name of author or authors and first name or initials, or name of organization
  b) Title of article in quotation marks
  c) Title of periodical in full and set in italics
  d) Volume, number, and, if available, part
  e) First and last pages of article
  f) Date of issue

[11] Boggs, S.A. and Fujimoto, N., "Techniques and instrumentation for measurement of transients in gas-insulated switchgear," IEEE Transactions on Electrical Installation, vol. ET-19, no. 2, pp.87–92, April 1984.

Format of a book reference:

[26] Peck, R.B., Hanson, W.E., and Thornburn, T.H., Foundation Engineering, 2nd ed. New York: McGraw-Hill, 1972, pp.230–292.

All references should be referred by the corresponding numbers in the text.

Figures

Figures should be black-and-white, clear, and drawn by the authors. Do not use figures or pictures downloaded from the Internet. Figures and pictures should be submitted also as separate files. Captions are obligatory. Within the text, references should be made by figure numbers, e.g. "see Fig. 2."
When using figures from other printed materials, exact references and note on copyright should be included. Obtaining the copyright is the responsibility of authors.

Contact address

Authors are requested to submit their papers electronically via the EasyChair system. The link for submission can be found on the journal's website:
www.infocommunications.hu/for-our-authors

If you have any question about the journal or the submission process, please do not hesitate to contact us via e-mail:
Pál Varga – Editor-in-Chief:
pvarga@hit.bme.hu

Rolland Vida – Associate Editor-in-Chief:
vida@tmit.bme.hu

legrand®

Everything that is electrical wiring

www.legrand.hu

SCIENTIFIC ASSOCIATION FOR INFOCOMMUNICATIONS

hte

FOUNDED IN 1949

SCIENTIFIC ASSOCIATION FOR INFOCOMMUNICATIONS HUNGARY

Who we are

Founded in 1949, the Scientific Association for Info-communications (formerly known as Scientific Society for Telecommunications) is a voluntary and autonomous professional society of engineers and economists, researchers and businessmen, managers and educational, regulatory and other professionals working in the fields of telecommunications, broadcasting, electronics, information and media technologies in Hungary.

Besides its 1000 individual members, the Scientific Association for Infocommunications (in Hungarian: HÍRKÖZLÉSI ÉS INFORMATIKAI TUDOMÁNYOS EGYESÜLET, HTE) has more than 60 corporate members as well. Among them there are large companies and small-and-medium enterprises with industrial, trade, service-providing, research and development activities, as well as educational institutions and research centers.

HTE is a Sister Society of the Institute of Electrical and Electronics Engineers, Inc. (IEEE) and the IEEE Communications Society.

What we do

HTE has a broad range of activities that aim to promote the convergence of information and communication technologies and the deployment of synergic applications and services, to broaden the knowledge and skills of our members, to facilitate the exchange of ideas and experiences, as well as to integrate and harmonize the professional opinions and standpoints derived from various group interests and market dynamics.

To achieve these goals, we…

- contribute to the analysis of technical, economic, and social questions related to our field of competence, and forward the synthesized opinion of our experts to scientific, legislative, industrial and educational organizations and institutions;
- follow the national and international trends and results related to our field of competence, foster the professional and business relations between foreign and Hungarian companies and institutes;
- organize an extensive range of lectures, seminars, debates, conferences, exhibitions, company presentations, and club events in order to transfer and deploy scientific, technical and economic knowledge and skills;
- promote professional secondary and higher education and take active part in the development of professional education, teaching and training;
- establish and maintain relations with other domestic and foreign fellow associations, IEEE sister societies;
- award prizes for outstanding scientific, educational, managerial, commercial and/or societal activities and achievements in the fields of infocommunication.

Contact information

President: **GÁBOR MAGYAR, PhD** • *elnok@hte.hu*
Secretary-General: **ERZSÉBET BÁNKUTI** • *bankutie@ahrt.hu*
Operations Director: **PÉTER NAGY** • *nagy.peter@hte.hu*
International Affairs: **ROLLAND VIDA, PhD** • *vida@tmit.bme.hu*

Address: H-1051 Budapest, Bajcsy-Zsilinszky str. 12, HUNGARY, Room: 502
Phone: +36 1 353 1027
E-mail: *info@hte.hu*, Web: *www.hte.hu*